MSc thesis in Mechanical Engineering

A Multi-Objective Optimization Model for Offshore Wind Farm Operations & Maintenance Fleet Selection

Jesse Bloothoofd
2023

TUDelft

MSc thesis in Mechanical Engineering

A multi-objective optimization model for offshore wind farm operations & maintenance fleet selection

Jesse Bloothoofd

A thesis submitted to the Delft University of Technology in partial fulfillment of the requirements for the degree of Master of Science in Mechanical Engineering.

To be defended publicly on Wednesday March 29, 2023 at 10:15 AM

Jesse Bloothoofd: *A multi-objective optimization model for offshore wind farm operations & maintenance fleet selection* (2023)

The work in this thesis was carried out at the:

TUDelft   Delft University of Technology

Preface

The Last Dance

With this thesis and graduation project, I close my final chapter as a student at the TU Delft. About six-and-a-half years ago I started my journey at the TU Delft with my Bachelor of Mechanical Engineering. My high school grades did not reflect those of the average TU Delft student. As a result, the first year was not pretty and I had to work hard to catch up. I convinced myself that abstract concepts and math were not my strongest points. But now that I am writing down the last sentences of my thesis, I think I was wrong. They were my strong points all along, but it just took a bit of effort to figure that out.

Acknowledgements

I would like to thank my supervisor Xiaoli for her dedicated guidance throughout my graduation project. She did not only supervise my graduation project but all three large projects of the second year. I always felt encouraged to use my creativity, which led to some very interesting projects. I would like to thank Rudy as well for his efforts and suggestions as graduation committee chair throughout my graduation project, and Mark for being part of the graduation committee and sparking my interest in mathematical optimization during his courses.

Next, I would like to thank the TNO wind energy department for the opportunity to combine my graduation project with an internship. In particular, I would like to thank my company supervisor Vinit for his suggestions and feedback during my internship and for his efforts to review the final draft of my thesis thousands of kilometers away.

At last, I would like to thank everyone in my personal life for their support throughout the years. Michelle, I would like to thank you for your unconditional support whenever I needed it. You made life so much easier during these last few months that I am tempted to call it our graduation instead of just mine. I would like to thank my parents for always giving me a place to stay in Alkmaar, for the number of times that they drove me to Delft or picked me up, and for the other countless times when they were there when I needed them. Also a special thanks to my friends and family from Alkmaar for all the great moments and for giving me a place to distract my mind from my studies, I cannot express how valuable these moments were to me to recharge. And last but not least, thanks to all the old roommates for the support and the laughs.

Abstract

Until recently, tenders in Europe were awarded to wind farm developers based on the highest auction prices or the lowest subsidized bids. The wind industry has suggested that non-price-related criteria should be considered for tenders, like plans to reduce greenhouse gas emissions. As a result of the sustainable tender criteria, greenhouse gas emissions are a relatively new KPI for offshore wind farm developers.

Studies have shown that the costs and wind farm availability are sensitive to the fleet composition and were commonly used as criteria in offshore wind fleet optimization models. Offshore wind greenhouse gas emissions were shown to be sensitive to the offshore wind fleet composition as well but thus far not used as criteria for fleet composition decision-making. This study aims to develop an offshore wind O&M multi-objective fleet optimization model that includes GHG emissions as the third criterion for the fleet composition. The model is rendered as a deterministic MIP problem. An epsilon constraint method-inspired approach is proposed to reformulate the multi-objective into a set of perturbed single-objective models, which can be solved using a commercial MIP solver.

Contents

List of Figures

List of Tables

List of Algorithms

1. Introduction

One of the recent conclusions at the COP27 climate conference in 2022 was that the 1.5°C global warming goal is still viable (Moosmann et al., 2022). However, warnings were given for the lack of efforts to phase out fossil fuels as a source of energy. It will take concrete and ambitious plans from nations all over the world to reduce their emissions in order to maintain the 1.5°C global warming goal (Paris Agreement, 2015). Wind energy is a promising renewable energy source for mitigating global warming (IRENA, 2019). In 2020, the total installed wind energy capacity in Europe was 220 Giga Watts (GW) (Komusanac et al., 2020), with offshore wind energy accounting for 25 GW. Offshore wind energy its share of total new installed wind energy has been steadily increasing (Komusanac et al., 2020). The outlook for offshore wind is positive in the long term as well, as Europe aims to increase the total offshore wind capacity to 400 GW by 2050 (Komusanac et al., 2020). Wind farm developers will need to build large-scale offshore wind farms in order to realize these ambitious plans.

Most offshore wind projects in Europe are awarded to wind farm developers using tenders. Once a tender is awarded, the wind farm developer is granted a permit for the construction, operation, and removal of the wind farm. Up till recently, the highest auction prices or the lowest subsidized bids serve as the criteria for awarding tenders (Wind & water works, 2022). However, the European wind industry has suggested that non-price-related criteria should be considered for tenders as well (WindEurope, 2022). These non-price-related criteria include sustainability and biodiversity-related criteria, such as plans to reduce greenhouse gas (GHG) emissions. This creates a strong incentive for offshore wind farm developers to propose environmentally friendly and sustainable strategies for the wind farm.

The vessel fleet composition during the wind farm operations and maintenance (O&M) phase is one of the strategies. The vessels are used to transport maintenance personnel, spare parts, and/or can perform heavy lifting. Offshore wind costs and wind farm availability are two key performance indicators (KPIs) that can be linked to the vessel fleet composition (Martin et al., 2016; Sperstad et al., 2017). Furthermore, as a result of sustainable tender criteria, GHG emissions are now an offshore wind KPI that can be linked to vessel fleet composition (Garcia-Teruel et al., 2022).

1.1. Problem statement

TNO is an independent scientific research institute in the Netherlands. TNO has dedicated efforts to the current energy transition problem. The wind energy department of TNO has played a contributing role as a consultant for the Dutch government as well as the wind energy industry. TNO has developed the UWiSE O&M Planner, an in-house O&M scheduling tool that can model and predict the costs of offshore wind maintenance activities during the entire O&M life cycle. The UWiSE O&M Planner can inform offshore wind O&M stakeholders about the costs and wind farm availability of required maintenance activities. One of the input parameters in the UWiSE O&M Planner is a selected fleet of maintenance vessels.

However, the maintenance vessel fleet composition is sometimes subject to change if maintenance vessels are temporarily chartered rather than owned by wind farm owners during the O&M phase. The vision for UWiSE O&M Planner is to incorporate an optimal fleet strategy to assist stakeholders in determining fleet composition.

The problem of determining the best fleet strategy for the UWiSE O&M Planner is related to maritime fleet size and mix problems. Several studies on maritime fleet size and mix problems have been done with the aim to develop decision-support tools for vessel fleet composition (Stålhane et al., 2020) based on the costs and/or wind farm availability. To the authors' best knowledge, there are no studies on offshore wind fleet size and mix problems that determine the fleet composition based on GHG emissions. This leads to the following problem statement:

> *Stakeholders have expressed interest in decision-support tools for offshore wind planning activities such as fleet composition. The majority of research on these decision-making tools has focused on lowering costs and increasing wind farm availability. However, research has demonstrated that GHG emissions in the O&M phase are also largely affected by fleet composition.*

1.2. Research goal

The goal of this study is to add the GHG emissions to the costs and wind farm availability as criteria for the offshore wind O&M fleet composition in a decision-support tool. This will be done by developing a multi-objective optimization model for offshore wind O&M fleet composition that is independent of the UWiSE O&M Planner.

1.3. Research questions

The following main research question has been defined to guide the research, based on the research goal:

- **Research question:** How can a multi-objective optimization model be formulated and solved to find an optimal vessel fleet selection for offshore wind O&M activities, based on the financial costs, the GHG emissions, and the wind farm availability as a result of the selected fleet?

A set of sub-questions have been defined in order to help in answering the main research question in a structured way.

- **Sub-question 1:** What optimization models exist to find the optimal fleet for offshore wind farm O&M?

- **Sub-question 2:** Which (parts of) existing optimization models can be adapted to formulate the fleet optimization model in the current study?

- **Sub-question 3:** How can GHG emissions be quantified and incorporated into the multi-objective fleet optimization model?

- **Sub-question 4:** Which algorithms can be used to find optimal solutions to the developed multi-objective fleet optimization model?

- **Sub-question 5:** How can the developed fleet optimization model be verified?

1.4. **Research scope**

This research has been performed as a graduation project to obtain an MSc in Mechanical Engineering at the TU Delft. The graduation project was combined with an internship at TNO. The incentive for TNO to have the fleet optimization model developed from the current study is to provide an optimal fleet selection for its in-house scheduling tool. The requirements were that the optimization model should be independent of the scheduling tool. The author of the current thesis was granted access to the scheduling tool but had no access to the source code or documentation on the model characteristics.

The scope of the research is to develop a deterministic vessel fleet optimization problem with strategic-level decision-making. Stochastic optimization, while useful for offshore wind O&M, is outside the scope of this study due to time and computational efficiency restrictions.

1.5. **Thesis outline**

The that follow will guide the reader through the research in the current study. The purpose of chapter 2 is to familiarize the reader with some of the concepts in offshore wind O&M. A number of offshore wind fleet optimization studies are evaluated with an emphasis on the identification of the research gaps that the current study attempts to fill. The offshore wind fleet optimization model that has been developed in the current study will be formulated in chapter 3. This chapter starts with the evaluation of some of the key aspects of offshore wind O&M that are important to incorporate into the fleet optimization model. The model itself will be covered in detail after, in which the formulation of the three objective functions and the constraints are explained. Some candidate approaches to find the optimal values to the fleet multi-objective optimization model will be discussed in chapter 4. One of these candidate approaches is selected and elaborated upon throughout the chapter. Two case studies for the fleet optimization model are defined in chapter 5 and the results of these case studies are evaluated. A discussion on the developed fleet optimization model, the approach that was used to find the optimal fleet in this model, and the results of the case studies can be found in chapter 6. This chapter ends with some of the limitations, some recommendations for practical implementations, and suggestions for future research based on the findings in the current study.

2. Literature review

The first part of this chapter includes an overview of various offshore wind O&M aspects. This is aimed to provide the reader with an overview of offshore wind O&M in general. The second part of this chapter includes a state-of-the-art review of offshore wind O&M fleet optimization studies. This is done to identify research gaps in the existing literature. By the end of this chapter, the reader should be familiar with some of the fundamental concepts, various decision-making strategies, the assets that can make up a fleet, and the current state of fleet optimization studies in offshore wind O&M.

2.1. Offshore wind O&M

An overview of offshore wind O&M has been compiled using various research efforts to direct the reader to more detailed analyses. The work of Rinaldi et al. (2021) evaluates existing research on offshore wind turbine O&M, lists some novelties, and provides a summary of the offshore wind O&M practices. The work of Merizalde et al. (2019) provides an overview and review of available maintenance models and methods. The work of Ramachandran et al. (2021) gives an overview of challenges and opportunities during the installation, O&M, and decommissioning phases of an offshore wind turbine. The work of Ren et al. (2021) contains a state-of-the-art literature review on offshore wind turbine maintenance, covering strategy selection, schedule optimization, onsite operations, repairs, assessment criteria, recycling, and environmental concerns. The work of Kolios and Brennan (2018) contains an overview of available O&M models/tools that are used (e.g. cost predictions). The work of Kang et al. (2019) contains a review of condition-based maintenance methods for offshore wind turbine O&M. The work of Shafiee (2015) contains a review of the maintenance logistics organization such as strategical issues, tactical issues, and supplementary issues.

The O&M phase of an offshore wind farm can be divided into three different sub-phases (Ren et al., 2021):

- *Maintenance strategy*: A strategy is a long-term plan for the wind farm that is chosen in the interest of optimizing its KPIs. A strategy could include using vibration sensors to monitor the condition of the main shaft of the generator.

- *Maintenance planning*: The planning is a medium-short-term plan where maintenance tasks are scheduled. An example of maintenance planning would be the optimal routing and scheduling of maintenance vessels.

- *Onsite maintenance*: The onsite maintenance entails the maintenance activities that will be carried out. An onsite maintenance procedure could be a minor repair or the total replacement of the generator its main shaft.

2.1.1. Maintenance strategy

The goal of O&M maintenance strategies of OWTs is to select a long-term plan that enhances offshore wind O&M criteria. The daily operations of an offshore wind farm require an efficient maintenance strategy (Ren et al., 2021). Because technicians must travel from a port to the wind farm, it is impossible to operate the wind farm continuously without any on-site maintenance delays. A maintenance crew needs to go to the wind farm frequently to prevent failures. However, due to the large numbers of maintenance personnel and vessels needed, frequent visits are ineffective and expensive. As a result, the frequency of maintenance is a trade-off between risks and resource management. A successful maintenance strategy aims at maximizing economic gain, increasing component life spans, minimizing the need for emergency repairs, cutting down on overtime labor costs, and lessening the stress that unpredictable equipment failures place on workers (Ren et al., 2021).

Maintenance strategies can be subdivided into corrective maintenance and preventive maintenance (Rinaldi et al., 2021). Corrective maintenance is performed on components that have already failed. Preventive maintenance, on the other hand, refers to maintenance tasks that are designed to keep a component from failing. Both types of maintenance have their own subcategories, as shown in fig. 2.1.

Corrective maintenance

Corrective maintenance is performed when a failure occurs in a wind turbine. Failures can occur on critical and non-critical components. If a critical component fails, the wind turbine cannot be operational until the failure is repaired. If a non-critical component fails, the wind turbine can still continue operations. The work of Rinaldi et al. (2021) further subdivides corrective maintenance of non-critical components into immediate, deferred, and opportunistic maintenance categories. If a wind turbine fails, immediate maintenance means that maintenance resources are allocated to the wind turbine failure right away. Deferred maintenance means that maintenance is postponed due to a lack of resources. Opportunistic maintenance is the decision to wait until an opportunity arises to make efficient use of resources. The benefit of the latter could be that maintenance costs are reduced if several breakdowns are handled in series immediately after each other Rinaldi et al. (2021).

Preventive maintenance

The goal of preventive maintenance is to try to prevent a breakdown from occurring. Preventive maintenance can be subdivided into periodic, predictive/condition-based, or proactive-based preventive maintenance (Rinaldi et al., 2021). Periodic/cyclic preventive maintenance is a periodically scheduled preventive maintenance operation. This could be the replacement of a specific part every 6 months. Predictive/condition-based maintenance is typically based on the monitoring of components or data. This could be vibration analysis or wear analysis which in turn could identify that a breakdown is about to happen. Proactive/model-driven preventive maintenance could be based on a model that predicts or simulates the process of breakdowns (Rinaldi et al., 2021).
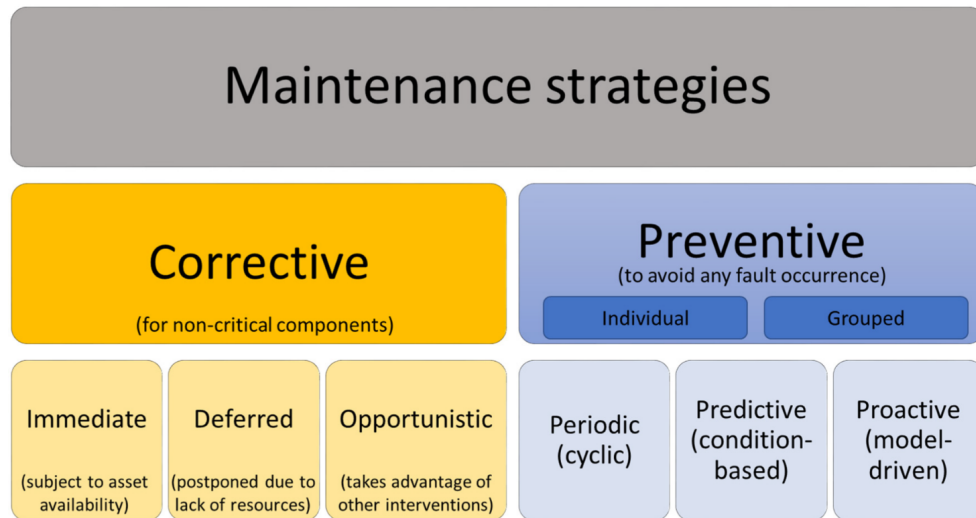
Figure 2.1.: Overview of different maintenance strategies.
Reprinted from "Current Status and Future Trends in the Operation and Maintenance of Offshore Wind Turbines: A Review", by Rinaldi et al. (2021), *Energies*, *14*, 2484

2.1.2. Maintenance planning

The maintenance planning phase is where the optimal scheduling of maintenance tasks is carried out. Maintaining wind farm reliability while minimizing maintenance LCOE is a complex management problem with many uncertainties (Ren et al., 2021). The environment and climate, management, aging, supply chain, electricity price fluctuations, technology advancements, risk analysis, interest rates, political tendencies, and the global market are all time-varying, unpredictable, or partially unpredictable factors. As a result, most maintenance policies and decision-making algorithms are designed to model and maximize short-term benefits, such as ensuring that the maintenance fleet and offshore wind turbines function properly (Ren et al., 2021).

The maintenance planning phase is divided into two parts: maintenance scheduling and route planning. Maintenance scheduling involves organizing maintenance tasks based on factors such as resource availability, potential loss of revenue due to turbine failure, and environmental conditions. On the other hand, route planning involves determining the most efficient route for a vessel to perform all maintenance tasks. Both can be addressed by using optimization models such as mixed integer linear models (Ren et al., 2021).

2.1.3. Onsite maintenance operations

The physical activities required to carry out maintenance are referred to as maintenance operations. These operations are performed after the planning phase, and their difficulty and complexity may vary depending on the type of maintenance required. Generally, maintenance operations can be categorized into two aspects: the actual maintenance procedures and the logistics involved in transporting spare parts and personnel to and from the offshore wind turbine site.
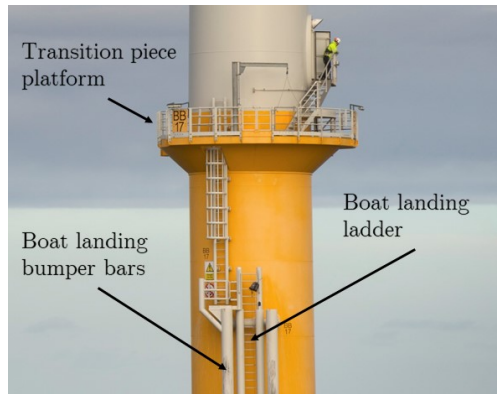
(a) Boat landing and transition piece.
From *Flickr*, by Wind Denmark, 2008.
Licensed under CC BY-NC 2.0 (edited).

(b) Hoisting platform.
From *Flickr*, by Wind Denmark, 2008.
Licensed under CC BY-NC 2.0 (edited)

Figure 2.2.: Offshore wind turbine access methods.

Logistics

To transport personnel and spare parts to an offshore wind turbine undergoing maintenance, three main access methods can be employed (Hu & Yung, 2020). These methods are categorized based on the access points on the offshore wind turbine for maintenance technicians:

- *Boat landing*: The technicians can enter the offshore wind turbine from the boat landing, which is at sea level. Technicians usually have to climb a ladder in order to get from the boat landing to the transition piece platform.

- *Transition piece*: The technicians can be directly transported to the platform on top of the transition piece.

- *Hoisting platform*: Some wind turbines have a dedicated platform on top of the nacelle where maintenance technicians can be dropped off by helicopter.

Various access vessel types or a helicopter can be used to access an offshore wind turbine for maintenance. Weather conditions are an important role in determining whether onsite maintenance operations can proceed safely. For instance, climbing a wind turbine is not permitted when wind speeds exceed 20 m/s (Ren et al., 2021), prohibiting maintenance tasks from being executed. The accessibility to the offshore wind turbine during maintenance operations may vary based on the method of transportation employed. For instance, wave heights exceeding a certain threshold can render it unsafe for the technicians to dock at the offshore wind turbine. These wave height thresholds may differ per type of transportation, as can be seen for a range of different CTVs in table 2.1. Thus, weather forecasts are essential in making informed decisions about maintenance operations.

The characteristics of generic vessel types and helicopters can be found below:

- *Crew Transfer Vessels (CTVs)*: Small vessels that are specifically designed for offshore wind turbine access. They are considered cost-effective and are a relatively fast solution (Hu & Yung, 2020). They can access the boat landing platform and can only stay at the wind farm for one day. A number of different CTV designs and characteristics can be found in table 2.1.

(a) Crew transfer vessel (CTV).
From *Flickr*, by Mark Kilner, 2018. Licensed under CC BY-NC-SA 2.0 (edited).

(b) Service operation vessel (SOV).
From *Wikimedia Commons*, by Saberwyn, 2011. Licensed under CC BY-SA 3.0 (edited)

Figure 2.3.: Figures of two offshore wind O&M vessels.

	Monohull	Catamaran	Trimaran	SWATH	SES
Length [m]	12-25	15-27	19-27	20-34	26-28
Top transit speed [knots]	15-25	18-27	18-22	18-23	35-39
Passenger capacity [-]	12	12	12	12/24	12/24
Cargo [tons]	5-10	10-15	1-5	2-10	3-5
H_s limit [m]	1-1.2	1.2-1.5	1.5-1.7	1.7-2	1.8-2.2

Table 2.1.: Table with the vessel characteristics of some CTV designs.
Reprinted with permission from "Offshore Wind Access Report 2022", by Dighe et al. (2022).
All rights reserved 2022 by TNO.

(a) Offshore helicopter.

From *Flickr*, by Colin Cooke, 2016. Licensed under CC BY-NC-SA 2.0 (edited).

(b) Jack-up vessel.

From *Flickr*, by Norbert Möller, 2018. Licensed under CC BY-NC-SA 2.0 (edited)

Figure 2.4.: Figures of a helicopter and a jack-up vessel.

- *Service Accommodation Transfer Vessels (SATVs)*: Medium-sized vessels designed for wind farms that are further from shore. They have an increased size over CTVs and they can stay at the wind farm for up to one week (Hu & Yung, 2020). Similarly to CTVs, they transfer technicians via the boat landing platform.

- *Service Operation Vessels (SOVs)*: Large vessels that are a step up from SATVs in size. This allows them to stay at wind farms for up to two weeks at a time. They are typically equipped with walk-to-work solutions such as motion-compensated gangways that allow the technicians to walk directly onto the transition piece platform (Hu & Yung, 2020).

- *Helicopters*: Helicopters are a fast way of transport towards and from the turbine and can drop personnel on a dedicated hoisting platform. The amount of weight in spare parts and tools that they can carry is limited and so is the amount of technicians that they can take with them. Since they can not always land and hoovering for long periods of time is not efficient, they generally go back to land, only to come back and pick up the technicians after they are done with the maintenance operations (Hu & Yung, 2020).

In some cases, motion-compensated cranes on SOVs may not be suitable for lifting heavy maintenance equipment due to their limited reach or weight capacity (Hu & Yung, 2020). For instance, lifting wind turbine blades may require heavy lifting capabilities that exceed the capacity of such cranes. In that case, two types of vessels are capable of performing the heavy lifting operations required for maintenance activities involving heavier components such as the gearbox, main shaft, bearing, transformer, and hub (Thomsen, 2014):

- *Crane vessels*: Generic crane vessels are vessels with one or more heavy cranes attached. Their floating platforms differ from ship-shaped hulls to semi-submersible designs (Naji Tahan, 2005).

- *Jack-up vessels*: A type of crane vessel that is more suitable for offshore wind turbine heavy lifting operations than generic crane vessels, as they can be jacked up to operate at the heights of offshore wind turbines (Thomsen, 2014). Additionally, they provide a large deck space for multiple components and are relatively stable (Shenton et al., 2014).

	Model	Algorithm	Objective(s)
Bolstad et al. (2022)	Two-stage SP	Heuristics (GRASP)	Cost
Stålhane et al. (2020)	Two-stage SP	L-shaped	Cost
Stålhane et al. (2019)	Two-stage SP	Matheuristic	Cost
Szpytko and Salgado (2019)	Two-stage SP	Unknown	EENS
Gutierrez-Alcoba et al. (2019)	Two-stage SP	Matheuristics	Cost
Rinaldi et al. (2019)	Sim	Heuristic (GA)	Cost, Reliability, Availability
Diran (2018)	DP	MIP	Cost
Liapodimitris (2017)	Sim	Heuristics (evolutionary)	Cost
Halvorsen-Weare et al. (2017)	Two-stage SP	Heuristics (GRASP, tabu)	Cost
Rinaldi et al. (2017)	Sim	Heuristics (GA)	Cost, Reliability
Stålhane et al. (2016)	Two-stage SP	MIP	Cost
Gundegjerde et al. (2015)	Three-stage SP	MIP	Cost
Dalgic et al. (2015)	Sim	Sim	Cost
Dalgic et al. (2014)	Sim	Sim	Cost
Halvorsen-Weare et al. (2013)	DP	MIP	Cost

Table 2.2.: Overview on offshore wind fleet optimization studies.
(DP = Discrete Programming, EENS = Expected Energy not Supply, GA = Genetic Algorithm, GRASP = Greedy Randomized Adaptive Search Procedure, MIP = Mixed Integer Programming, Sim = Simulation, SP = Stochastic Programming)

Maintenance procedures

Wind turbines are intricate structures comprising numerous components and subsystems that vary among manufacturers. Hence, failure rates and maintenance requirements differ by turbine type, location, and load history. The study by Carroll et al. (2015) evaluated the failure rate distribution of generic components in 350 offshore wind turbines across Europe. The failure rate distribution is available in appendix C, fig. C.1. The study reveals that wind turbine blades and gearboxes are the most commonly replaced components due to major failures, necessitating the use of heavy lifting vessels for replacement. Major and minor repairs are most common in the pitch control/hydraulics of the wind turbine and in the other component categories.

2.2. Review of fleet optimization studies in offshore wind

A relationship between the costs, wind farm availability, and vessel fleet composition had been identified in chapter 1. Numerous studies have been aimed at formulating and solving offshore wind fleet optimization models. A selection of these offshore wind fleet optimization models will be reviewed in the section below. This should give the reader an overview of the various modeling approaches and solution methodologies for these types of models. An overview of these studies in a tabular form can be found in table 2.2.

2.2.1. Offshore wind fleet optimization studies

The studies of Halvorsen-Weare et al. (2013) and Diran (2018) have investigated ways to develop a deterministic fleet optimization model that is solved using Mixed-Integer Programming (MIP). Some of the gaps that were identified in deterministic models were that they did

not capture the highly uncertain nature of processes in offshore wind O&M. The studies of Gundegjerde et al. (2015) and Stålhane et al. (2016) introduced multi-stage stochastic modeling to offshore wind fleet optimization in order to incorporate the uncertainty of parameters into decision-making. Both studies have solved the fleet optimization models using MIP. One conclusion that was drawn was that if the planning aspect of the models would be become more detailed, the model would quickly become too impractical to solve. A number of different multi-stage stochastic programming models were developed and investigated alternative ways to solve the fleet optimization models. The study of Gutierrez-Alcoba et al. (2019) investigated ways to include heuristics for maintenance scheduling. The study of Stålhane et al. (2019) investigated using Dantiz-Wolfe reformulation methods and metaheuristics for fleet optimization models. The studies Stålhane et al. (2020) and Bolstad et al. (2022) attempt to solve an offshore wind O&M fleet optimization model using an L-shaped and a heuristic GRASP method, respectively.

A different approach to the analytical models from the formerly listed studies is by means of simulation. The studies of Dalgic et al. (2014) and Dalgic et al. (2015) include a simulation-based approach to evaluate an optimal CTV fleet selection and to evaluate the effects of a mothership concept for offshore wind O&M, respectively. The studies of Rinaldi et al. (2017) and Rinaldi et al. (2019), by using genetic algorithms to find sets of optimal solutions based upon multiple objective functions from a surrogate O&M simulation model.

The trend that the offshore wind industry is looking to move from a preventive strategy to a condition-based monitoring strategy has been identified and related to offshore wind optimization studies by Stålhane et al. (2019). The only study that includes a predictive maintenance strategy approach in the offshore wind fleet optimization literature so far is the work of Szpytko and Salgado (2019).

It has been found that the optimization models that are used in these fleet optimization studies vary in model formulation. The two most common approaches for modeling offshore wind fleet optimization models were simulation-based models and MIP models. A noticeable amount of the MIP models were multi-stage stochastic optimization models, which are used to account for uncertain occurrences in offshore wind fleet optimization models. Only two studies were identified that included multiple objectives. Both of these studies were solved using genetic algorithms and a simulation-based surrogate model. It was also found that almost all optimization studies included at least the cost as an objective function and no offshore wind fleet optimization studies have included the GHG emissions as (part of) the objective function(s).

A number of gaps in existing literature could be identified. Some of the foremost gaps mentioned in former studies are the inclusion of condition-based monitoring strategies in offshore wind O&M fleet optimization models (Stålhane et al., 2019) and the need to find more efficient methods to solve large instances of fleet optimization models Stålhane et al. (2020). Another gap that had not been identified before was that no offshore wind fleet optimization studies included GHG emissions as their objective function. The introduction chapter in the current study already covered why GHG emissions are recently introduced as an offshore wind KPI, which is why the lack of coverage in fleet optimization models is considered a gap. The second identified gap was that there is a limited amount of offshore wind fleet optimization studies with multiple objectives. None of the multi-objective fleet optimization studies used exact methods to solve the optimization model and they all relied on metaheuristics. While many metaheuristics are known to provide decent solutions within a short amount of time, they are not guaranteed to converge to a true optimal value within a finite amount of time. Exact methods for multi-objective optimization models on the other hand do converge within a finite amount of time.

2.3. Concluding remarks

The first part of this chapter includes a literature review on some of the different aspects of offshore wind O&M and on fleet optimization models for offshore wind O&M. It was found that there is a wide range of frameworks to categorize different offshore wind O&M aspects. The current literature review presents the categorization of different phases within O&M, distinguishing between maintenance strategy, maintenance planning, and onsite maintenance operations. There are two types of maintenance strategies, each with its own set of subcategories. The goal of preventive maintenance is to keep failures from happening, whereas the goal of corrective maintenance is to replace and/or repair failures that have already happened. A number of different offshore wind O&M assets that are used during maintenance were evaluated. They are categorized into personnel access vehicles and heavy-lifting vessels.

The second part of this chapter focussed on answering first research sub-question, which was formulated as:

- **Sub-question 1:** What optimization models exist to find the optimal fleet for offshore wind farm O&M?

A number of fleet optimization studies in the offshore wind were reviewed in order to answer this research sub-question. Simulation-based models and MIP models were commonly used for fleet optimization studies in offshore wind. Only two studies were found that included multiple objectives. Both of these studies used metaheuristics as the methodology to solve the multi-objective model. None of the reviewed studies included GHG emissions as the objective function.

By answering research sub-question 1, two gaps in fleet optimization studies for offshore wind were identified. The first gap is that none of the offshore wind fleet optimization studies include GHG emissions as the objective function. The second gap is that the number of multi-objective optimization studies in offshore wind O&M is scarce and all solving methodologies use metaheuristics.

3. Offshore wind fleet optimization model

The current chapter is divided into two sections. The first section will define the scope of the model. The second section will go over the mathematical formulation of the fleet optimization model. The model in this study is a modified version of the model in Bolstad et al. (2022) and Stålhane et al. (2020).

3.1. Scope of the model

The fleet optimization model of the current study is written as a deterministic MIP problem. The model considers a single wind farm with a fixed number of turbines and a single maintenance base. The main variables of interest in the model are vessel charter decisions based on the costs, time-based wind farm availability, and GHG emissions. The charter decisions fall within tactical-level[1] decision-making (Shafiee, 2015). A corrective-preventive maintenance strategy is used in the model.

Additional operational-level elements of offshore wind O&M are included in the model to ensure that the fleets meet the requirements for operational-level decision-making such as completing all maintenance tasks. Variables like the number of man-hours spent on maintenance tasks, when vessels are used, when maintenance tasks are completed, and whether maintenance tasks are not completed are used to quantify the objective functions and define operational-level constraints. Transit is limited to movement between the wind farm and the maintenance base only and the transit between wind turbines is ignored.

3.1.1. Costs

The costs are commonly used criteria in offshore wind O&M simulations (Sperstad et al., 2017) and fleet optimization models (see table 2.2). It can be concluded by evaluating the simulation and optimization models that there are a number of important aspects in offshore wind O&M cost modeling:

- *Vessel costs*: The costs can be divided into two categories: vessel acquisition costs and fleet ownership costs. The vessels can be acquired by purchasing the vessels or chartering the vessels. Costs associated with fleet ownership may include docking and vessel maintenance.

- *Transit costs*: When vessels are used, they consume fuel. Transit costs are the expenses incurred as a result of using the vessels.

- *Maintenance costs*: The maintenance costs are the costs associated with carrying out the maintenance tasks. This includes the costs of spare parts, tools, and hiring maintenance technicians.

---

[1]Strategic, tactical, and operational-level are adjectives used to categorize decisions or plans based on their scope, time horizon, and focus.

- *Downtime costs*: A wind turbine can stop producing energy for a variety of reasons. It is a decrease in revenue if a wind turbine stops producing energy. A shutdown can occur as a result of the failure of a critical component. The wind turbine can also be shut down for maintenance on non-critical failures.

The vessel costs in the current study are limited to chartering costs only. Vessels can only be chartered from the beginning to the end of a month, and chartering the vessel for longer periods of time may result in a lower monthly cost. Aside from charter costs, the model includes fixed monthly costs to account for a variety of costs associated with owning a vessel fleet. The Transit costs are based on the costs of fuel. Because the prices of different types of marine fuel vary, the option to calculate fuel costs per fuel type has been added. The maintenance costs are calculated per hour that is worked on the maintenance task. If the spare part costs per maintenance operation are known, the costs can be divided by the time required to complete the maintenance task to obtain the spare part costs per hour. It is assumed that maintenance technicians are hired on a daily basis, and crew costs are added each time a vessel is used for transportation on a given day. Downtime costs are based on the number of hours that are being worked on a task for preventive maintenance. Corrective maintenance tasks are assumed to be the result of a critical failure and thus cause downtime from the moment the failure occurs until it is repaired.

3.1.2. Wind farm availability

Wind farm availability can be defined in two ways: time-based wind farm availability and production-based wind farm availability (Wright & Falbe-Hansen, 2017). The production-based wind farm availability is calculated by dividing the energy produced by the energy expected. The time-based wind farm availability can be divided into two subcategories: full-period definition and wind-in-limits definition. The full period definition is calculated by dividing the number of hours available by the number of hours in a year, whereas the wind-in-limits definition is calculated by dividing the number of hours the wind turbine is generating power by the number of hours that the wind is between cut-in and cut-out (Wright & Falbe-Hansen, 2017).

The current study will use the time-based full-period wind farm availability definition. The availability is calculated for the entire wind farm by summing up the number of hours available from all turbines. The number of hours in a year is multiplied by the number of turbines to balance out the nominator and denominator in the time-based full-period wind farm availability definition. The number of hours available for each turbine is calculated by subtracting the number of hours of downtime from the number of hours in a year. This can be expressed in equation form as:

$$\text{Availability}_{\text{full}-\text{period}}^{\text{Time}-\text{Based}} = \frac{\sum_{\text{Turbines}}(\text{HoursPerYear} - \text{TurbineDowntime})}{(\text{NumberOfTurbines})(\text{HoursPerYear})} \tag{3.1}$$

3.1.3. GHG emissions

The emissions of GHGs through human activities are linked to global warming. According to the Kyoto Protocol (Kyoto Protocol, 1997), GHGs are carbon dioxide (CO2), methane (CH4), nitrous oxide (N2O), hydrofluorocarbons (HFCs), perfluorocarbons (PFCs), and sulfur

hexafluoride (SF6). Some gasses have a stronger greenhouse effect than others. GHG emissions are uniformly quantified in terms of CO2 equivalent (CO2e) by multiplying gasses by a respective multiplication factor.

The quantifications of GHG emissions can be done following a range of scopes (Ranganathan et al., 2004). Scope 1 emissions only include emissions from direct sources. Scope 2 also takes into account indirect emissions caused by energy consumption. Scope 3 emissions now add emissions that are caused by the upstream and downstream flow of used services and products (Ranganathan et al., 2004).

Only direct emissions (scope 1) will be modeled in this study. The only direct emissions that fell within scope 1 that could be identified in offshore wind O&M were vessel emissions. The engines of vessels are assumed to be running during transit and while loitering/idling[2]. The amount of fuel used during transit is calculated based on the distance from the maintenance base to the wind farm, the vessel transit speed, and the vessel fuel usage per unit of time. The emissions produced while idling/loitering are proportional to the time spent on maintenance. The emissions are calculated in units of CO2e. Depending on the fuel used, vessels can emit varying amounts of CO2e per liter of fuel. The GHG gasses used to calculate CO2e per liter of fuel are the proportions of CO2, CH4, and N2O produced by fuel combustion.

3.2. Mathematical formulation of the optimization model

The fleet optimization model developed and used by Bolstad et al. (2022) and Stålhane et al. (2020) has been modified to fit the purposes of the current study. There are several reasons why this model was chosen over the other offshore wind O&M fleet optimization models. First and foremost, the scope of their model is similar to the scope set for the model in the current study. Second, the variables used in the models of these two studies are well suited to formulate a GHG emission and time-based wind farm availability objective function.

3.2.1. Notations

Indices

n	Denotes the month number
l	Denotes the month number when a vessel contract expires
p	Denotes the day number
τ	Denotes the turbine number
m	Denotes the maintenance task number
v	Denotes the vessel type number

---

[2]Loitering/idling means that a vessel remains in position for an extended period of time, but still runs an engine or generator to power auxiliary systems.

Sets

N	Set of all months
V	Set of all vessels
L	Denotes until which month a vessel is chartered
M	Set of all maintenance tasks
M^{PREV}	Set of all preventive maintenance tasks
M^{CORR}	Set of all corrective maintenance tasks
T	Set of all wind turbines
P	Set of all days
P_n	Set of all days that belong to month n
A_n	The set of all ancestor months

Coefficients and parameters

C^{TC}_{nvl}	Chartering cost for vessel of type v in month n with expiration in l
C^F_{nv}	Fixed costs of operating vessel of type v in month n
G_v	Capacity that a vessel of type v uses
M^D	Vessel capacity of the base
C^M_{mv}	The costs of using vessel v on maintenance task m per manhour
C^{DTC}_p	Downtime costs per day of a turbine on day p
M^{CREW}_v	Crew size of a vessel type v
$P^{BD}_{m\tau}$	Day on which a breakdown of maintenance type m on turbine τ happens
C^V_v	Costs of using a vessel of type v for transit per hour
T^T_v	Amount of time it takes to travel back and forth to the wind farm with a vessel of type v
C^P_m	Penalty costs of failing to complete the maintenance task m by the end of the planning horizon
$C^{GHG-TRANSIT}_v$	Amount of GHG emissions by using a vessel of type v for traveling per trip to the wind turbine and back
$C^{GHG-IDLE}_v$	Amount of GHG emissions due to idling per hour
$T^M_{m\tau}$	Amount of manhours that maintenance task m requires for turbine τ before it is completed
T^{MAX}	Maximum amount of hours that can be worked on a day

M_v^K	Maximum weather condition that a vessel of type v can operate in
U_{pv}	Weather condition on day p
M^{BIG}	Big-M number used for linearization of cost objective function

Variables

x_{nvl}	Amount of vessels of type v chartered in month n until month l
w_{nv}	Amount of vessels of type v available due to long time chartering in month n
u_{npv}	Amount of vessels of type v used for maintenance in month n on day p
$t_{pmv\tau}$	Amount of manhours that vessels of type v conduct on maintenance task m on turbine τ on day p
$t_{pmv\tau}^{LIN}$	Variable of the amount of manhours that vessels of type v conduct on maintenance task m on turbine τ on day p and is used for linearization
$\gamma_{pm\tau}$	$\begin{cases} 1 & \text{if task } m \text{ on turbine } \tau \text{ is completed on day } p \\ 0 & \text{if task } m \text{ on turbine } \tau \text{ is not completed on day } p \end{cases}$
$\beta_{m\tau}$	$\begin{cases} 1 & \text{if task is not completed by the planning horizon end} \\ 0 & \text{if task is completed by the planning horizon end} \end{cases}$

3.2.2. Objective functions

Cost objective function

$$z^{Cost} = \sum_{n\in N}\sum_{v\in V}\sum_{l\in L} C_{nvl}^{TC} x_{nvl} \tag{3.2a}$$

$$+ \sum_{n\in N}\sum_{v\in V} C_{nv}^{F} w_{nv} \tag{3.2b}$$

$$+ \sum_{p\in P}\sum_{\tau\in T}\sum_{m\in M}\sum_{v\in V} C_{mv}^{M} t_{pmv\tau} \tag{3.2c}$$

$$+ \sum_{p\in P}\sum_{\tau\in T}\sum_{m\in M^{PREV}}\sum_{v\in V} C_{p}^{DTC}\frac{t_{pmv\tau}}{24M_{v}^{CREW}} \tag{3.2d}$$

$$+ \sum_{p\in P}\sum_{\tau\in T}\sum_{m\in M^{CORR}} C_{p}^{DTC}(p - P_{m\tau}^{BD})\gamma_{pm\tau} \tag{3.2e}$$

$$+ \sum_{p\in P}\sum_{\tau\in T}\sum_{m\in M^{CORR}}\sum_{v\in V} C_{p}^{DTC}\frac{t_{pmv\tau}^{LIN}}{24M_{v}^{CREW}} \tag{3.2f}$$

$$+ \sum_{\tau\in T}\sum_{m\in M^{CORR}} C_{p}^{DTC}\beta_{m\tau}(|P| - P_{m\tau}^{BD}) \tag{3.2g}$$

$$+ \sum_{n \in N} \sum_{p \in P_n} \sum_{v \in V} C_v^V u_{npv} T_v^T \tag{3.2h}$$

$$+ \sum_{m \in M} \sum_{\tau \in T} C_m^P \beta_{m\tau} \tag{3.2i}$$

The term in eq. (3.2a) are the charter costs for chartering a vessel of type v from month n until month l. The variable x_{nvl} is defined as the number of vessels of type v that are chartered from month n until month l. In the case that $x_{1,4,2} = 3$, this would indicate that 3 units of vessel type 4 should be chartered from month 1 to month 2, meaning that the vessel is chartered for 2 months in total. The parameter C_{nvl}^{TC} denotes the costs of chartering a vessel of type v from month n until month l. The set N is the set of all months. A set V is defined as the set that includes all vessel types. The set L is the set that indicates until which months vessels can be chartered.

The term in eq. (3.2b) consists of the fixed costs of owning a vessel fleet. The variable w_{nv} denotes the number of vessels of type v in month n. The variable w_{nv} is different from x_{nvl} as the latter denotes the number of contracts and the length of the contracts that are required, while the former denotes the actual fleet size in a certain month as a result of the contract length x_{nvl}. The parameter C_{nv}^F denotes the fixed costs of owning a vessel of type v in month n.

The term in eq. (3.2c) is the costs due to conducting maintenance per man-hour of work. The variable $t_{pmv\tau}$ is the variable that denotes the number of man-hours a vessel of type v conducts on maintenance task m. The parameter C_{mv}^M are the costs of conducting maintenance on task m while using vessel v per man-hour worked on a task.

The term in eq. (3.2d) are the downtime costs due to preventive maintenance. The parameter M_v^{CREW} represents the number of technicians in the crew. The amount of days that the wind turbine is offline due to maintenance on the wind turbine is expressed as the number of man-hours $t_{pmv\tau}$ divided by the amount of crew M_v^{CREW} and by 24 hours. The parameter C_p^{DTC} is a parameter that is equal to the number of costs lost for every 24 hour of wind turbine downtime on a given day p.

The downtime costs due to corrective maintenance tasks on a critical failure can be found in eq. (3.2e), eq. (3.2f) and eq. (3.2g). The variable $\gamma_{pm\tau}$ is a binary variable that is equal to 1 if a maintenance operation m on wind turbine τ is completed on the day p and is equal to 0 if it is not completed on this day. The binary variable $\beta_{m\tau}$ is a binary variable that is equal to 1 if the maintenance task m on wind turbine τ is not completed by the end of the planning horizon and equal to 0 if it is completed somewhere in the planning horizon. The parameter $P_{m\tau}^{BD}$ denotes the day on which the critical failure occurs. The parameter $|P|$ stands for the total amount of days in the planning horizon. In case a maintenance task is completed on the day p, eq. (3.2e) counts the number of days between the occurrence of the breakdown and the repair of the breakdown. This term is only added when the maintenance is completed on that specific day because only then it is multiplied with $\gamma_{pm\tau} = 1$. The number of days between the critical failure and the repair is then multiplied by the costs of downtime C_p^{DTC}. It could be that there is still time that is spent on a maintenance task on the day it is completed. This still causes the wind turbine to be broken down at the first part of the day. This is accounted for by eq. (3.2f), by summing up the number of hours that are being worked on a wind turbine on the day that it is completed. Note that $t_{pmv\tau}^{LIN}$ is a linearization of $t_{pmv\tau}\gamma_{pm\tau}$ using the big-M method, so only the amount of hours that are worked on the day on which the maintenance tasks are completed are nonzero. In the case that a maintenance task is not completed, there are still downtime costs. Therefore, the amount of downtime is formulated

in eq. (3.2g) as a function of the variable $\beta_{m\tau}$ in case the maintenance task is not completed in the planning horizon.

The costs due to using a maintenance vehicle to travel to the wind farm and back and additional penalty costs if maintenance operations are not completed by the end of the month can be found in eq. (3.2h) and eq. (3.2i), respectively. The variable u_{npv} is defined as the number of vessels of type v that are used for transit to the wind farm and back in month n on the day p. The parameter C_v^V denotes the number of costs of using a maintenance vessel at operating speeds per hour, while the parameter T_v^T denotes the amount of time it takes for a vessel of type v for transit to the wind farm and back.

GHG emissions objective function

$$z^{Emissions} = \sum_{n \in N} \sum_{p \in P_n} \sum_{v \in V} C_v^{GHG-TRANSIT} u_{npv} \tag{3.3a}$$

$$+ \sum_{p \in P} \sum_{v \in V} \sum_{m \in M} \sum_{\tau \in T} C_v^{GHG-IDLE} \frac{t_{pmv\tau}}{M_v^{CREW}} \tag{3.3b}$$

The first term in the objective function is the amount of GHG emissions that are emitted by vessels during transit to the wind farm. The parameter $C_v^{GHG-TRANSIT}$ quantifies the amount of GHG emissions that a vessel of type v emits in transit.

The second term in the objective function is the amount of GHG emissions that the vessels emit due to idling. The parameter $C_v^{GHG-IDLE}$ quantifies the amount of GHG emissions that a vessel of type v emits when powering auxiliary systems while the vessel waits until the maintenance task is completed.

Wind farm availability objective function

$$z^{Availability} = 1 - \frac{1}{|P|\,|T|} \left(\sum_{m \in M^{CORR}} \sum_{\tau \in T} \beta_{m\tau}(|P| - P_{m\tau}^{BD}) \right. \tag{3.4a}$$

$$+ \sum_{p \in P} \sum_{\tau \in T} \sum_{m \in M^{CORR}} (p - P_{m\tau}^{BD}) \gamma_{pm\tau} \tag{3.4b}$$

$$+ \sum_{p \in P} \sum_{\tau \in T} \sum_{m \in M^{CORR}} \sum_{v \in V} \frac{t_{pmv\tau}^{LIN}}{24 M_v^{CREW}} \tag{3.4c}$$

$$\left. + \sum_{p \in P} \sum_{\tau \in T} \sum_{m \in M^{PREV}} \sum_{v \in V} \frac{t_{pmv\tau}}{24 M_v^{CREW}} \right) \tag{3.4d}$$

The terms in eq. (3.4a), eq. (3.4b) and eq. (3.4c) represent the total downtime due to corrective maintenance. The second term in eq. (3.4d) is the loss of time-based wind farm availability due to preventive maintenance operations. The first part in eq. (3.4a) is the total amount of availability, represented by 1. The time-based availability function will be divided by the total number of turbines and the total number of days in the planning horizon, $|P|$ and $|T|$ respectively. This will return the time-based wind farm availability over the entire planning horizon, rather than the time-based availability of individual turbines.

3.2.3. Constraints

Vessel balance constraints

The first constraint in eq. (3.5) is a constraint that balances the number of new vessel contracts and expired vessel contracts against the fleet size in each month. It is defined as:

$$\sum_{l \in L} x_{nvl} + w_{a(n)v} - \sum_{n' \in A_n} x_{n'v\,a(n)} = w_{nv} \qquad\qquad \forall n \in N \backslash \{1\}, v \in V, n \leq l \qquad (3.5)$$

This constraint relates the number of vessels of type v in month n that are available to use for maintenance activities, w_{nv}, to the sum of newly chartered vessels in month n until month l, $\sum_{l \in L} x_{nvl}$, plus the number of available vessels from last month, $w_{a(n)v}$, minus the number of vessels of which the contract ended in the previous month, $\sum_{n' \in A_n} x_{n'v\,a(n)}$. The set A_n is the set of all months that lie behind month n. E.g. the set $A_{n=3} = \{1, 2\}$ and the set $A_{n=5} = \{1, 2, 3, 4\}$. Besides the set of all ancestor nodes, $a(n)$ denotes the ancestor node before node n. E.g. if $n = 3$, then $a(3) = 2$ and if $n = 5$, then $a(5) = 4$. This constraint holds for all $n \in N$ with the exception of $n = 1$, because no ancestor nodes exist for the first month. Additionally, the constraint only holds such that $n \leq l$ because a vessel cannot be chartered until a month that lies in history.

The second constraint in eq. (3.6) is similar to the first constraint but is specifically modeled for the first month $n = 1$. It is defined as:

$$\sum_{l \in L} x_{nvl} = w_{nv} \qquad\qquad \forall n = 1, v \in V \qquad (3.6)$$

This constraint sets the number of vessels of type v in month n equal to the number of charter contracts that start in month $n = 1$ until month l.

The third constraint in eq. (3.7) sets a limit to the maximum amount of docking space that is available at the maintenance base. This is defined as:

$$\sum_{v \in V} G_v w_{nv} \leq M^D \qquad\qquad \forall n \in N \qquad (3.7)$$

The term on the left-hand side of the equation in this constraint is the number of vessels of type v that are part of the fleet in month n, multiplied by the size G_v of the vessel. The right-hand side of the equation is the maximum available space of the maintenance base M^D.

The fourth constraint in eq. (3.8) is defined as:

$$u_{npv} \leq w_{nv} \qquad\qquad \forall n \in N, p \in P, v \in V \qquad (3.8)$$

This constraint makes sure that the number of vessels that are used for maintenance, u_{npv}, cannot exceed the number of vessels that are available in the fleet, w_{nv}.

Weather accessibility constraints

The fifth constraint in eq. (3.9) is defined as:

$$(M_v^K - U_{pv}) \sum_{m \in M} \sum_{\tau \in T} t_{pmv\tau} \geq 0 \qquad \forall p \in P, v \in V \qquad (3.9)$$

The constraint makes sure that vessels cannot be used for maintenance if the weather conditions exceed the maximum conditions that the vessel can operate in. The parameter $(M_v^K$ is defined as the weather condition in which a vessel of type v can operate. The parameter U_{pv} denotes the weather condition in month n on day p. Some maintenance vehicles could have different limiting types of weather conditions, e.g. wave height for vessels and wind speed for helicopters. For that reason, U_{pv} could also be a different type of weather condition depending on the vessel type v. The constraint subtracts U_{pv} from M_v^K and is multiplied by the sum of manhours that a spends on a task on a given day. In the case that $M_v^K - U_{pv}$ is smaller than 0, the sum of manhours that a vessel spends working on a task has to be equal to zero in order to not violate the right-hand side condition. This can only occur if the weather value U_{pv} is higher than the maximum weather conditions that a vessel can operate in M_v^K. In the case that $M_v^K - U_{pv}$ is larger than 0, the sum of manhours that a maintenance vehicle works on, is not constrained by the weather.

Maintenance constraints

The sixth constraint in eq. (3.10) is defined as:

$$\sum_{m \in M} \sum_{\tau \in T} t_{pmv\tau} \leq E_v M_v^{CREW}(T^{MAX} - T_v^T) u_{npv} \qquad \forall n \in N, p \in P_n, v \in V \qquad (3.10)$$

This constraint makes sure that if the total amount of man-hours $t_{pmv\tau}$ that is worked on a maintenance task m on vessel τ on day p in month n by vessel v is larger than 0, the right amount of vessels u_{npv} are used for the maintenance operation. Additionally, this constraint sets an upper limit to the amount of time that can be worked on a maintenance task by u_{npv} amount of vessels. This is defined as $T^{MAX} - T_v^T$, which is the maximum amount of operating time minus the time needed to travel to the wind farm and back. An efficiency factor E_v can be set to account for loss of productivity of the crew.

The seventh constraint in eq. (3.11) ensures that maintenance tasks are uncompleted as long as there are not enough man-hours worked on a maintenance task. This is formulated as:

$$\sum_{p \in P} \sum_{v \in V} t_{pmv\tau} \geq T_m^M(1 - \beta_{m\tau}) \qquad \forall m \in M, \tau \in T \qquad (3.11)$$

This constraint makes sure that if not enough time is spent on a maintenance operation, the task will be assigned as uncompleted. The parameter T_m^M is the required amount of manhours needed to complete maintenance task m.

The eighth constraint in eq. (3.12) is defined as:

$$\sum_{p' \in \{(p+1),\dots,|P|\}} \sum_{v \in V} t_{p'mv\tau} \leq T_m^M (1 - \gamma_{pm\tau}) \qquad\qquad \forall p \in P, m \in M, \tau \in T \qquad (3.12)$$

This constraint ensures that once a maintenance task is completed, that no more hours are put into the maintenance operation on the following days after the task is completed. Additionally, it limits the number of hours that are worked on a maintenance task m on the following days p' to be no more than the maximum amount of hours that are required for a maintenance task if it is not completed. In the case that $\gamma_{pm\tau} = 1$, the right-hand side of the equation becomes equal to 0. If the right-hand side of the equation is equal to zero, that means that the left-hand side of the equation has to be less or equal to zero. Since negative worked man-hours $t_{pmv\tau}$ are not possible, the only feasible condition that satisfies this constraint is that the left-hand side sum is equal to 0 as well. Note that the sum of man-hours that are being worked on is summed over $p' \in \{(p+1),\dots,|P|$, which represents the set of remaining days after day p.

The ninth constraint in eq. (3.13) is defined as:

$$\sum_{p \in P} \gamma_{pm\tau} + \beta_{m\tau} = 1 \qquad\qquad \forall m \in M, \tau \in T \qquad (3.13)$$

This constraint ensures that a maintenance task is either completed on a particular day or not completed by the end of the month. This is formulated by summing up the variable which is defined to be equal to 1 if a maintenance task is completed on a particular day p, $\gamma_{pm\tau}$ and adding the binary variable $\beta_{m\tau}$ that is defined to be equal to 1 if the maintenance task is not completed by the end of the year. Since all variables in the constraint are binary variables, only one of the variables on the left-hand side can be equal to 1. Therefore, the maintenance task can only be completed once or can remain uncompleted at the end of the planning horizon.

The tenth constraint in eq. (3.14) is defined as:

$$\sum_{v \in V} \left(\frac{t_{pmv\tau}}{M_v^{CREW}} \right) \leq T^{MAX} \qquad\qquad \forall m \in M, \tau \in T, p \in P \qquad (3.14)$$

This constraint ensures that the maximum amount of hours that all vessels can work on a maintenance task on a given day does not exceed the maximum amount of hours that can be worked on a day. The reason for adding this constraint is to avoid situations where several maintenance vehicles can work on the maintenance task simultaneously and complete it faster, while this might be infeasible. In the constraint, this is expressed on the left-hand side by summing up the number of hours that each vessel of type v works on a task m from turbine τ on day p in month m and dividing this value by the crew size M_v^{CREW}. On the right-hand side, there is the maximum amount of hours that can be worked on maintenance tasks each day.

The eleventh constraint in eq. (3.15) is defined as:

$$(p - P_{m\tau}^{BD}) \sum_{v \in V} t_{pmv\tau} \geq 0 \qquad\qquad \forall p \in P, m \in M^{CORR}, \tau \in T \qquad (3.15)$$

This constraint makes sure that no hours can be worked on a corrective maintenance task if the breakdown of the turbine did not occur yet. This is expressed by subtracting the current day p by the parameter that represents the day that the breakdown occurs $P_{m\tau}^{BD}$ and multiplying this with the number of man-hours that each vessel puts in this task. In the case that the current day is less or equal to the day that the breakdown occur, $p - P_{m\tau}^{BD} \leq 0$, that means that the sum of man-hours that are worked on that task has to be equal to 0 in order to satisfy the right-hand side of the constraint. In other words, the maintenance tasks cannot be worked on. In the case that the current day is larger than the day that the breakdown occurs, the sum of man-hours can take on any positive value or 0, thus the maintenance tasks can be worked on.

Together with eq. (3.12), the twelfth constraint in eq. (3.16) ensures that the binary variable $\gamma_{pm\tau}$ should be equal to 1 once a maintenance task is completed on a specific day p. It is defined as:

$$\sum_{v \in V} t_{pmv\tau} \geq \gamma_{pm\tau} \qquad\qquad \forall p \in P, m \in M, \tau \in T \qquad (3.16)$$

$$(3.17)$$

The constraint in eq. (3.12) on its own is not enough to ensure that $\gamma_{pm\tau} = 1$ only on the day that the last man-hours are worked on a maintenance task. This is because the constraint in eq. (3.12) allows any day p that follows once the last hours have been put into a maintenance task to be set as the day when a maintenance task is completed, even if there are no man-hours worked on the task on these days. It is desired that only the day on which the last man-hours are worked on a maintenance task is labeled as the day when the maintenance task is completed. The constraint in eq. (3.16) now ensures this by summing up the number of hours that are worked by each vessel on a given maintenance task on the left-hand side of the constraint. Additionally, $\gamma_{pm\tau}$ is put on the right-hand side of the constraint. This means that at least 1 man-hour should be worked on the maintenance task before it can be considered completed on this day.

The thirteenth constraint can be used to ensure that some maintenance tasks cannot be started earlier than another maintenance task has been completed. It is formulated as:

$$\sum_{v \in V} \sum_{p' \in \{0,...,p\}} t_{p,m_2,v,\tau} \leq (1 - \gamma_{p,m_1,\tau}) T_{m_2}^M \qquad\qquad \forall p \in P, \tau \in T \qquad (3.18)$$

The maintenance task m_1 denotes the maintenance task number that should be completed before the maintenance task m_2. The variable $\gamma_{p,m_1,\tau} = 1$ if the first maintenance task is completed. If this is the case, the right-hand side of this constraint becomes equal to 0. The remaining left-hand side of the constraint is the number of man-hours that are worked on the second maintenance task from day 0 until day p. The left-hand side and right-hand side together make sure that the number of man-hours that are worked on the second maintenance task m_2 is equal 0 up until m_1 is completed.

Big-M Constraints

Both the cost objective function and the time-based wind farm availability objective function include a formulation for the downtime of the wind turbine. Part of the original formulation

of these two objective functions is nonlinear. The nonlinear part of the objective functions is formulated as:

$$\frac{t_{pmv\tau}}{24M_v^{CREW}}\gamma_{pm\tau} \tag{3.19}$$

The multiplication of $t_{pmv\tau}$ with $\gamma_{pm\tau}$ causes this nonlinearity, even though one is a binary variable and the other is a continuous variable. The big-M method is used to linearize this part of the objective functions, and the proof can be found in appendix B.2. A new variable will be introduced that will substitute $t_{pmv\tau}$ in the objective function which will be labeled as $t_{pmv\tau}^{LIN}$. A large number M^{BIG} is introduced such that $M^{BIG} >> t_{pmv\tau}$. The goal is to define a set of constraints that will make the value of $t_{pmv\tau}^{LIN} = 0$ in the case that $\gamma_{pm\tau} = 0$, as this was also the desired effect of the nonlinear formulation. Additionally, it is desired that $t_{pmv\tau}^{LIN} = t_{pmv\tau}$ in the case that $\gamma_{pm\tau} = 0$ as this was also the desired behavior of the nonlinear formulation. To do this, a constraint will be added that relates $t_{pmv\tau}$ to $t_{pmv\tau}^{LIN}\tau$. This constraint is formulated as:

$$t_{pmv\tau}^{LIN} \geq t_{pmv\tau} - M^{BIG}(1 - \gamma_{pm\tau}) \qquad \forall v \in V, p \in P, m \in M^{CORR}, \tau \in T \tag{3.20}$$

In the case that $\gamma_{pm\tau} = 1$, the term $M^{BIG}(1 - \gamma_{pm\tau})$ on the right hand side of the equation will be 0. This means that the constraint changes in $t_{pmv\tau}^{LIN} \geq t_{pmv\tau}$. In the case that $\gamma_{pm\tau} = 0$, the second term on the right-hand side of the constraint will not become zero. Since the assumption was made that $M^{BIG} >> t_{pmv\tau}$, the entire right-hand side of the equation will be a negative number and the equation changes to $t_{pmv\tau}^{LIN} \approx -M^{BIG}$.

Another constraint will be added and is defined as:

$$t_{pmv\tau}^{LIN} \leq M^{BIG}\gamma_{pm\tau} \qquad \forall v \in V, p \in P, m \in M^{CORR}, \tau \in T \tag{3.21}$$

If the binary variable $\gamma_{pm\tau} = 1$, the constraint changes into $t_{pmv\tau}^{CORR} \leq M$. If the binary variable $\gamma_{pm\tau} = 0$, $t_{pmv\tau}^{CORR} \leq 0$.

One last constraint will be added that once again relates $t_{pmv\tau}^{CORR}$ to $t_{pmv\tau}$:

$$0 \leq t_{pmv\tau}^{LIN} \leq t_{pmv\tau} \qquad \forall v \in V, p \in P, m \in M^{CORR}, \tau \in T \tag{3.22}$$

This sets an low bound to $t_{pmv\tau}^{LIN}$ of 0 and a high bound that is equal to $t_{npmv\tau}$. The proof of the Big-M method can be found in appendix B.2.

Integrality constraints

The last constraints set the maximum limits of the variables x_{nvl} and w_{nv} to integer values only. These constraints are defined as:

$$x_{nvl} \in \mathbb{Z}_{\geq 0} \qquad\qquad \forall n \in N, v \in V, l \in L \qquad (3.23)$$

$$w_{nv} \in \mathbb{Z}_{\geq 0} \qquad\qquad \forall n \in N, v \in V \qquad\qquad (3.24)$$

The last constraints are defined as:

$$t_{pmv\tau} \in \mathbb{R}_{\geq 0} \qquad\qquad \forall p \in P, v \in V, m \in M, \tau \in T \quad (3.25)$$

$$u_{npv} \in \mathbb{Z}_{\geq 0} \qquad\qquad \forall n \in N p \in P, v \in V \qquad\qquad (3.26)$$

$$\gamma_{pm\tau} = \begin{cases} 1 & \text{if task is completed on day } p \\ 0 & \text{if task is not completed on day } p \end{cases} \qquad \forall p \in P, m \in M, \tau \in T \qquad (3.27)$$

$$\beta_{m\tau} = \begin{cases} 1 & \begin{array}{l}\text{if the task is not completed by the} \\ \text{end of the planning horizon}\end{array} \\ 0 & \begin{array}{l}\text{if the task is completed by the end} \\ \text{of the planning horizon}\end{array} \end{cases} \qquad \forall m \in M, \tau \in T \qquad (3.28)$$

These constraints ensure that the amount of manhours that are used to conduct maintenance on a wind turbine $t_{pmv\tau}$ is limited to positive continuous values, that the amount of vessels that are used for maintenance tasks u_{npv} is limited to positive integer values and that the variables which denote that a maintenance task is completed $\gamma_{pm\tau}$ or when a maintenance task is not completed $\beta_{m\tau}$ are both binary variables.

3.3. Concluding remarks

This chapter addressed the scope and mathematical formulation of the offshore O&M fleet optimization model used in the current study. Some of the efforts in this chapter were directed toward answering the second research sub-question, which was phrased as follows:

- **Sub-question 2:** Which (parts of) existing optimization models can be adapted to formulate the fleet optimization model in the current study?

Two fleet optimization studies (Bolstad et al., 2022; Stålhane et al., 2020) with similar fleet optimization models were identified as suitable for modification in the current study. These studies were chosen based on their suitability for quantifying GHG emissions and time-based wind farm availability. In order to formulate the model in the current study, parts of the models from these studies were removed, changed, or added from/to the existing fleet optimization study. The following are some of the key differences and changes between the two models:

1. The current model is formulated as a deterministic model, while the model of Stålhane et al. (2020) and Bolstad et al. (2022) is a multi-stage stochastic model

2. The current model does not have a variable maintenance base, while the model of Stålhane et al. (2020) and Bolstad et al. (2022) does.

3. The current model does not support multiple wind farms, while the model of Stålhane et al. (2020) and Bolstad et al. (2022) does.

4. The current model has introduced the set of all wind turbines T for the variable formulation.

5. The current model has two additional objective functions which quantify the GHG emissions and the time-based wind farm availability.

6. The current model has added constraints to set additional limitations on the maximum amount of man-hours, ensure that no man-hours can be worked on a task with a critical failure before it has occurred, ensure that maintenance tasks are completed on the day that the last man-hour has been worked on the task and ensure that can be used to ensure that on maintenance task cannot be started before another maintenance task is completed in eqs. (3.14) to (3.16) and (3.18), respectively.

7. The current model does not use symmetry-breaking constraints, while the model of Stålhane et al. (2020) does.

8. The current model has a linearized cost objective function formulation that estimates the downtime due to remaining man-hours that are worked on the maintenance tasks with a critical failure.

Some of the efforts in this chapter were directed toward answering the third research sub-question, which was phrased as follows:

- **Sub-question 3:** How can GHG emissions be quantified and incorporated into the multi-objective fleet optimization model?

It was discovered that the scope of GHG emissions quantification can be limited to only direct emissions or can include indirect emissions as well. The current study only quantifies GHG emissions from direct emissions as units of CO2e. The GHG emissions from vessels are calculated both while they are in use for transit and while they are idling/loitering. The fleet optimization model in the current study simplifies transit by ignoring transit between wind turbines and only considering transit between the maintenance base and the wind farm. This means that the time spent in transit between wind turbines is excluded from the GHG calculation.

4. Optimization technique for solving a multi-objective model

In this chapter, a method for optimizing the developed fleet optimization model will be chosen. The chapter will begin with an assessment of some methods for optimizing the fleet optimization model. One of the methods will then be chosen to be used in the current study. First, the method will be applied to a two-objective optimization model. Following that, the method will be applied to a three-objective optimization model.

4.1. Multi-objective optimization methods

Models with multiple objective functions are known as multi-objective optimization models. The methods for solving multi-objective models are classified into two types (Gunantara, 2018). The first method is the scalarization method, which combines multiple objective functions into a single scalar fitness function and yields only one solution. The second method is the Pareto method, which treats the objective functions as independent vectors and yields one or more solutions. The Pareto method has one advantage over the scalarization method in that it shows an overview of the trade-offs between solutions, whereas the scalarization method does not show trade-offs between solutions. Only Pareto methods are considered in the current study because the ability to see tradeoffs between solutions provides more information to work with for decision-making.

In the literature, a wide variety of algorithms and/or techniques for solving multi-objective optimization models have been studied. Three Pareto methods were chosen as candidates to solve the fleet optimization model developed in chapter 3:

- *Genetic methods*: Genetic methods are biological evolution-inspired methods for solving optimization problems. They typically have one or more fitness functions and find solutions through mechanisms such as reproduction, mutation, recombination, and selection. There are many different types of genetic algorithms, such as single-objective and multi-objective genetic algorithms. Multi-objective genetic algorithms can be used to estimate a set of non-dominated solutions on the Pareto front. Genetic algorithms are classified as metaheuristics, which means that there is no guarantee that they will converge in a finite amount of time.

- *Weighted sum method*: The weighted sum method combines multiple objective functions into one objective function. Each individual objective function is multiplied by a respective weight. Solving the models for multiple weight perturbations will yield a set of non-dominated solutions on the Pareto front. The method does not solve the optimization model, but rather modifies the model formulation so that it can be used to find and estimate a set of non-dominated Pareto solutions.

- *Epsilon constraint method*: The epsilon constraint method changes the model formulation by setting some of the objectives as constraints. The model is then solved several times, with the objective functions set as constraints being perturbed with each iteration. Similarly to the weighted sum method, this method does not solve the optimization model directly but modifies the model formulation so that it can be used to find and estimate a set of non-dominated solutions on the Pareto front.

Genetic algorithms are built with inherent mechanisms that allow them to find feasible solutions to optimization models while also approximating a set of non-dominated Pareto optimal solutions. The benefit of this is that they are a complete package for solving multi-objective optimization models and approximating a set of non-dominated Pareto solutions. On the contrary, the epsilon constraint method and the weighted sum method only reformulate the models such that they can be solved using single objective optimization methods. MIP is an option for solving the individual perturbed optimization problems as a result of using the epsilon constraint method and the weighted sum method.

There are also advantages to using the epsilon constraint method or the weighted sum method in combination with MIP. Unlike genetic algorithms, MIP is an exact method. It is guaranteed to converge to a globally optimal solution in a finite amount of time. Furthermore, MIP applications often use the MIP gap to quantify the level of convergence during the solving procedure, whereas genetic algorithms do not have this capability. At last, some of the underlying techniques in MIP are inherently designed to deal with constraints, whereas many genetic algorithms struggle with heavily constrained optimization problems.

The performance of the method depends on the choice of the model. Different genetic algorithms were used during earlier stages of the fleet optimization model development. The fleet optimization model was too heavily constrained for many genetic algorithms to solve efficiently with a good distribution of solutions, which turned out to be a recurring issue throughout multiple iterations of the model development. The epsilon constraint method was then used, and it proved to be more effective at finding feasible solutions to the fleet optimization model in the current study. Because of its ability to deal with constraints consistently, the epsilon constraint method was chosen as the method for solving the optimization model in the current study.

4.2. Epsilon constraint method for two objectives

This section elaborates on the implementation of the epsilon constraint method for two objectives, which serves as an introduction to the epsilon constraint method for three objectives, which is later used to solve the fleet optimization model in this study. In algorithm 4.1, a pseudo-code has been described for calculating the Pareto front for two objective functions. Other algorithms that are called by algorithm 4.1 can be found in algorithm 4.2 and algorithm 4.3. The process of solving the perturbed problems using the epsilon constraint method for two objectives can be found in fig. 4.2.

Let us define an optimization model with variables $x_1, x_2, ...x_n$ and two objective functions $f_1(x_n)$ and $f_2(x_n)$, with the goal of minimizing the objective functions. The problem of solving this optimization model can be expressed as follows:

$$\text{minimize} \quad \{f_1(x_n), f_2(x_n)\} \tag{4.1}$$

a) min(f_1) max(f_1)

b) $f_1 \leq \min(f_1)$

c) $f_1 \leq \min(f_1) + \epsilon_1$

d) $f_1 \leq \min(f_1) + \epsilon_2$

e) $f_1 \leq \min(f_1) + \epsilon_7$

f) $f_1 \leq \min(f_1) + \epsilon_{11}$
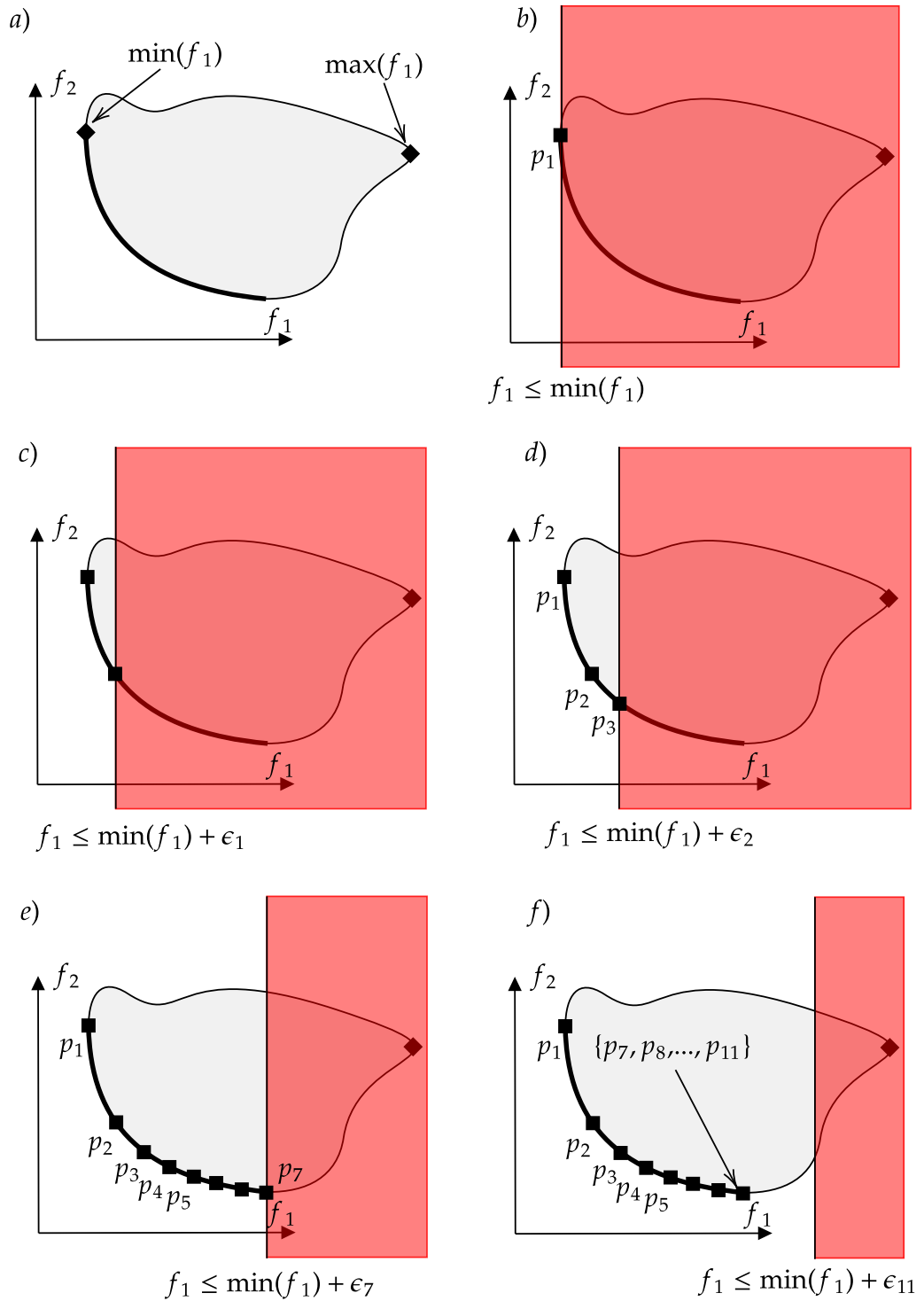
Figure 4.1.: Epsilon constraint method for two objectives.
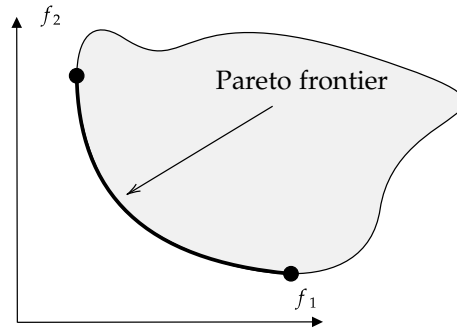
Figure 4.2.: Feasible objective space and Pareto front.
Visual representation of the Pareto front (bold) and the feasible objective space (light grey).

Let us define a set of equality constraints, $h_i(x_n)$, and inequality constraints, $g_j(x_n)$:

$$h_i(x_n) = 0 \qquad\qquad \forall i \in I \qquad\qquad (4.2)$$
$$g_j(x_n) \leq 0 \qquad\qquad \forall j \in J \qquad\qquad (4.3)$$

The objective functions $f_1(x_n)$ and $f_2(x_n)$ are subjected these sets of constraints. By combining them together, the constrained optimization problem can be expressed as follows:

$$\text{minimize} \quad \{f_1(x_n), f_2(x_n)\} \qquad\qquad (4.4)$$

$$h_i(x_n) = 0 \qquad\qquad \forall i \in I \qquad\qquad (4.5)$$
$$g_j(x_n) \leq 0 \qquad\qquad \forall j \in J \qquad\qquad (4.6)$$

The actual Pareto front of the model is depicted in fig. 4.2. The light grey area represents the model's feasible space, and an arrow points to the Pareto frontier, which is represented by a bold black line. Remember that the actual Pareto front is unknown at this point and is only shown to make the steps easier to follow.

Now that the model is defined in eq. (4.4), the maximum value of $f_1(x_n)$ and the minimum value of $f_1(x_n)$ are calculated independently from $f_2(x_n)$. In other words, the model in eq. (4.4) is solved as a minimization and maximization problem without $f_2(x_n)$. This is depicted in fig. 4.1 at step a), where it can be seen that the solutions to both optimization problems are located on the far left and far right ends of the feasible space. The pseudo algorithm that belongs to this step is algorithm 4.2. We now have an upper and lower bound for all feasible solutions $f_1(x_n)$.

The next step is to change $f_1(x_n)$ from an objective function to the left-hand side of an "$\leq$" constraint. The right-hand side of this constraint will be a constant C_1. The updated problem can now be expressed as:

$$\text{minimize} \quad \{f_1(x_n)\} \tag{4.7}$$

$$h_i(x_n) = 0 \qquad\qquad\qquad\qquad\qquad \forall i \in I \tag{4.8}$$
$$g_j(x_n) \leq 0 \qquad\qquad\qquad\qquad\qquad \forall j \in J \tag{4.9}$$
$$f_1(x_n) \leq C_1 \tag{4.10}$$

The problem in eq. (4.7) is now solved multiple times for perturbed C_1 values. Let us start with setting C_1 equal to the lower bound of $f_1(x_n)$ which was found earlier:

$$C_1 = min(f_1) \tag{4.11}$$

Solving the optimization problem in eq. (4.7) with this value of C_1 is depicted in fig. 4.1 at step b). It can be observed that all but the most left part of the feasible space is removed by eq. (4.10). The Pareto optimal solution that belongs to the perturbed problem that was solved is now referred to as p_1.

Let us perturb the value of C_1 by adding a value ϵ_1 to it. The new value for C_1 is now defined as:

$$C_1 = min(f_1) + \epsilon_1 \tag{4.12}$$

Solving the optimization problem in eq. (4.7) with this perturbed value of C_1 is depicted in fig. 4.1 at step c). When compared to step b), step c) now leaves a larger portion of the original feasible space feasible. By solving this perturbed problem, the solution will lie in the feasible space at the lowest possible value for $f_2(x_n)$ in step c), and it can be seen that this solution lies on the Pareto front. The Pareto optimal solution that belongs to the perturbed problem that was solved is now referred to as p_2.

This process can be repeated for multiple perturbations of C_1. This is depicted in fig. 4.1 in steps d), e), and f). By looking at fig. 4.1, it becomes clear why the minimum and maximum values for $f_1(x_n)$ were calculated. If C_1 is set too small, the model could become infeasible. If the perturbed values for C_1 are set too high, there is a risk of missing solutions in the far left region of the feasible space. If the minimum and maximum values of $f_1(x_n)$ are known, they can be used as upper and lower bounds for perturbed C_1 values.

Note that once a perturbation of C_1 reveals the global minimum of the problem, perturbations of C_1 with larger values do not lead to new solutions on the Pareto front. This can be seen in fig. 4.1 in step f), where an arrow is used to indicate the location in the feasible regions where solutions $\{p_7, p_8, ..., p_{11},\}$ are the same. On the one hand, it is desirable that these solutions are located in the same location in the feasible space and not further to the right. If not, they would not lie on the Pareto front. On the other hand, each point requires an optimization model to be solved and since these stacked points lie on the same spot, they do not give any additional information on the shape of the Pareto front. This makes them of little use and requires unnecessary computational power.

Algorithm 4.1: EPSILON CONSTRAINT METHOD TWO OBJECTIVE ($NumberOfShifts$)

Input: $NumberOfShifts \leftarrow$ number of times the constraint it shifted between
        $MinBound, MaxBound$
Output: $p_i \leftarrow$ Pareto points

1 MinBound = BOUNDS TWO OBJECTIVE ($f_1(x), Optimize =' min'$);
2 MaxBound = BOUNDS TWO OBJECTIVE ($f_1(x), Optimize =' max'$);
3 **for** $i \leftarrow 0$ **to** $NumberOfShifts$ **do**
4 $\quad$ $\epsilon = i/NumberOfShifts$;
5 $\quad$ p_i = FIND PARETO POINT ($f_2(x), f_1(x), \epsilon, MinBound, MaxBound$);
   $\quad$ // p_i contains the Pareto point locations $[f_1(x^{Optim}), \min(f_2)]$

Algorithm 4.2: BOUNDS TWO OBJECTIVE ($f_1(x_n), Optimize$)

Input: $f_1(x_n) \leftarrow$ objective function
$Optimize \leftarrow$ variable that states if the model should be optimized or minimized
Output: $\min(f_1)$ and $\max(f_1)$

1 **if** $Optimize = 'min'$ **then**
2 $\quad$ RunMIPSolver($f_1(x_n)$, minimize);
3 $\quad$ **return** $\min(f_1)$
4 **if** $Optimize = 'max'$ **then**
5 $\quad$ RunMIPSolver($f_1(x_n)$, maximize);
6 $\quad$ **return** $\max(f_1)$

Algorithm 4.3: FIND PARETO POINT TWO OBJECTIVE] ($f_2(x_n), f_1(x_n), \epsilon, MinBound,$
$MaxBound$)

Input: $f_2(x_n) \leftarrow$ objective function to be solved
$f_1(x_n) \leftarrow$ objective function to be set as constraint
$[MinBound, MaxBound] \leftarrow$ bounds over which to shift the constraint over
$\epsilon \leftarrow$ constraint shift size coefficient
Output: $\min(f_2) \leftarrow$ the optimal objective values
$x_n^{Optim} \leftarrow$ the variables that belong to this optimal value
$f_1(x_n^{Optim}) \leftarrow$ the corresponding value for the first objective function

1 AddConstraint($f_1(x_n) \leq MinBound + \epsilon(MaxBound - MinBound)$);
2 RunMIPSolver($f_2(x_n)$, minimize);
3 **return** $x_n^{Optim}, \min(f_2), f_1(x_n^{Optim})$
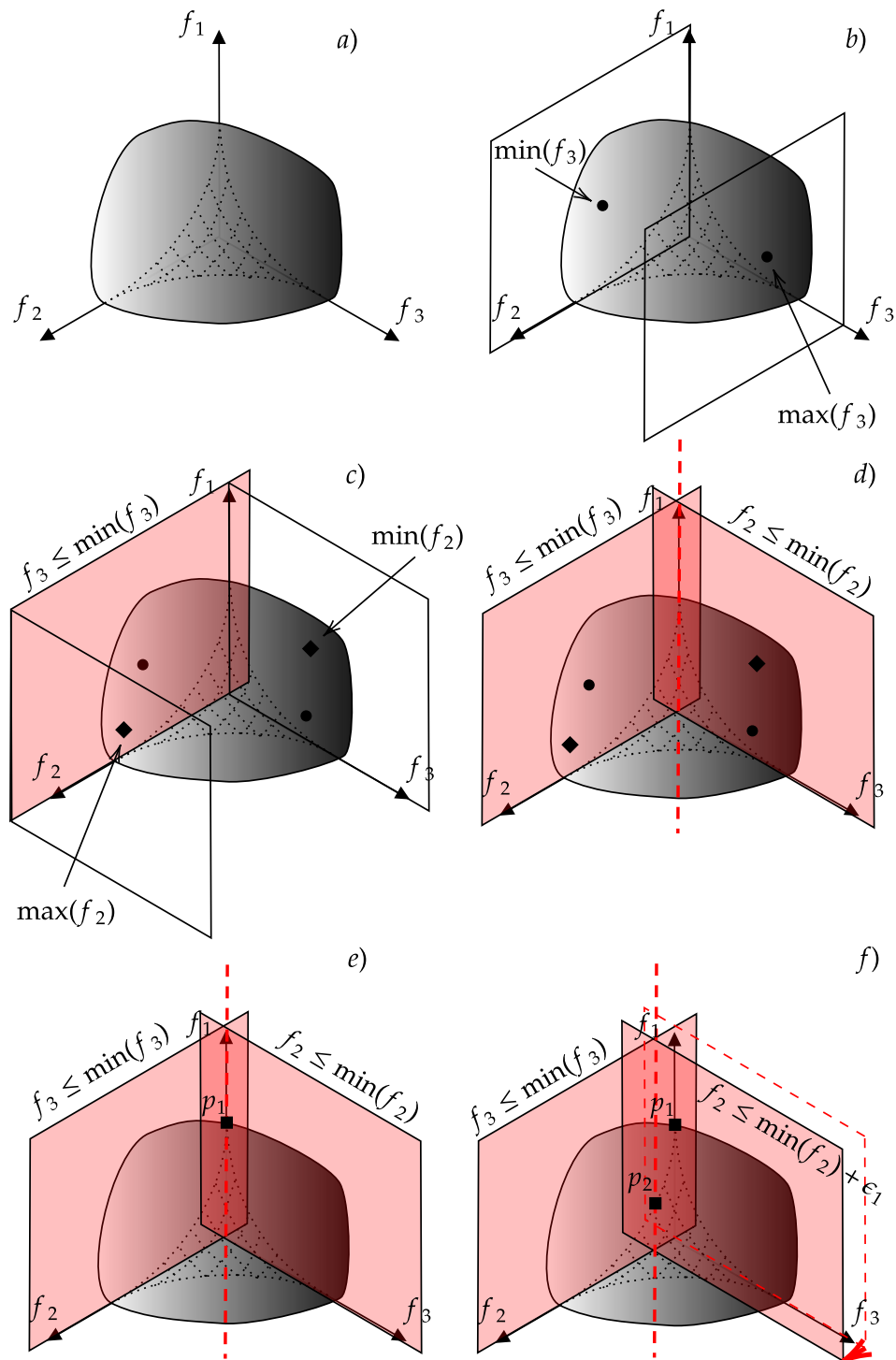
Figure 4.3.: Epsilon constraint method for three objectives (part 1).
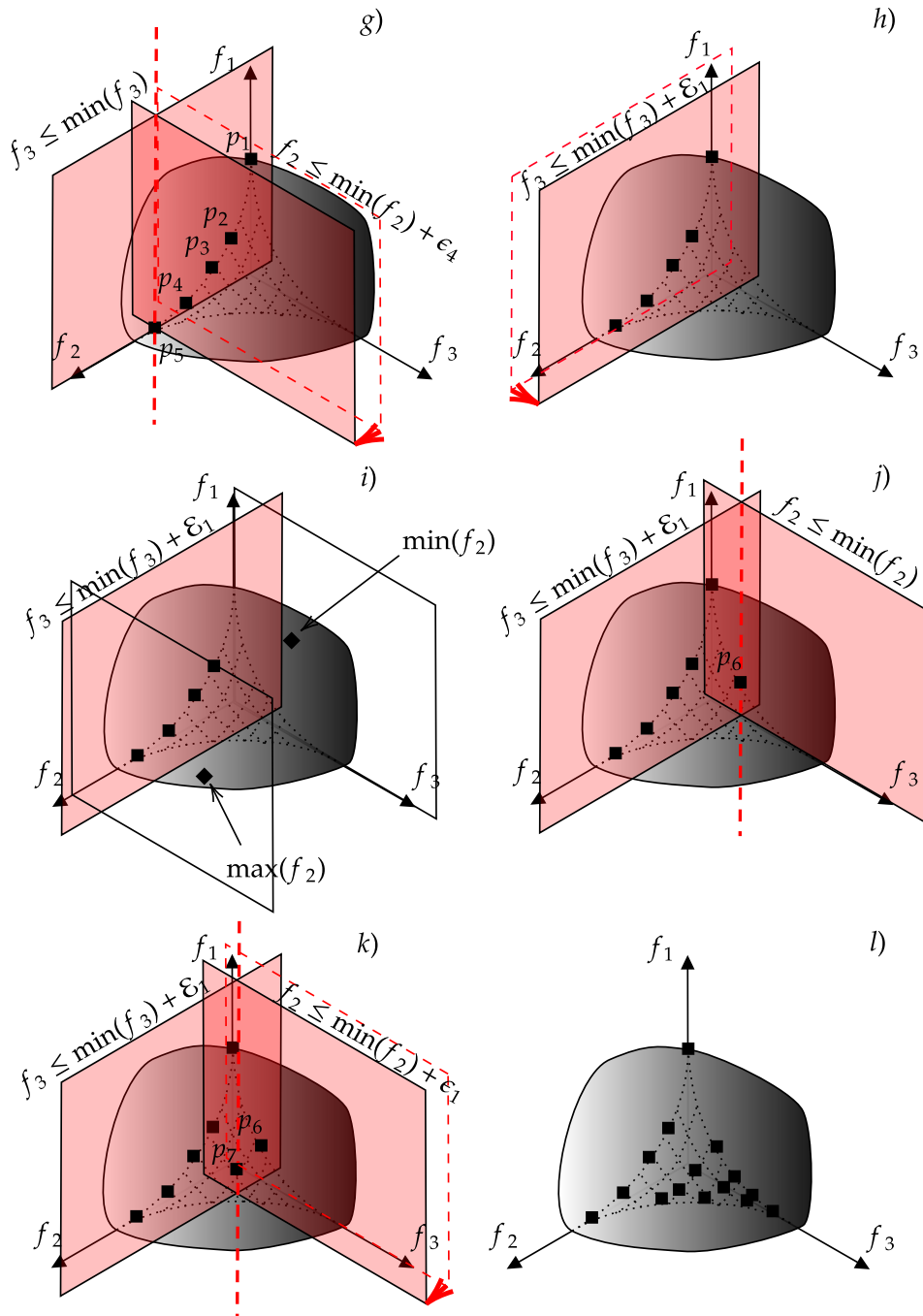
Figure 4.4.: Epsilon constraint method for three objectives (part 2).

4.3. Epsilon constraint method for three objectives

After discussing the epsilon constraint method implementation for two objectives in the previous section, the current section will discuss the epsilon constraint method implementation for three objectives. A pseudo-code for calculating the Pareto front for three objective functions is described in algorithm 4.4. Other algorithms that are used in algorithm 4.1 can be found in algorithm 4.5 and algorithm 4.6.

Let us define a minimization optimization problem with three objective functions $f_1(x_n)$, $f_2(x_n)$, and $f_3(x_n)$ which are subjected to a set of equality constraints, $h_i(x_n)$, and inequality constraints, $g_j(x_n)$:

$$\text{minimize}\{f_1(x_n), f_2(x_n), f_3(x_n)\} \tag{4.13}$$

$$h_i(x_n) = 0 \qquad\qquad\qquad\qquad \forall i \in I \tag{4.14}$$
$$g_j(x_n) \leq 0 \qquad\qquad\qquad\qquad \forall j \in J \tag{4.15}$$

It was observed in fig. 4.1 that the feasible region for a two-objective optimization problem can be plotted in two-dimensional objective space. Analogous to this, the feasible space for a three-objective optimization problem can be plotted in three-dimensional objective space. The feasible space for three objectives is depicted as a three-dimensional space in fig. 4.3. The Pareto front for three objectives can now be represented as a surface rather than a line, which is depicted using grid lines in fig. 4.3 at step a). As with the two-objective variant, the actual Pareto front is unknown beforehand and is only shown to make the steps easier to follow.

The maximum and minimum of the objective function $f_3(x_n)$ are calculated first as shown in fig. 4.3 at step b). The pseudo algorithm that corresponds to this process is algorithm 4.5 and is depicted in fig. 4.3 in b). This is equal to solving the following optimization problems:

$$\text{minimize}\{f_3(x_n)\} \tag{4.16}$$
$$\text{maximize}\{f_3(x_n)\} \tag{4.17}$$

$$h_i(x_n) = 0 \qquad\qquad\qquad\qquad \forall i \in I \tag{4.18}$$
$$g_j(x_n) \leq 0 \qquad\qquad\qquad\qquad \forall j \in J \tag{4.19}$$

Similarly, the maximum and minimum of the objective function $f_2(x_n)$ are calculated. However, this time an inequality constraint is added with $f_3(x_n)$ on the left-hand-side of the equation and the parameter C_3 on the right-hand-side of the equation. This is depicted in fig. 4.3 in c) equal to solving the following optimization problems:

$$\text{minimize}\{f_2(x_n)\} \tag{4.20}$$
$$\text{maximize}\{f_2(x_n)\} \tag{4.21}$$

$$h_i(x_n) = 0 \qquad\qquad\qquad\qquad \forall i \in I \tag{4.22}$$
$$g_j(x_n) \leq 0 \qquad\qquad\qquad\qquad \forall j \in J \tag{4.23}$$
$$f_3(x_n) \leq C_3 \tag{4.24}$$

Remember that setting an objective function as an inequality constraint in a two-objective space can be visualized as a line parallel to the objective direction in the objective space and an infeasible surface on either side. In a three-objective space, this line becomes a plane that is parallel to the objective direction in the objective space instead and the infeasible surface on either side now becomes an infeasible volume, as can be observed in fig. 4.3 and fig. 4.4.

Reflection

Let us reflect back on what has been done so far, and compare it to the steps made for the epsilon constraint method for two objectives.

- A minimization problem was defined with three objectives.

- Four problems were then solved, which were the minimum and maximum values for $f_3(x_n)$ and $f_2(x_n)$. These values will serve the same purpose as the minimum and maximum values for $f_2(x_n)$ in the epsilon constraint method for two objectives: to set minimum and maximum bounds for the perturbations.

One particular detail that is different from the two-objective method is that an objective function is already set as constraints while calculating the minimum and maximum bounds for the perturbations in eq. (4.24). This is because the minimum and maximum values of $f_2(x_n)$ can vary for different perturbations of C_3, analogous to how the width of a shape can vary over its length.

The objective functions $f_2(x_n)$ and $f_3(x_n)$ are then changed to left-hand-side constraints in problem eq. (4.13). The parameter C_3 is introduced on the right-hand side of $f_3(x_n)$, and the parameter C_2 is introduced on the left-hand side of $f_2(x_n)$. These modifications result in the following new formulation:

$$\text{minimize}\{f_1(x_n)\} \tag{4.25}$$

$$h_i(x_n) = 0 \qquad\qquad \forall i \in I \tag{4.26}$$
$$g_j(x_n) \leq 0 \qquad\qquad \forall j \in J \tag{4.27}$$
$$f_3(x_n) \leq C_3 \tag{4.28}$$
$$f_2(x_n) \leq C_2 \tag{4.29}$$

Let us select the lower bounds of the objective functions as the initial values for C_3 and C_2, which are $\min(f_3)$ and $\min(f_2)$, respectively.

$$C_2 = \min(f_2) \tag{4.30}$$
$$C_3 = \min(f_3) \tag{4.31}$$

This is shown in fig. 4.3 at step d), where the constraints remove a large portion of the feasible space. Solving this problem will yield the solution with the lowest value of $f_1(x_n)$ in

the feasible region. This solution is labeled as p_1 in fig. 4.3 at step e). The problem is now solved again by perturbing C_2 while leaving C_3 unchanged. This will achieved by adding a perturbation ϵ_1 to $\min(f_2)$, such that:

$$C_2 = \min(f_2) + \epsilon_1 \tag{4.32}$$
$$C_3 = \min(f_3) \tag{4.33}$$

The solution p_2 is obtained by solving the model with these updated perturbations. The solution p_2 has the lowest $f_1(x_n)$ value in the feasible region, as shown in fig. 4.3 at step f). The process of solving the model for various perturbations of C_2 while maintaining C_3 constant can be repeated several times. This is shown in fig. 4.4 at step g).

The value of C_3 will be perturbed after solving the model several times for different perturbations of C_2. This will be accomplished by adding a perturbation $\mathcal{E}_1$ to C_3, as shown in fig. 4.4 at step h). For each perturbation of C_3, new minimum and maximum bounds for $f_2(x_n)$ must be calculated, implying that eq. (4.20) and eq. (4.21) must be solved again. The updated upper and lower bounds of C_2 are shown in fig. 4.4 at step i). Once these new bounds are determined, the process of solving the model with $f_1(x_n)$ as the objective function and various perturbations for C_2 repeats. The process of finding new solutions for other perturbations of C_2 is depicted in fig. 4.4 at steps j) and k). After solving the model for sufficient perturbations of C_2 and C_3, a set of solutions on the Pareto front is obtained, as shown in fig. 4.4 at step l).

Algorithm 4.4: EPSILON CONSTRAINT METHOD THREE OBJECTIVE ($NumberOfShiftsF2$, $NumberOfShiftsF3$)

Input: $NumberOfShiftsF2 \leftarrow$ number of times the constraint it shifted between $MinBoundF2$, $MaxBoundF2$
$NumberOfShiftsF3 \leftarrow$ number of times the constraint it shifted between $MinBoundF3$, $MaxBoundF3$
Output: Pareto points p_i

1 MinBoundF3 = BOUNDS THREE OBJECTIVE ($f_3(x)$, $Optimize =' min'$);
2 MaxBoundF3 = BOUNDS THREE OBJECTIVE ($f_3(x)$, $Optimize =' max'$);
3 **for** $i \leftarrow 0$ **to** $NumberOfShiftsF3$ **do**
4 $\quad$ $\mathcal{E} = i/NumberOfShiftsF3$;
5 $\quad$ MinBoundF2 = BOUNDS THREE OBJECTIVE ($f_2(x)$, $Optimize =' min'$);
6 $\quad$ MaxBoundF2 = BOUNDS THREE OBJECTIVE ($f_2(x)$, $Optimize =' max'$);
7 $\quad$ **for** $i \leftarrow 0$ **to** $NumberOfShiftsF3$ **do**
8 $\quad\quad$ $\epsilon = i/NumberOfShiftsF3$;
9 $\quad\quad$ FIND PARETO POINT THREE OBJECTIVE ($f_1(x_n)$, $f_2(x_n)$, $f_3(x_n)$,
$\quad\quad$ $[MinBoundF2, MaxBoundF2]$, ϵ, $[MinBoundF3, MaxBoundF3]$, $\mathcal{E}$);
$\quad\quad$ // p_i contains the Pareto point locations $[f_1(x^{Optim}), \min(f_2)]$

4.4. Improving the selection of C_2 and C_3

The minimum and maximum bounds for C_2 and C_3 perturbations in section 4.3 ensure that the constraints set during each optimization model evaluation iterate over the entire feasible

---

Algorithm 4.5: BOUNDS THREE OBJECTIVE ($f(x_n)$, *Optimize*)

Input: $f(x_n) \leftarrow$ objective function
Optimize $\leftarrow$ variable that states if the model should be optimized or minimized
Output: $\min(f_1)$ and $\max(f_1)$

1 **if** $f(x_n) = f_2(x)$ **then**
2   **if** *Optimize* $= 'min'$ **then**
3   AddConstraint($f_3(x_n) \leq MinBound + \mathcal{E}(MaxBound - MinBound)$);
4   RunMIPSolver($f_2(x_n)$, minimize);
5   **return** $\min(f_2)$
6   **if** *Optimize* $= 'max'$ **then**
7   AddConstraint($f_3(x_n) \leq MinBoundF3 + \mathcal{E}(MaxBoundF3 - MinBoundF3)$);
8   RunMIPSolver($f_2(x_n)$, maximize);
9   **return** $\max(f_2)$
10 **if** $f(x_n) = f_3(x)$ **then**
11   **if** *Optimize* $= 'min'$ **then**
12   RunMIPSolver($f_3(x_n)$, minimize);
13   **return** $\min(f_3)$
14   **if** *Optimize* $= 'max'$ **then**
15   RunMIPSolver($f_3(x_n)$, maximize);
16   **return** $\max(f_3)$

Algorithm 4.6: FIND PARETO POINT THREE OBJECTIVE ($f_1(x_n)$, $f_2(x_n)$, $f_3(x_n)$, $[MinBoundF2, MaxBoundF2]$, ϵ, $[MinBoundF3, MaxBoundF3]$, $\mathcal{E}$)

Input: $f_1(x_n) \leftarrow$ objective function to be solved
$f_2(x_n) \leftarrow$ objective function to be set as constraint
$f_3(x_n) \leftarrow$ objective function to be set as constraint
$[MinBoundF2, MaxBoundF2] \leftarrow$ bounds over which to shift the constraint over
$\epsilon \leftarrow$ constraint shift size coefficient
$[MinBoundF3, MaxBoundF3] \leftarrow$ bounds over which to shift the constraint over
$\mathcal{E} \leftarrow$ constraint shift size coefficient
Output: $\min(f_1) \leftarrow$ the optimal objective values
$x_n^{Optim} \leftarrow$ the variables that belong to this optimal value
$f_2(x_n^{Optim}) \leftarrow$ the corresponding value for the second objective function
$f_3(x_n^{Optim}) \leftarrow$ the corresponding value for the third objective function

1 AddConstraint($f_3(x_n) \leq MinBoundF3 + \mathcal{E}(MaxBoundF3 - MinBoundF3)$);
2 AddConstraint($f_2(x_n) \leq MinBoundF2 + \epsilon(MaxBoundF2 - MinBoundF2)$);
3 RunMIPSolver($f_1(x_n)$, minimize);
4 **return** $x_n^{Optim}, \min(f_1), f_2(x_n^{Optim}), f_3(x_n^{Optim})$

region of the solution space. However, the disadvantage of this method is that some solutions may accumulate in the same location in the feasible region. A visualization of the accumulated points for the two objective epsilon constraint methods can be found in fig. 4.1, where the points $p_7, p_8, ..., p_{11}$ all share the same combination of values for f_1 and f_2. The accumulated solutions require a model to be solved, but they do not provide a new Pareto optimal solution with unique corresponding objective values.

To reduce computational expenses, each Pareto point should ideally have objective function values that differ from other solutions. Simultaneously, the range over which the Pareto points are calculated should ideally still cover the entire Pareto front. One way to satisfy these requirements is to set the point in the objective space where all Pareto points stack in fig. 4.1 as the maximum bound because every solution beyond this point is not a Pareto optimal solution. It can be seen in fig. 4.1 for two objectives that this point can be found by finding by removing $f_1(x_n)$ from the model and finding $\min(f_2(x_n))$ because it lies at the minimum value of $f_2(x_n)$. The variables that belong to the solution of $\min(f_2(x_n))$ can then be used to find the corresponding objective function value for f_1. This value of f_1 is then set as the new maximum bound for $f_1(x_n)$, as this is the location in fig. 4.1 where all the Pareto optimal solutions accumulate. By employing this new upper bound, all perturbations of C_1 are now on the Pareto front.

The point that we are looking for by minimizing the model for $f_2(x_n)$ is known as one of the anchor points. The Nadir point, which is defined as the combination of the worst possible values for each objective in the set of all non-dominated Pareto optimal solutions, is a more generalized feature of the model we are looking for (Mesquita-Cunha et al., 2022). For models with more than two objective functions, the Nadir point can be found using the anchor points. For models with more than two objective functions, anchor points can no longer be used to find the exact Nadir point and can only be used as an estimate (Deb & Miettinen, 2009; Isermann & Steuer, 1988). Algorithms have been developed to determine the exact Nadir point (Jorge, 2009), but combining this with the epsilon constraint method can significantly complicate the algorithm (Nikas et al., 2022). The current study will not incorporate an exact method to find the Nadir point and instead use a similar approach to payoff tables made up of anchor points from Mavrotas and Florios (2013). This keeps the implementation of the epsilon constraint method relatively simple, but it can lead to underestimation of upper bounds.

The following changes are made to find the bounds for C_2 and C_3 in section 4.3. First, the upper and lower bounds for $f_3(x_n)$ are determined. The method for determining the lower bound remains unchanged, and it is determined by solving the model and minimizing $f_3(x_n)$ independently of the other objective functions. The problem that has to be solved is formulated as:

$$\text{minimize}\{f_3(x_n)\} \tag{4.34}$$

$$h_i(x_n) = 0 \qquad\qquad\qquad \forall i \in I \tag{4.35}$$
$$g_j(x_n) \leq 0 \qquad\qquad\qquad \forall j \in J \tag{4.36}$$

Finding the upper bound is now slightly different, as the model is solved twice now. The first time it is solved for $f_1(x_n)$, independently of the other objective functions, and the second time it is solved for $f_2(x_n)$, independently of the other objective functions. The highest value of f_3 from both solutions is then set as the upper bound for $f_3(x_n)$. This is formulated as solving the problems:

$$\text{minimize}\{f_1(x_n)\} \tag{4.37}$$
$$\text{minimize}\{f_2(x_n)\} \tag{4.38}$$

$$h_i(x_n) = 0 \qquad\qquad\qquad \forall i \in I \tag{4.39}$$
$$g_j(x_n) \leq 0 \qquad\qquad\qquad \forall j \in J \tag{4.40}$$

A similar process follows for the bounds of C_2. The upper and lower bounds for C_2 must be found for every perturbation of C_3, just as in algorithm 4.4. Finding the lower bound of C_2 is obtained by solving the model for $f_2(x_n)$.

$$\text{minimize}\{f_2(x_n)\} \tag{4.41}$$

$$h_i(x_n) = 0 \qquad\qquad\qquad \forall i \in I \tag{4.42}$$
$$g_j(x_n) \leq 0 \qquad\qquad\qquad \forall j \in J \tag{4.43}$$
$$f_3(x_n) \leq C_3 \tag{4.44}$$

Since an equality constraint for $f_3(x_n)$ is added to the model while finding the bounds for C_2, the value of $f_3(x_n)$ is fixed. To find the upper bound of C_2, only the minimum of $f_1(x_n)$ now has to be found and the value of f_3 that belongs to this solution is extracted.

$$\text{minimize}\{f_1(x_n)\} \tag{4.45}$$

$$h_i(x_n) = 0 \qquad\qquad\qquad \forall i \in I \tag{4.46}$$
$$g_j(x_n) \leq 0 \qquad\qquad\qquad \forall j \in J \tag{4.47}$$
$$f_3(x_n) \leq C_3 \tag{4.48}$$

The current method that is used to improve the selection of C_2 and C_3 is similar to the payoff table method as both approaches use anchor points to estimate the upper bounds. The current method calculates the bounds for C_2 for each perturbation of C_3. The advantage is that it ensures that the combinations of C_2 and C_3 are within the feasible space, thus not leading to infeasible models. The disadvantage of this is that it requires two additional problems to be solved to find the upper and lower bounds of C_2 for each perturbation of C_3. Although the epsilon constraint method in the current model is solved with an exact solving method by using MIP, this is not sufficient to guarantee that all solutions are non-dominated (Mavrotas, 2009).

4.5. Parallelization of the problems

A part of the epsilon constraint method can be solved in parallel after finding the bounds of C_3. This can be done by making blocks of problems that have to be solved. The first part of each block consists of determining the bounds of C_2 that belong to a respective perturbation of

C_3, after which the perturbations of C_2 are determined. The second part of each block consists of solving the combinations of C_2 and C_3 that will estimate the Pareto optimal solutions.

A process flow diagram of the epsilon constraint method for three objective functions can be found in fig. 4.5. The perturbations of C_2 and C_3 are indicated with indices j and i, respectively. Since new perturbations of C_2 are determined for every perturbation of C_3, it has both indices i and j. A verification of the epsilon constraint method against a genetic algorithm can be found in appendix B.3.

4.6. Concluding remarks

The purpose of this chapter was to provide an answer to the fourth research question, which was defined as:

- **Sub-question 4:** Which algorithms can be used to find optimal solutions to the developed multi-objective fleet optimization model?

In order to answer this research question, a number of multi-objective algorithms and reformulation methods were evaluated and considered as candidates to solve the fleet optimization model in the current study. The three candidates were genetic algorithms, the weighted sum method, and the epsilon constraint method. Several attempts were made to solve early adaptations of the fleet optimization model using various genetic algorithms, but they were unsuccessful. This was likely a result of the heavy constraint characteristic of the fleet optimization model, which genetic algorithms are known to have issues with. This was most likely due to the heavily constrained characteristic of the fleet optimization model, which genetic algorithms are known to struggle with.

The epsilon constraint method was deemed superior to the weighted sum method because the former can capture convex hulls in the Pareto front while the latter cannot. It was found that the epsilon constraint method could be used in combination with MIP. Unlike genetic algorithms, MIP is an exact method. Early adaptions of the fleet optimization model were more successfully solved using MIP in combination with the epsilon constraint method than genetic algorithms. This led to the consideration that the epsilon constraint method in combination with MIP is the most suitable approach for the fleet optimization model in the current study.

Despite the fact that it is chosen as the most optimal approach, the epsilon constraint method implementation in the current study has some known limitations:

- Despite the fact that it is used in combination with an exact MIP solver, this does not guarantee that the epsilon constraint method is found exactly. This is because it is not guaranteed that all solutions are non-dominated Pareto solutions.

- Since the bounds over which the perturbations are selected are calculated using an approach that is analogous to approximating the Nadir point, it is not guaranteed that the epsilon constraint method iterates over the full range of the Pareto front.
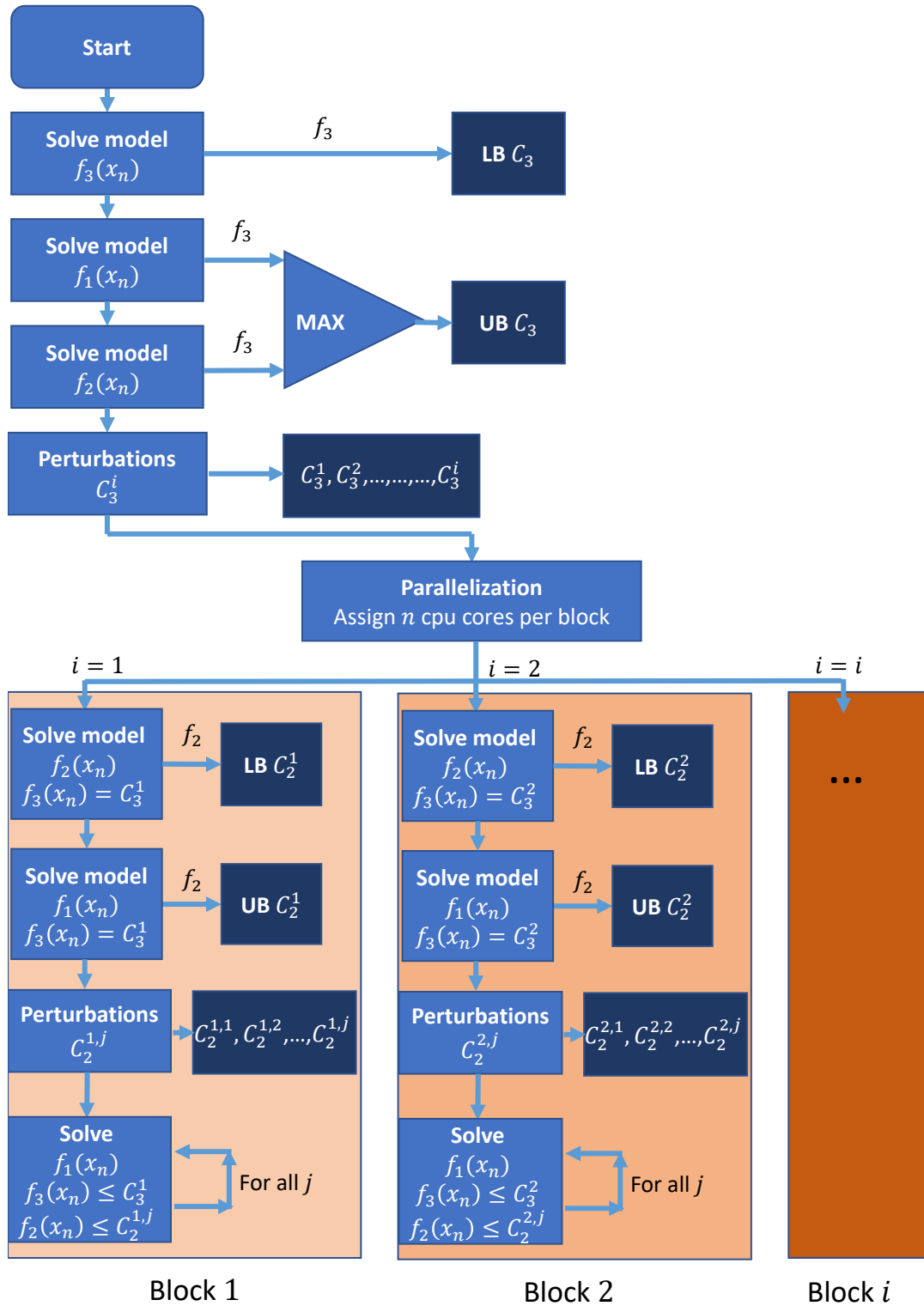
Figure 4.5.: Parallelization of the epsilon constraint method.

5. Case study

Two case studies will be defined and implemented in this chapter for the previously defined optimization offshore wind O&M fleet optimization model in chapter 3. The first case study compares objective function values to an offshore wind O&M cost estimation tool and is limited to preventive maintenance. The second case study now includes corrective maintenance tasks, and the results of this case study will be thoroughly evaluated. The case studies will be solved using the fleet optimization model and epsilon constraint method with three objectives from chapter 4. At the end of this chapter, the case study results are presented and evaluated.

5.1. Case study methodology
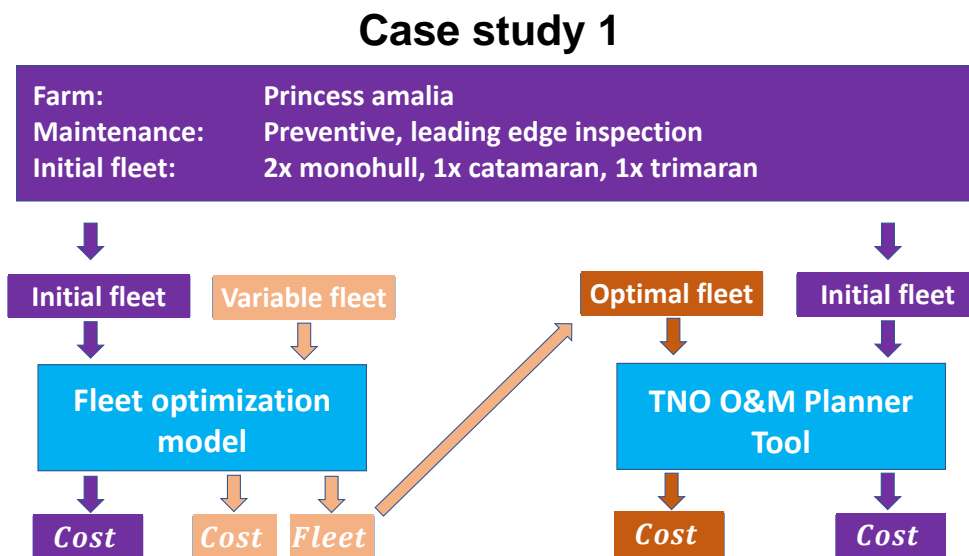
Figure 5.1.: Overview of case study 1.

An overview of case study 1 is shown in fig. 5.1. Case study 1 compares the estimated costs of the fleet optimization model to an offshore wind O&M cost modeling tool. The cost estimation tool that will be used for the comparison is the UWiSE O&M Planner. An initial unoptimized fleet is defined for case study 1, which is inserted in the UWiSE O&M Planner. By constraining the fleet composition variables with constraints, this initial unoptimized fleet is also used as the fleet in the optimization model. The constraints are then removed from the fleet optimization model, allowing the fleet composition to be variable again. The fleet optimization model is then solved and proposes a number of optimal fleets. One of these fleets is then selected and used as the fleet composition in the UWiSE O&M Planner. The

results of all these runs will be examined, allowing for comparisons between the optimization model results and the UWiSE O&M Planner.

Case study 2
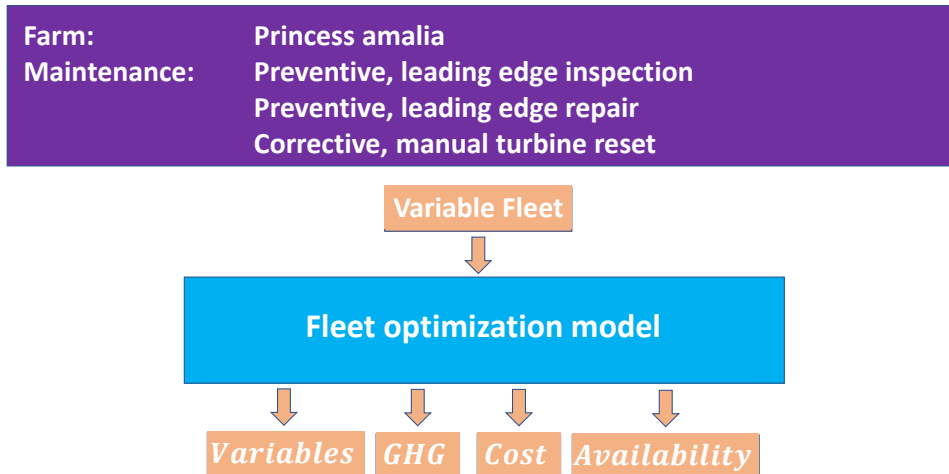
Figure 5.2.: Overview of case study 2.

An overview of case study 2 can be found in fig. 5.2. The purpose of case study 2 is to demonstrate the fleet optimization model with a larger variety of maintenance types compared to case study 1.

5.2. Case studies definition

Both case studies are based on the currently operational Princess Amalia Wind Farm in the Netherlands and located offshore 23 kilometers from IJmuiden. The wind farm has been commissioned in 2008 and consists of 60 Vestas V80 wind turbines with a maximum rated power of 2 MW each, giving it a total capacity of 120 MW.

Case study 1 will only include a visual inspection of the wind turbine blades, which is modeled as a preventive maintenance task required for all wind turbines in the Princess Amalia wind farm. In addition to the visual inspection, case study 2 will require a leading edge protection maintenance task and a corrective maintenance task due to a critical failure. The maintenance vessels available for charter in both case studies are a variety of different types of CTVs distinguished by their hull design.

The sections that follow will go into greater detail about the case studies.

Time horizon

Case study 1 has a one-year time horizon, while Case Study 2 has a six-month time horizon. Each year is made up of 12 months, with each month consisting of 30 days. In reality, each month can have more or fewer days than 30. This means that if a vessel is chartered in the sixth month, it will be from the 30th of May to the 29th of June rather than from the 1st of

	Maintenance type	Hours required [h]	Costs per task [€]
Maintenance task 1	Critical failure (Corrective)	6	500
Maintenance task 2	Visual inspection (Preventive)	6	250
Maintenance task 3	Coating reapplication (Preventive)	8	500

Table 5.1.: Table with maintenance task parameters.

	Inspection results per year				
	2012	2014	2015	2016	2017
Category 1	2%	0%	33%	0%	8%
Category 2	27%	26%	15%	63%	77%
Category 3	67%	68%	46%	37%	14%
Category 4	5%	6%	6%	0%	1%
Category 5	0%	0%	0%	0%	0%

Table 5.2.: Table with values for the damage category distribution per year.

June to the 30th of June. If a vessel is chartered in the sixth month in the model, the month is still referred to as June. The historical data used in this model will be implemented so that the final day of the 1-year planning horizon falls on December 26th.

The maximum amount of hours that maintenance engineers can work on a maintenance task is assumed to be 10 hours. The shift starts at 08:00 and ends at 18:00.

Maintenance tasks

The leading edges of the wind turbines are protected with a coating. This coating can deteriorate over time, exposing and damaging the laminate of the wind turbine blades. The first maintenance task is to visually inspect the leading edges of the wind turbine blades for damage to the coating. This maintenance task is included in both case studies 1 and 2. If the visual inspection revealed that the coating on the blade had sustained significant damage, a follow-up maintenance task has to be executed to reapply the coating. This follow-up maintenance task is only included in case study 2. The final maintenance task is a corrective maintenance task for a critical failure that has rendered the wind turbine non-functional. This maintenance task is only included in case study 2 as well.

The level of damage on wind turbine blades is classified by categorizing the damage into five levels. The first category indicates that there is no significant damage to the leading edge protection of the blade. The second category indicates that the leading edge has minor damage, but no action is required at this time. The third category indicates that the leading edge protection has been almost completely compromised. The fourth category indicates that parts of the laminate are now exposed. The fifth and final category indicates that the laminate has been penetrated. An overview of the inspection results per year can be found in table 5.2.

	Type	Crew [teams]	Weather limits	Speed [m/s]	Docking space
CTV 1	Monohull	1	$H_s^{max} = 1.1[m]$	8	1 [Dock space]
CTV 2	Catamaran	1	$H_s^{max} = 1.35[m]$	14	1 [Dock space]
CTV 3	Trimaran	1	$H_s^{max} = 1.6[m]$	16	1 [Dock space]

Table 5.3.: Table with maintenance vessel parameters.

	Fuel		Costs		
	Type	Consumption [l/h]	Charter [€/day]	Fuel [€/l]	Fixed [€/month]
CTV 1	MFO	180	3500	1.64	2000
CTV 2	MFO	130	4500	1.64	2000
CTV 3	MFO	150	5000	1.64	2000

Table 5.4.: Table with maintenance vessel parameters on fuel and costs.

Up to category 3, technicians who access the turbine via rope can apply a new layer of protective coating to the wind turbine blade. Categories 4 and 5 require the removal of the turbine blade from the wind turbine using heavy lifting equipment. Only damages up to category 3 are considered in this case study. Technicians will use ropes to gain access to the blades for both visual inspections (case studies 1 and 2) and coating reapplication (case study 2). The critical failure corrective maintenance task (case study 2) is assumed to be repairable without the use of heavy lifting vessels. The wind turbine will have to be shut down for both the visual inspection and the application of the protective coating, so it will not be producing power in the meantime. The maintenance task of applying a protective coating to the wind turbine blade can only be performed after the visual inspection of the wind turbine has been completed. All turbines must have been inspected at least once over the course of a year. It is assumed that a single crew can complete the visual inspection in about 6 hours and apply the protective coating in about 8 hours. A single inspection on a wind turbine will cost €250 per task.

The number of turbines with category 3 damage will be determined using data from 2017 (see table 5.2). As a result, the total number of turbines that require the protective coating is rounded to 9 turbines. The coating is assumed to be required for turbine numbers 0-8, and maintenance personnel can only begin working on it after the visual inspection of the turbine has been completed. Each protective coating will take 8 hours to apply and will cost €500 per task.

It is assumed that one critical failure occurs at one of the 60 turbines each month on average. This will be modeled as a corrective maintenance task that leaves the wind turbine non-operational after the critical failure occurs. Once the critical failure is repaired, the turbine will be operational again. The costs of a critical failure are assumed to be €500 per task, with the required hours to repair the turbine being 6.

Maintenance vessels

In case studies 1 and 2, there are three different maintenance vessels to choose from for the fleet composition, and all vessel assumptions are the same for both case studies. The three

options consist of CTVs with different types of hull designs. There are three types of CTV hulls: monohull, catamaran, and trimaran. The different designs of the vessel hulls give them unique characteristics, such as transit speed. The number of vessels is chosen as a unit of docking space in the maintenance base capacity constraint because the vessels are assumed to be roughly the same size. The units that are used to determine the capacity of a vessel are typically expressed as the number of maintenance technicians it can transport. However, it is assumed in both case studies that each vessel can only carry one maintenance team at a time with each team consisting of three technicians. The costs of the vessels are assumed to be charter costs, fuel costs, and fixed costs associated with upkeep costs. During rough sea states, the CTVs have limited access to the wind farm. This is assumed to be the significant wave height H_s for the CTVs.

The vessel specifications can be found in table 5.3 and table 5.4. Some of the CTV specifications, such as the operational speed and the H_s limit, are based on the typical characteristics of these types of hull designs (Hu & Yung, 2020). The costs of chartering the maintenance vessels were estimated based on values from literature (Dewan & Asgarpour, 2016). The fuel type for the CTVs is assumed to be MFO (Gray, 2021). The fuel prices are calculated using Dutch fuel prices in 2022. The relatively better fuel economy of catamaran and trimaran hull designs was one of the reasons for their introduction (Hu & Yung, 2020). The fuel economy of the catamaran is based on the specifications of the CWind Endurance SWATH CTV, while the monohull and trimaran hull designs fuel economies are estimated. The terms in the charter contract likely determine which types of vessel upkeep costs are or are not covered by the charter company. Since no data on the fixed costs were available, the fixed costs are estimated.

The costs of the maintenance vessel charter prices are assigned to the parameter C_{nvl}^{TC} in the model. The fixed costs of the vessels are assigned to C_{nv}^{F} parameter in the model. The costs of fuel consumption are assigned to the C_v^V parameter in the model.

Maintenance crew

It is assumed in both case studies that one maintenance crew consists of three technicians. It is assumed that each vessel can only carry one team of maintenance technicians on board the maintenance vessel, regardless of the actual maximum capacity of the maintenance vessel. There is a maximum of four maintenance crews that can be hired on a given day. Because each vessel can only carry one maintenance team, the maximum number of maintenance vessels is four. On any given day, there is no minimum number of crews that must be hired.

A crew is not considered to be employed by the wind farm operator but rather is hired from another company on a per-day basis. This means that the costs of a maintenance crew are fixed for each day they are used, regardless of how many hours they work on maintenance tasks. The costs of the crew are added to the parameter C_v for this reason, as this parameter is multiplied by the variable u_{npv} which determines how many maintenance vessels are used for maintenance activities on a given day. The day rate of a technician is assumed to be $1000 €/day$.

Environmental conditions

The significant wave height H_s for vessels represents is used as the sea state condition that can limit the accessibility of maintenance vessels to the wind farm. The H_s values are based on the hourly historical significant wave height data from the Princess Amalia wind farm in

	Month											
	J	F	M	A	M	J	J	A	S	O	N	D
Capacity factor	0.5	0.49	0.4	0.29	0.3	0.28	0.28	0.29	0.28	0.38	0.45	0.5
Electricity price [€/MWh]	67	67	67	67	68	69	72	73	75	77	81	80

Table 5.5.: Table the capacity factor and electricity prices that are used in the case study for each month.

2016. To be compatible with the model, the hourly historical significant wave height data must be converted to daily historical significant wave height data. This is accomplished by calculating the daily average significant wave height.

Charter costs

Longer-term vessel contracts are typically less expensive than shorter-term contracts (Dalgic et al., 2013). As a result, a discount factor is used to account for this. The monthly cost of chartering a vessel is added to the parameter C_{nvl}^{TC}. The following equation was used to include lower prices for longer periods of time:

$$C_{nvl}^{TC} = (\text{CharterCostsPerDay}[€/day])(\text{MonthSize}[day])(l - n + 1)(\text{DiscountFactor})^{l-n} \quad (5.1)$$

To convert the charter costs of a single day to a single month, the charter costs per day are multiplied by the month size. The multiplication with $(l - n + 1)$ is necessary to calculate the costs for multiple months without a discount. The final multiplication with the discount factor is then performed to reduce the charter costs per month as the charter length increases. The discount factor used in both case studies was set at 0.95.

Downtime costs

The downtime costs are assigned to the parameter C_p^{DTC}. This parameter is defined as the cost of downtime per day when the wind turbine is not operational. The downtime cost parameter C_p^{DTC} in the current case studies is calculated as follows:

$$C_p^{DTC} = 24(\text{RatedTurbinePower})(\text{ElectricityPricePerMWh})(\text{CapacityFactor}) \quad (5.2)$$

The 24 in the equation is required to convert the units to the amount of power generated per day. This is then multiplied by the rated power of the wind turbine and the current electricity prices per MWh. The wind turbine capacity factor is assumed to be different for each month and is based on the historical capacity factor of the Belgian North Sea because other data was unavailable. The electricity prices are based on 2016 electricity prices in the Netherlands. The capacity factor and electricity price values for each month can be found in table 5.5.

Maintenance vessel transit time, transit costs, and loitering costs

The transit time of the maintenance vessels is defined in the parameter T_v^T. The total amount of time a vessel spends in transit on a given day is defined as the transit time. The transit time of the maintenance vessels is assumed to be constant and unaffected by environmental factors such as wave height or wind speed. It is assumed that vessels will remain at the wind turbine while maintenance is performed by the technicians. The average distance from the IJmuiden port to the wind turbines is 23.8[km], which is used to calculate the distance to the wind farm. The parameter T_v^T is calculated as follows:

$$T_v^T = \frac{2(\text{DistanceToWindFarm}[m])}{\text{VesselSpeed}[m/s]} \tag{5.3}$$

The amount of transit costs are added to the parameter C_v^T. The transit costs for all vessel types are calculated in a similar manner and are defined as follows:

$$C_v^T = (\text{FuelPerHour}[l/h])(\text{FuelCost}[\text{\euro}/l]) \tag{5.4}$$

It is also assumed that the vessels will consume fuel while loitering. Estimates of the amount of fuel consumed during loitering are made in section 5.2. The total costs of loitering are calculated as a function of the amount of time spent working on a maintenance task. It is therefore added to the parameter C_{mv}^M because this parameter is multiplied by the number of man-hours spent on a maintenance task $t_{pmv\tau}$. It is calculated as follows:

$$C_{mv}^M = (\text{FuelPerHourIdling}[l/h])(\text{FuelCost}[\text{\euro}/l])/M_v^{CREW} \tag{5.5}$$

The value is divided by M_v^{CREW} to obtain the number of hours that are being worked on a task rather than the number of man-hours of work.

Emissions

In the current study, the emissions quantification for the fleet optimization model was limited to direct emissions only. The vessels used for maintenance are assumed to be the only sources of direct emissions. These vessels use fuel while traveling between the maintenance base and the wind farm. Furthermore, it is assumed that vessels use generators to power auxiliary systems on board the vessel while the crew performs maintenance tasks at the wind turbine. These emissions are referred to as loitering emissions. Since the fleet optimization model in the current study only considers transit between the wind farm and the maintenance base, emissions from moving from one wind turbine to another are not modeled.

The parameters used to quantify GHG emissions from loitering and transit are $C_v^{GHG-IDLE}$ and $C_v^{GHG-TRANSIT}$, respectively. The parameter that quantifies the number of emissions during transit is defined as follows:

$$C_v^{GHG-TRANSIT} = \frac{\text{DistanceTraveled}[m]}{\text{vesselSpeed}[m/s]} \frac{(\text{FuelPerHour}[l/h])(\text{FuelEmissions}[kgCO2e/l])}{3600[s/h]} \tag{5.6}$$

The first fraction in eq. (5.6) calculates the time spent in transit by dividing the distance between the wind turbine farm and the maintenance base by the assumed operational speed of the maintenance vessel. The second fraction multiplies the amount of fuel consumed per hour by the number of emissions associated with the fuel type used. The second fraction is divided by $3600[s/h]$ to convert the units of time to seconds.

For the case studies, emissions from idling will be calculated as a result of the fuel consumed by marine generators. For all CTV types, it is assumed that the Cummins Onan 13.5 kVa/230V generator is used. During idling, the assumption is made that both generators run at maximum power. At maximum power, each generator consumes approximately 17 liters of fuel per hour, for a total of 34 liters per hour for two generators. It is assumed that the fuel used in the generators is the same type as the fuel used in the engines used for the propulsion of the ship. The amount of emissions caused by maintenance vessel idling is calculated as follows:

$$C_v^{GHG-IDLE} = (\text{FuelPerHour}[l/h])(\text{FuelEmissions}[kgCO2e/l]) \tag{5.7}$$

The number of fuel emissions associated with a specific fuel type is calculated in units of $kgCO2e$ per liter of fuel burned. The unit $CO2e$ converts the GHG contributions of other gases to the amount of $CO2$ required to achieve the same GHG effects. The Kyoto Protocol (Kyoto Protocol, 1997) has identified six greenhouse gases (GHGs):

1. Carbon dioxide

2. Methane

3. Nitrogen dioxide

4. Hydrofluorocarbons

5. Perfluorocarbons

6. Sulphur hexafluoride

Carbon dioxide, methane, and nitrogen dioxide are the only GHGs associated with fuel combustion. When a fuel is burned, it emits a different concentration of carbon dioxide, methane, and nitrogen dioxide. The emissions in $CO2e$ can be calculated by multiplying methane and nitrogen dioxide levels by an emission factor.

For the case studies, it is assumed that the fuel used by CTVs is Marine Fuel Oil (MFO). The amount of carbon dioxide, methane, and nitrogen dioxide emitted by burning a liter of MFO can be found in eq. (5.8c). Carbon dioxide, methane, and nitrogen dioxide emission factors can be found in table 5.6.

The amount of GHG emissions due to burning a liter of fuel is calculated as:

$$\text{FuelEmissions}[kgCO2e/l] = \text{CO2PerLFuel}[kgCO2e/l] \tag{5.8a}$$
$$+ (\text{CH4PerLFuel}[kgCH4/l])(\text{CH4Factor}[kgCO2e/kgCH4]) \tag{5.8b}$$
$$+ (\text{N2OPerLFuel}[kgN2O/l])(\text{N2OFactor}[kgCO2e/kgN2O]) \tag{5.8c}$$

	CO2PerLFuel $[kgCO2e/l]$	CH4PerLFuel $[kgCH4/l]$	N2OPerLFuel $[kgN2O/l]$
MFO	11.27	0.45E-3	0.09E-3

Table 5.6.: Table with the amount of CO2, CH4 and N2O emissions per fuel type.

CH4Factor $[kgCO2e/kgCH4]$	N2OFactor $[kgCO2e/kgN2O]$
25	298

Table 5.7.: Table of the emission factors of CH4 and N2O.

Completing maintenance tasks

For the purposes of this case study, it is assumed that all maintenance tasks will be completed by the end of the planning horizon. One technique to achieve this is by imposing an arbitrarily high penalty for failing to complete maintenance tasks. However, if the penalties are not set high enough, this could still result in solutions with uncompleted maintenance tasks. A constraint can be added to ensure that the model only provides solutions where all maintenance tasks are completed by the end of the planning horizon by enforcing $\beta_{m\tau} = 0$. This constraint is formulated as:

$$\beta_{m\tau} = 0 \qquad\qquad \forall m \in M, \tau \in T \qquad\qquad (5.9)$$

5.3. Computational setup

The models are solved using the commercial optimization solver Gurobi v.10.0.1 using an academic license. A computing cluster with two Intel Xeon Gold 6326 16 cores 32 threads CPUs running at 2.90GHz and 130762 MB of RAM is used to solve the case studies.

The Pareto fronts of the case studies will be approximated using the methodology described in section 4.3 and section 4.4. The respective objective functions to f_1, f_2 and f_3 from section 4.3 and section 4.4 are z^{Costs}, $z^{Availability}$ and $z^{Emissions}$. Similarly, the respective perturbations are changed from C_1, C_2 and C_3 to C_{Costs}, $C_{Availability}$ and $C_{Emissions}$. Both case studies will have 8 perturbations of the $z^{Availability}$ constraint and 8 perturbations of the $z^{Emissions}$ constraint, meaning that the model will be solved $8 * 8 = 64$ times.

Some termination criteria have been established in order to avoid lengthy solution times. The first termination criterion is when a solution with a MIP gap less than 2% is found. The second stopping criterion is after running the model for longer than 10800 seconds. The value of 10800 seconds was determined by experimenting and determining which time limits would result in either good convergence of the MIP gap or a MIP gap less than 2%.

5.4. Case study results

The case study findings are split into two sections. The first section discusses the findings of case study 1, while the second discusses the findings of case study 2.

5.4.1. Case study 1 results

The Pareto front

The Pareto front of case study 1 is depicted in fig. 5.3 by plotting the solutions to the model perturbations. The x-axis of the plot represents the objective function for the GHG emissions, while the y-axis represents the objective function for the costs. The color of the plotted points represents the availability objective function. A plot of the same Pareto front in three spatial dimensions can be found in fig. C.2.
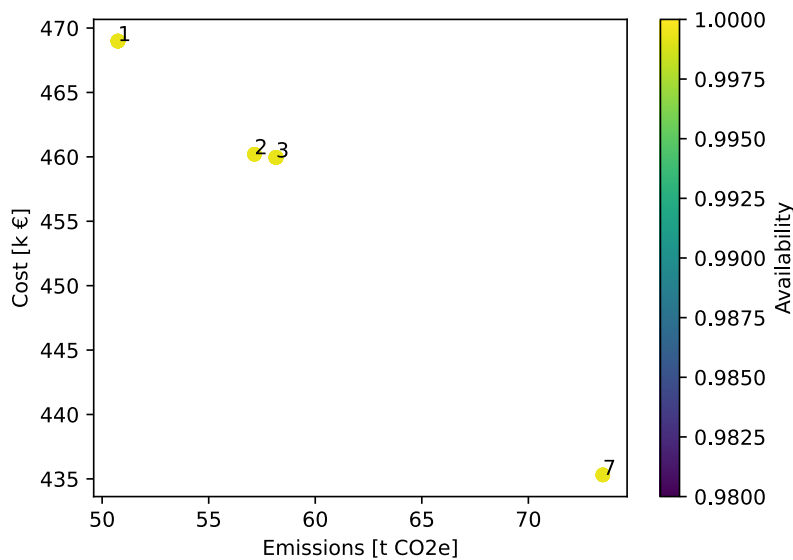
Figure 5.3.: Case study 1 Pareto front.

It can be seen that the Pareto front in fig. 5.3 shows four distinct solutions with unique objective function values. The first thing to notice is that the values for the time-based wind farm availability objective function are identical across all solutions. This is consistent with the observation that all maintenance tasks in case study 1 are preventive maintenance. Preventive maintenance is modeled so that wind turbines are only shut down when maintenance tasks are completed. Because each solution in the Pareto front plot must complete the same number of preventive maintenance tasks and each task requires the same number of hours to be worked on, the solutions have the same time-based wind farm availability estimates.

Each solution in fig. 5.3 has a time-based availability of 0.9993056. A manual calculation can be used to verify this value by looking at the definition of the time-based wind farm availability function. Each wind turbine requires one preventive maintenance inspection, which takes 6 hours or 1/4 days to complete. This maintenance will result in the same amount of downtime for the wind turbine. Case study 1 has a planning horizon of 360

	Fleet composition		
	Monohull	Catamaran	Trimaran
1	-	1 [Jun, Jul]	-
2	1 [Apr]	1 [Sep]	-
3	1 [Apr]	1 [Feb]	-
7	1 [Jun, Jul]	-	-

Table 5.8.: Objective functions and fleet compositions of case study 1.

	Optimization model		UWiSE O&M Planner	
	Solution 1	Solution 7	Solution 1	Solution 7
Vessel type 0	-	1 [June, July]	-	1 [June, July]
Vessel type 1	1 [June, July]	-	1 [June, July]	-
Vessel type 2	-	-	-	-
Total costs	€469.0*k*	€435.3*k*	€476.7*k*	€408.3*k*
Time-based availability	99.93%	99.93%	99.76%	99.77%
GHG emissions	50.7 t CO2e	73.5*t* CO2e	-	-

Table 5.9.: Table with a summary of the small case study results from the optimization model and the UWiSE O&M Planner

days, so the time-based availability of the entire wind farm can be calculated as $1 - \frac{1}{360}\frac{1}{4}\frac{1}{60} * 60 = 0.9993056$. When different vessel types are modeled to have different crew sizes on each vessel, the time-based wind farm availability for preventive maintenance tasks can be different.

The fleet composition of each unique solution in the Pareto front in fig. 5.3 varies. The fleet compositions are shown in table 5.8. Solution number 1 charters a vessel of type 1 (catamaran) beginning in June and ending at the end of July. It is the most expensive solution, but it also produces the least emissions. Solutions 2 and 3 have similar compositions, but the months in which the vessels are chartered differ. The more expensive solution charters a vessel of type 0 in April and a vessel of type 1 in September, whereas the less expensive solution charters a vessel of type 0 in April and a vessel of type 1 in June. Finally, solution 7 is the solution with the lowest costs and highest emissions is located on the far right. In June and July, this solution charters a vessel of type 0.

Two of the fleets from the Pareto front in fig. 5.3 are selected as the optimal fleets. Case study 1 is now run using the UWiSE O&M Planner, together with both optimal fleets. For demonstration purposes, the fleets of solution numbers 1 and 7 have been selected. The results of case study 1 with these fleets for the UWiSE O&M Planner can be found alongside the optimization model in table 5.9. The cost estimation of both models with the initial fleet are €712.0*k* and €712.2*k*, respectively. The costs of the optimized fleet are €435.3*k* and €412.1*k*, respectively.

5.4.2. Case study 2 results

The Pareto front

The Pareto front of case study 2 is plotted in fig. 5.4. Similarly to the Pareto front plots of case study 1, this was achieved by creating a scatter plot of the objective functions from the case study 2 solutions. There are two plots with the same Pareto front in fig. 5.4. The left and right plots differ in that the right plot highlights some of the solutions by indicating the solution number with an arrow, whereas the left plot is left blank. The x-axis of both plots represents the GHG emission objective function and the y-axis represents the cost objective function. The color of the plotted points represents the availability objective function. The plots in fig. C.4 and fig. C.3 contain plots of the Pareto front from case study 2 in three spatial directions rather than two with a color plot. When compared to the results of case study 1, it is evident that the amount of unique solutions is greater for case study 2. It can also be seen that the solutions now have distinct time-based wind farm availability objective function values, as the plotted points have different color shades.
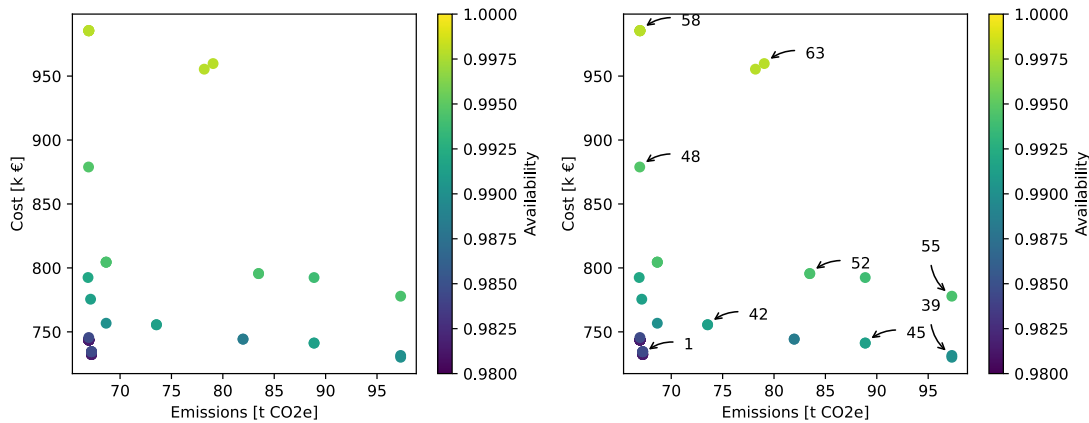
Figure 5.4.: Plot of the Pareto front of case study 2.

The fleet compositions that belong to the set of numbered solutions in fig. 5.4 can be found in table 5.11. The objective function values that belong to the numbered solutions can be found in table 5.10.

The results of the fleet compositions in table 5.10 show that not all solutions have at least one vessel available each month, despite the fact that critical failure corrective maintenance tasks occur once a month. Some solutions have the same vessel in their fleet every month (e.g., solution 58), whereas others have mixed fleet compositions across multiple months (e.g. solution 63). In any given month, none of the solutions have a fleet that consists of more than one vessel.

Convergence to optimality can be visualized by plotting the incumbent (best integer solution), best bound (lower bound to the model), and MIP gap over time. A plot like this can be found in fig. 5.5 for solution number 60. An arrow marks the points where the fleet composition variables w_{nv} are updated during the solving procedure. This plot shows that the solution has converged to a MIP gap less than the stopping criterion of 2% at just over 200 seconds. Another convergence plot can be found in fig. 5.6 for solution number 48, but this time without highlighting the points in time during the solving procedure where the fleet

	Objectives		
	f^{Cost}	$f^{Emissions}$	$f^{Availability}$
	$[k\,\text{€}]$	$[t\ CO2e]$	
1	732	67.2	0.981
39	731	97.3	0.990
42	756	73.5	0.991
45	741	88.9	0.991
48	879	66.9	0.995
52	796	83.5	0.994
55	778	97.3	0.994
58	986	70.0	0.998
63	960	79.0	0.998

Table 5.10.: Table with the objective function values of a selection of solutions.

	Fleet composition		
	Monohull	Catamaran	Trimaran
1	-	1 [Jun]	1 [Apr]
39	1 [Mar, May, Jun]	1 [Apr]	-
42	1 [Apr]	1 [Feb, Jun]	-
45	1 [Apr, Jun]	1 [Feb]	-
48	-	1 [Feb, Mar]	1 [May, Jun]
52	1 [Jan, May, Jun]	1 [Mar]	-
55	1 [Jan, Mar, May, Jun]	-	-
58	-	-	1 [Jan, Feb, Mar, Apr, May, Jun]
63	1 [Mar, Apr, May, Jun]	-	1 [Jan, Feb]

Table 5.11.: Table with the fleet compositions of a selection of solutions.

composition variables w_{nv} are updated. It is clear that the solution did not reach a MIP gap of less than 2% before the 10800 seconds stopping criteria was met. The difference between the incumbent and best bound ceased to improve after 2000 seconds. A similar phenomenon occurred with solution 24, where the MIP gap ceased to grow. All other solutions reached a MIP gap of less than 2% before the time limit of 10800 seconds was reached.

Variables

The fleet composition variables were already evaluated in section 5.4.1 and section 5.4.2. The variable u_{npv} denotes how many vessels of type v are used on the day p in month n. Because many of the variables in the fleet optimization model are defined in terms of the day p, a calendar-type plot can be created to provide an overview of these variables. Each month is defined to be 30 days long, so u_{npv} is plotted in 6 blocks of 30 days. For each vessel type, an additional row of calendar days can be plotted. For solution number 55, the calendar plot for the variable u_{npv} can be found in fig. 5.7.

One of the constraints in the fleet optimization model restricts vessel accessibility in certain weather conditions. The wave height was set to be the limiting factor for the weather conditions in both case studies 1 and 2. If the maximum wave height at which a v vessel can operate, M_v^K, is less than the average wave height on a given day, U_{pv}, the vessel cannot be used on that day. The days when certain vessels are unable to operate due to weather restrictions can be plotted using a calendar-type plot by marking the days where M_v^K is less than U_{pv} as 0. If M_v^K is greater than U_{pv}, the value on the given day in the calendar plot is 1. This vessel accessibility plot can be found in fig. 5.8.

When comparing fig. 5.7 to fig. 5.8, it is evident that vessels are only used on days when there are no weather restrictions on the given vessel type. It can also be seen in the fig. 5.8 that certain vessel types may be utilized on more days than others. This is to be expected given that the hull designs of some vessel types were defined to have lower wave height limitations than other hull designs for both case studies 1 and 2. The trimaran hull design had the highest maximum operable significant wave heights of any hull design, followed by the catamaran and mono-hull, respectively. This is evident in fig. 5.8, where the catamaran can be used on more days than the mono-hull, and the trimaran can be used on more days than both the mono-hull and the catamaran.

A similar plot to the one made for u_{npv} can be made for the number of man-hours spent on a maintenance task, $t_{pmv\tau}$. The number of variables of $t_{pmv\tau}$ is significantly larger than the number of variables u_{npv} because the former is defined for every maintenance task m and wind turbine τ as well. For that reason, a subset of all variables $t_{pmv\tau}$ are plotted. A calendar-type plot for turbine 5 maintenance task 0 (corrective, critical failure) can be found in fig. 5.9. A calendar-type plot for turbine 5 maintenance task 0 (preventive, coating reapplication) can be found in fig. 5.10. Both plots make use of variables from solution 55.

Finally, the variables $\gamma_{pm\tau}$, which indicate when a maintenance task is completed, can be plotted. Recall that this is a binary variable and its value is equal to 1 if the maintenance task is completed and equal to 0 if a maintenance task is not completed. The variable $\gamma_{pm\tau}$ can be plotted in a calendar-type plot similar manner as had been done for u_{npv} and $t_{pmv\tau}$. A plot can be found in fig. 5.11 for solution number 55, maintenance task 2, and turbine 5.
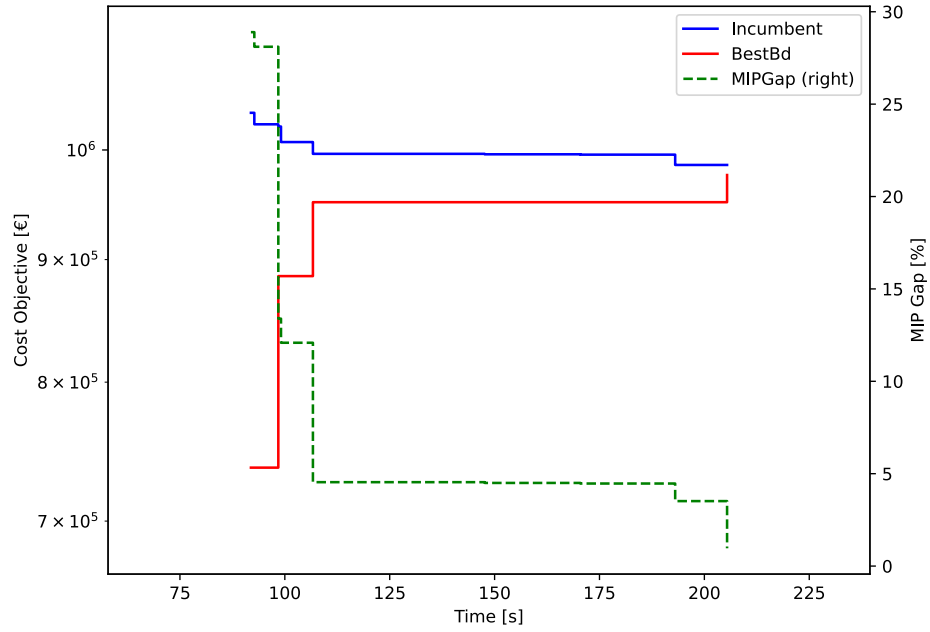
Figure 5.5.: Convergence over time for solution 60.
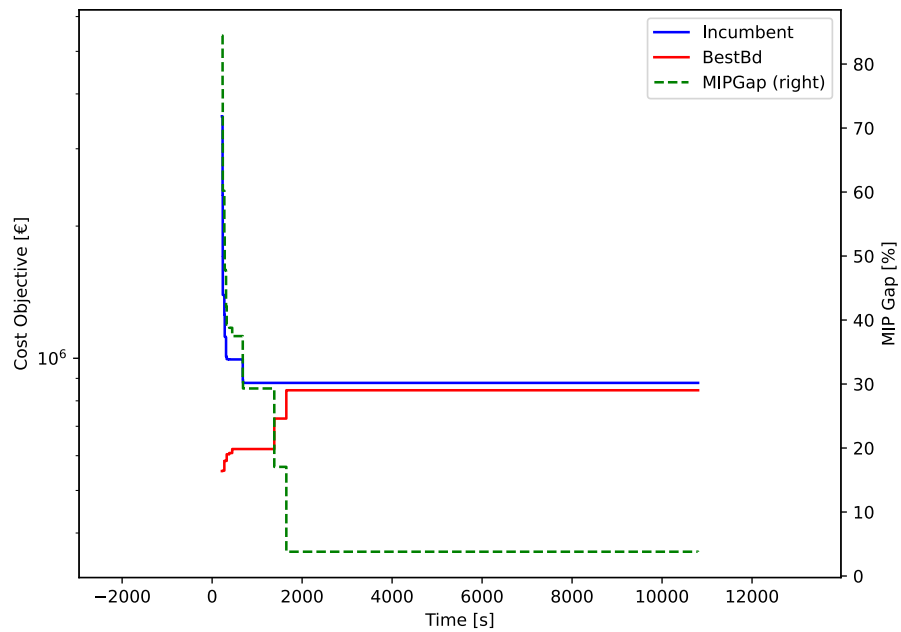
Figure 5.6.: Convergence over time for solution 48.

Values for u_{npv}
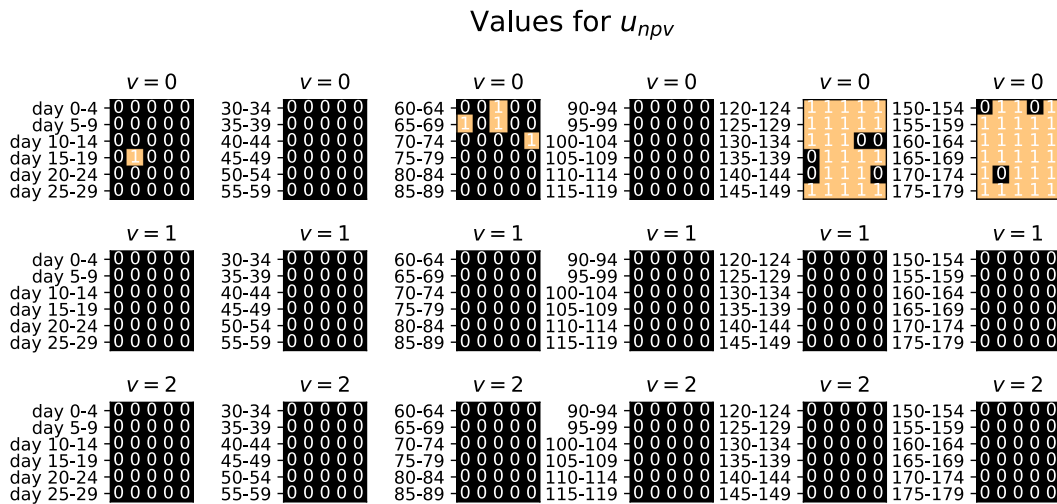
Figure 5.7.: Variable that denotes when a vessel is used, u_{npv}, for solution 55.

Accessabillity of vessels
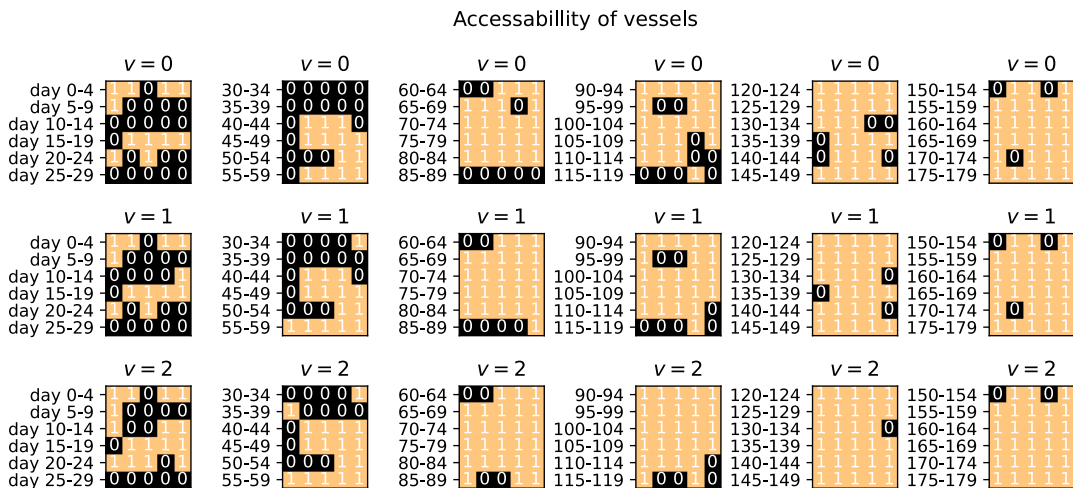
Figure 5.8.: Days on which vessels cannot be used due to weather restrictions.

Values for $t_{pmv\tau}$ for (task 0) at (turbine 5)

Figure 5.9.: Variable that denotes the hours worked, $t_{pmv\tau}$, for task 0 and turbine number 5 of solution number 55.

Values for $t_{pmv\tau}$ for (task 2) at (turbine 5)

Figure 5.10.: Variable that denotes the hours worked, $t_{pmv\tau}$ for task 2 and turbine number 5 of solution number 55.

Values for $\gamma_{pm\tau}$ for (task 2) for (turbine 5)

Figure 5.11.: Variable that denotes when a task is finished, $\gamma_{pm\tau}$ for task 2 and turbine number 5 of solution number 55.

5.5. Concluding remarks

The purpose of this chapter was to answer to the fifth and final research sub-question, which was formulated as follows:

- **Sub-question 5:** How can the developed fleet optimization model be verified?

Two case studies had been developed to answer this sub-question. Maintenance activities at the Princess Amalia wind farm near IJmuiden are the focus of both case studies. The first case study has been implemented in both the fleet optimization model and the UWiSE O&M Planner, which is an offshore wind O&M cost estimation tool. The goal of Case study 1 is to compare the cost estimates of the UWiSE O&M Planner to those of the fleet optimization model. Case study 2 includes a broader range of maintenance task types. The goal of this case study is to evaluate all of the maintenance task types defined in the fleet optimization model. The results and variables of case study 2 are examined in greater depth to determine whether the model works as intended. A calendar-based framework had been developed that can help with the verification of constraints by visualizing the variables.

For case study 1, the results showed that the UWiSE O&M Planner and the optimization model had similar cost estimations. However, the findings suggested that there are inherent differences between the two models. The second case study investigated various methods for plotting the variables, which can be used to confirm that the model works as intended.

6. Discussion

The current chapter discusses the developed fleet optimization model, the approach used to solve the multi-objective model, and the results of the case studies. The chapter will start off with some of the key findings of the current study. The results are then interpreted in the section that follows. The limitations of the current study are assessed based on the key findings and interpretation of the results. Finally, several recommendations for practical applications and future research on the model are given.

6.1. Key findings

Two case studies have been developed and incorporated into the offshore wind fleet optimization model in the current study. The purpose of case study 1 was to compare the costs of the fleet optimization model and an offshore wind O&M cost modeling tool. Case study 2 was developed to assess a wider range of maintenance types supported by the fleet optimization model.

The Pareto front from Case Study 1 revealed a limited number of unique solutions. Using the epsilon constraint method, only four solutions with a unique combination of costs, GHG emissions, and wind farm availability objective functions were found. All of the solutions from case study 1 had the same availability values. The fleet compositions of the solutions all consisted of fleet sizes of no more than one vessel per month. The uniqueness of the solutions was most characterized by the vessel types in the solutions and the months in which they were chartered. Case study 1 cost estimations revealed similar results between the UWiSE O&M Planner and the optimization model, but hinted that both models are fundamentally different.

The solutions from case study 2 contained a greater number and a greater variety of unique fleet compositions than those of case study 1. All solutions used fleet sizes that were never larger than one vessel in a given month. Despite the fact that corrective maintenance for a critical failure was modeled to occur once a month, some solutions did not charter a vessel in that month. These corrective maintenance tasks were then postponed until the fleet consisted of at least one vessel in a month. This resulted in lower availability compared to solutions that chartered vessels over long periods of time, but also a lower cost because fewer vessels were chartered. In almost all solutions, preventive maintenance tasks were completed over several days rather than all at once. Except for two solutions, all reached a lower MIP gap than 2% before reaching the 10800 run time stopping criteria.

6.2. Interpretation of the results

The smaller number of maintenance tasks included in case study 1 could explain the lower variety of solutions compared to case study 2. If the number of maintenance tasks is greater, more vessels are required to transport enough maintenance technicians to the wind farm to

complete all maintenance tasks. If more vessels are required, more fleet compositions are possible, and the number of Pareto optimal fleet compositions may increase as a result.

The lack of corrective maintenance tasks with critical failures in case study 1 could explain why there is no variation in the time-based wind farm availability objective function of the solutions. For case studies that only include preventive maintenance tasks, the only contribution to wind turbine downtime is when the turbine is shut down for maintenance. Because all maintenance tasks are completed in the same amount of time by all vessel types, the fleet composition has no effect on the wind farm availability objective function. If the wind farm availability objective function was quantified as production based rather than time-based, the influence of the varying wind farm capacity factor in each month could potentially lead to more diverse wind farm availability objective function values. The low amount of unique solutions in case study 1 may also be related to the uniform wind farm availability objective function values, as the diversity in wind farm availability values in case study 2 was paired with a significantly greater number of unique solutions.

The cost estimations for case study 1 between the fleet optimization model and the UWiSE O&M Planner were relatively similar. The optimization model estimated a higher cost for solution number 1, whereas the UWiSE O&M Planner estimated a higher cost for solution number 7. This could imply that the close estimates are coincidental and that the intrinsic cost quantification of the two models varies more for different solutions or case studies. The wind farm availability functions are relatively different between the fleet optimization model and the UWiSE O&M Planner, which could be due to a difference in wind farm availability quantification.

Both case studies 1 and 2 had fleet sizes of no more than one vessel in any given month. One possible explanation for this in case study 1 is that if vessels are chartered for multiple months in a row, a discount is given. As a result, chartering a vessel for two months in a row is more cost-efficient than chartering two vessels in a single month. A similar explanation could clarify the phenomenon in case study 2 as well. Furthermore, case study 2 has an incentive to charter at least one vessel every month in order to repair a turbine breakdown as soon as it occurs to maintain high wind farm availability. The majority of the preventive maintenance tasks in fig. 5.7 are scheduled in months 4 and 5, when the wind turbine downtime costs are lower than in previous months due to lower electricity prices and wind farm capacity factor. This indicates that the optimization model takes advantage of scheduling preventive maintenance tasks these months. If vessels are chartered in earlier months, they are only utilized for corrective maintenance tasks. This means that there is plenty of room left to utilize the remaining vessels, and it is not necessary to have a fleet size larger than one vessel at any given time.

The number of hours worked on the preventive maintenance task in fig. 5.10 shows that the amount of work on that task is spread out over several days. This is inefficient compared to completing the tasks on the same day. One possible explanation is that the model does not account for the lost time, additional costs, and additional GHG emissions caused by transit between wind turbines. Spreading out work on preventive maintenance tasks does not have a negative impact on the objective function values if these factors are ignored.

Before the time limit was reached, most solutions for case study 2 and all solutions for case study 1 converged to a MIP gap of less than 2%. In case study 2, an interesting phenomenon occurred when the two solutions did not converge in time. During the solving procedure, the MIP gap appears to stop improving at a point in time. Similar phenomena occurred during earlier adaptations of the fleet optimization model during the design phase of the model. One possible cause could be a weak MIP model formulation (Klotz & Newman, 2013), but this would not explain why it occurs in only a subset of the perturbed models of case study

2. Another possible cause is thought to be the unusually high number of variables in a constraint by setting the objective functions as a constraint, as opposed to regular constraints, which could be difficult for the MIP solver to deal with. Both potential causes are speculative, and the precise cause of this phenomenon is unknown.

6.3. Limitations

The simplification of the routing is one of the limitations of the model. The effects of this simplification were apparent during the evaluation of the solutions of case study 2, where the preventive maintenance tasks were spread out over several days. This is considered inefficient because the maintenance vessel and technicians must be transported multiple times throughout the wind farm. The model does not penalize this because it does not model transit in between the wind turbines. As a result, the amount of available time to work on maintenance tasks is overestimated, while the cost and GHG emission objective functions are underestimated.

Another limitation is the deterministic nature of the model. Many offshore wind O&M fleet optimization models in table 2.2 included multi-stage stochastic optimization models to account for uncertainty in fleet optimization decision-making. Many arguments can be made for the importance of incorporating uncertainty in O&M fleet optimization models, as many aspects of offshore wind O&M are inherently uncertain. Weather, unexpected breakdowns, and electricity prices are examples of uncertainty in offshore wind O&M.

Despite its shortcomings, the model was successful in incorporating a GHG emission objective function into an offshore wind fleet optimization model. Given the inherent uncertainty in offshore wind O&M, the use of multi-stage stochastic fleet optimization models, as found in many other fleet optimization studies, is a reasonable modeling choice. However, these multi-stage optimization models can be computationally intensive. This study solves a multi-objective model using the epsilon constraint method in combination with MIP, which offers the flexibility to choose from various fleet compositions based on multiple KPIs. Unfortunately, this flexibility comes with a high computational cost as the model has to be solved multiple times. The combination of a multi-stage model and the multi-objective optimization method that was developed in the current study could risk becoming an optimization approach that is too computationally expensive to solve efficiently.

6.4. Recommendations

Because the model does not account for uncertainty, it is recommended to take a conservative approach when selecting parameters and configuring the fleet optimization model. One practical example would be to see if the historical weather data includes unusually good weather in a month where bad weather is expected. It is also recommended that the vessel types used as fleet composition candidates are limited to those that move to and from the wind farm once per day, such as CTVs. Although the model is not necessarily limited to specific vessel types, it is expected that other vessel types, such as SOVs, will not be accurately modeled because they can stay offshore for several days.

Future research could look into the possibility of incorporating stochastics into the fleet optimization model. Multi-stage optimization models are a common approach for modeling

uncertainty in offshore wind fleet optimization studies, but they make the models compu-
tationally expensive to solve. Therefore, future research could explore efficient methods for
combining multi-stage and multi-objective models. Additionally, alternative approaches for
incorporating uncertainty, such as robust optimization, could be investigated to compare their
effectiveness. To enhance the accuracy of the fleet optimization model, it would be valuable
to investigate the benefits of a higher fidelity transit model as well as scope 2 or scope 3 GHG
quantification methods.

7. Conclusion

The current study is aimed at developing a multi-objective optimization model that chooses an offshore wind O&M fleet based on costs, wind farm availability, and GHG emissions. To the authors best knowledge, this study is the first to include GHG emissions in an offshore wind O&M fleet optimization study.

The central research question of the current study was formulated as follows:

- How can a multi-objective optimization model be formulated to find an optimal vessel fleet selection for offshore wind O&M activities, based on the financial costs, the GHG emissions, and the time-based wind farm availability as a result of the selected fleet?

The cost objective function takes into account vessel charter costs, vessel usage costs, maintenance operation costs, and profit loss due to wind farm downtime. The GHG emission objective function quantifies direct emissions as a result of vessel transit and powering the vessel auxiliary systems during maintenance tasks. The time-based wind farm availability is based on the amount of downtime of a wind turbine, where corrective maintenance tasks cause downtime from the moment that a breakdown occurs and preventive maintenance tasks only cause downtime while maintenance is executed. The epsilon constraint method is used as a reformulation method for the fleet optimization model. The multi-objective optimization model is converted into a single objective model that is solved multiple times. The other two objective functions are set as constraints that are perturbed each time the model is solved. The Pareto front of the model is estimated by solving these perturbed single-objective models with a commercial MIP solver. The Pareto front can be used to compare trade-offs between solutions.

It is suggested that stochastics be included in the fleet optimization model for future research. Furthermore, there is plenty of room to improve the quantification of transit so that transit between wind turbines is accounted for. One approach that looks promising for this is the pattern-based approach from the studies of (Gutierrez-Alcoba et al., 2019) and (Stålhane et al., 2019). Incorporating scope 2 and scope 3 emissions to account for indirect emissions could be a novel approach to quantifying GHG emissions for offshore wind fleet composition decisions for future studies.

A. Research paper

A multi-objective optimization model for offshore wind farm operations & maintenance fleet selection

J.S. Bloothoofd

ABSTRACT Until recently, tenders in Europe were awarded to wind farm developers based on the highest auction prices or the lowest subsidized bids. The wind industry has suggested that non-price-related criteria should be considered for tenders, like plans to reduce greenhouse gas emissions. As a result of the sustainable tender criteria, greenhouse gas emissions are a relatively new KPI for offshore wind farm developers.

Studies have shown that the costs and wind farm availability are sensitive to the fleet composition and were commonly used as criteria in offshore wind fleet optimization models. Offshore wind greenhouse gas emissions were shown to be sensitive to the offshore wind fleet composition as well but thus far not used as criteria for fleet composition decision-making. This study aims to develop an offshore wind O&M multi-objective fleet optimization model that includes GHG emissions as the third criterion for the fleet composition. The model is rendered as a deterministic MIP problem. An epsilon constraint method-inspired approach is proposed to reformulate the multi-objective into a set of perturbed single-objective models, which can be solved using a commercial MIP solver.

I. INTRODUCTION

One of the recent conclusions at the COP27 climate conference in 2022 was that the 1.5°C global warming goal is still viable[1]. However, warnings were given for the lack of efforts to phase out fossil fuels as a source of energy. It will take concrete and ambitious plans from nations all over the world to reduce their emissions in order to maintain the 1.5°C global warming goal[2]. Wind energy is a promising renewable energy source for mitigating global warming[3]. In 2020, the total installed wind energy capacity in Europe was 220 Giga Watts (GW)[4], with offshore wind energy accounting for 25 GW. Offshore wind energy its share of total new installed wind energy has been steadily increasing[4]. The outlook for offshore wind is positive in the long term as well, as Europe aims to increase the total offshore wind capacity to 400 GW by 2050[4]. Wind farm developers will need to build large-scale offshore wind farms in order to realize these ambitious plans. Most offshore wind projects in Europe are awarded to wind farm developers using tenders. Once a tender is awarded, the wind farm developer is granted a permit for the construction, operation, and removal of the wind farm. Up till recently, the highest auction prices or the lowest subsidized bids serve as the criteria for awarding tenders[5]. However, the European wind industry has suggested that non-price-related criteria should be considered for tenders as well[6]. These non-price-related criteria include sustainability and biodiversity-related criteria, such as plans to reduce greenhouse gas (GHG) emissions. This creates a strong incentive for offshore wind farm developers to propose environmentally friendly and sustainable strategies for the wind farm. The vessel fleet composition during the wind farm operations and maintenance (O&M) phase is one of the strategies. The vessels are used to transport maintenance personnel, spare parts, and/or can perform heavy lifting. Offshore wind costs and wind farm availability are two key performance indicators (KPIs) that can be linked to the vessel fleet composition[7,8]. Furthermore, as a result of sustainable tender criteria, GHG emissions are now an offshore wind KPI that can be linked to vessel fleet composition[9].

There is an extensive amount of literature on fleet optimization models in offshore wind. The studies of Halvorsen-Weare et al.[10] and Diran[11] have investigated ways to develop a deterministic fleet optimization model that is solved using Mixed-Integer Programming (MIP). Some of the gaps that were identified in deterministic models were that they did not capture the highly uncertain nature of processes in offshore wind O&M. The studies of Gundegjerde et al.[12] and Stålhane et al.[13] introduced multi-stage stochastic modeling to offshore wind fleet optimization in order to incorporate the uncertainty of parameters into decision-making. Both studies have solved the fleet optimization models using MIP. One conclusion that was drawn was that if the planning aspect of the models would be become more detailed, the model would quickly become too impractical to solve. A number of different multi-stage stochastic programming models were developed and investigated alternative ways to solve the fleet optimization models. The study of Gutierrez-Alcoba et al.[14] investigated ways to include heuristics for maintenance scheduling. The study of Stålhane et al.[15] investigated using Dantiz-Wolfe reformulation methods and metaheuristics for fleet optimization models. The studies Stålhane et al.[16] and Bolstad et al.[17] attempt to solve an offshore wind O&M fleet optimization model using an L-shaped and a heuristic GRASP method, respectively. A different approach to the analytical models from the formerly listed studies is by means of simulation. The studies of Dalgic et al.[18] and Dalgic et al.[19] include a simulation-based approach to evaluate an optimal CTV fleet selection and to evaluate the effects of a mothership concept for offshore wind O&M, respectively. The studies of Rinaldi, Thies, and Johanning[20] and Rinaldi et al.[21], by using genetic algorithms to find sets of optimal solutions based upon multiple objective functions from a surrogate O&M simulation model.

Stakeholders have expressed interest in decision-support tools for offshore wind planning activities such as fleet composition. The majority of research on these decision-making tools has focused on lowering costs and increasing wind farm availability. However, research has demonstrated that GHG emissions in the O&M phase are also largely affected by fleet composition. To the best of the authors' knowledge, cur-

rent offshore wind studies have yet to incorporate greenhouse gas (GHG) emissions into O&M fleet composition decision-making, despite suggestions from the industry to award offshore wind farm tenders to wind farm developers based on non-monetary criteria, such as environmental impact. This highlights a need for further research into the integration of GHG emissions as a key consideration in the fleet composition decision-making process for offshore wind energy, in order to maximize the industry its contribution to sustainability and climate change mitigation.

The goal of this study is to add the GHG emissions to the costs and wind farm availability as criteria for a multi-objective optimization model for offshore wind O&M fleet composition decision-making. The model in the current study is based on the offshore wind fleet optimization model of Bolstad *et al.* [17] and Stålhane *et al.* [16]. The structure of the current study begins with the fleet optimization model development. After that, a method is introduced that reformulates the fleet optimization model into multiple single-objective models. The developed fleet optimization model and the reformulation method will be applied to two case studies.

II. METHODS

A. Fleet optimization model

The model accounts for the presence of a single wind farm, which comprises a specific number of turbines, and a single maintenance base. A time horizon in the model specifies the duration over which the fleet optimization is evaluated, which is expressed in terms of months and days. Additionally, the model defines the maximum number of work hours per day in which maintenance can be executed. The time lost due to transit is deducted from the amount of time available for maintenance tasks on any given day. A maximum fleet size can be set to take into account the maximum number of maintenance vehicles imposed by maintenance base size restrictions.

The strategy in this model is a combination of corrective and preventive maintenance operations. The model differentiates maintenance tasks based on the number of tasks, the cost of the operation, and the number of hours of work required before completion. Corrective maintenance tasks are assumed to be performed as a result of a critical failure, and the wind turbine is rendered inoperable until repaired. Preventive maintenance tasks can be completed at any time during the planning horizon and only cause downtime when technicians are working on the wind turbine. The wind farm availability is calculated as a function of downtime and is time-based. It can be modeled that one maintenance task cannot begin until another maintenance task is completed. All maintenance technicians on a vessel are assumed to be able to work on a maintenance task at the same time. Work on maintenance tasks is measured in manhours, so a vessel with three maintenance technicians can complete three manhours of work in one hour. The model keeps track of whether or not maintenance tasks are completed by evaluating if sufficient man-hours are assigned to the task.

It is assumed that a vessel can be chartered only from the start to the end of a month. Long charter contracts can be set to be less expensive per month than short charter contracts. Aside from chartering costs, vessels may have fixed costs associated with them for owning the vessel for a set period of time. The model will account for only transit between the maintenance base and the wind farm. Weather conditions may prevent vessels from being used on a given day if the conditions are worse than the maximum rated conditions that a vessel can operate in. The simplified transit assumptions represent CTVs because they travel to and from the wind farm once per day. Other maintenance vehicles, such as helicopters or SOVs, travel to and from the wind farm multiple times a day or can stay offshore for extended periods of time and are thus not accurately quantified in the model.

Only direct emissions from vessels are used to calculate GHG emissions. The amount of fuel used by a vessel depends on how much time it spends in transit and how much fuel it uses while idling/loitering. To account for differences in fuel costs and emissions, different fuel types can be used for different vessel types. The vessel speed and the distance between the maintenance base and the wind farm determine the amount of transit time and the amount of time spent idling/loitering depends on the number of hours that are being worked on a maintenance task.

It is possible to assign penalty costs if maintenance tasks are not completed by the end of the planning horizon. If all maintenance tasks must be completed, the model can force all solutions to finish the maintenance tasks. The model also includes the costs of maintenance technicians and incorporates historical electricity prices and wind turbine capacity factors to estimate the lost electricity produced during downtime.

1. Indices

n	Denotes the month number
l	Denotes the month number when a vessel contract expires
p	Denotes the day number
τ	Denotes the turbine number
m	Denotes the maintenance task number
v	Denotes the vessel type number

2. Sets

N	Set of all months
V	Set of all vessels
L	Denotes until which month a vessel is chartered
M	Denotes the number of maintenance activities
M^{PREV}	Set of all preventive maintenance tasks

M^{CORR}	Set of all corrective maintenance tasks
T	Set of all wind turbines
P	Set of all days
P_n	Set of all days that belong to month n
A_n	The set of all ancestor months

3. Coefficients and parameters

C_{nvl}^{TC}	Chartering cost for vessel of type v in month n with expiration in l
C_{nv}^{F}	Fixed costs of operating vessel of type v in month n
G_v	Capacity that a vessel of type v uses
M^D	Vessel capacity of the base
C_{mv}^{M}	The costs of using vessel v on maintenance task m per manhour
C_p^{DTC}	Downtime costs per day of a turbine on day p
M_v^{CREW}	Crew size of a vessel type v
$P_{m\tau}^{BD}$	Day on which a breakdown of maintenance type m on turbine τ happens
C_v^V	Costs of using a vessel of type v for transit per hour
T_v^T	Amount of time it takes to travel back and forth to the wind farm with a vessel of type v
C_m^P	Penalty costs of failing to complete the maintenance task m by the end of the planning horizon
$C_v^{GHG-TRANSIT}$	Amount of GHG emissions by using a vessel of type v for transit per trip to the wind turbine and back
$C_v^{GHG-IDLE}$	Amount of GHG emissions due to idling per hour
$T_{m\tau}^M$	Amount of manhours that maintenance task m requires for turbine τ before it is completed
T^{MAX}	Maximum amount of hours that can be worked on a day
M_v^K	Maximum weather condition that a vessel of type v can operate in
U_{pv}	Weather condition on day p
M^{BIG}	Big-M number used for linearization of cost objective function

4. Variables

x_{nvl}	Amount of vessels of type v chartered in month n until month l
w_{nv}	Amount of vessels of type v available due to long time chartering in month n
u_{npv}	Amount of vessels of type v used for maintenance in month n on day p

$t_{pmv\tau}$	Amount of manhours that vessels of type v conduct on maintenance task m on turbine τ on day p
$t_{pmv\tau}^{LIN}$	Variable of the amount of manhours that vessels of type v conduct on maintenance task m on turbine τ on day p and is used for linearization
$\gamma_{pm\tau}$	$\begin{cases} 1 & \text{if task } m \text{ on turbine } \tau \text{ is completed on day } p \\ 0 & \text{if task } m \text{ on turbine } \tau \text{ is not completed on day } p \end{cases}$
$\beta_{m\tau}$	$\begin{cases} 1 & \text{if task is not completed by the planning horizon end} \\ 0 & \text{if task is completed by the planning horizon end} \end{cases}$

5. Objective functions

$$z^{Cost} = \sum_{n\in N}\sum_{v\in V}\sum_{l\in L} C_{nvl}^{TC} x_{nvl} \tag{1a}$$

$$+ \sum_{n\in N}\sum_{v\in V} C_{nv}^{F} w_{nv} \tag{1b}$$

$$+ \sum_{p\in P}\sum_{\tau\in T}\sum_{m\in M}\sum_{v\in V} C_{mv}^{M} t_{pmv\tau} \tag{1c}$$

$$+ \sum_{p\in P}\sum_{\tau\in T}\sum_{m\in M^{PREV}}\sum_{v\in V} C_p^{DTC} \frac{t_{pmv\tau}}{24M_v^{CREW}} \tag{1d}$$

$$+ \sum_{p\in P}\sum_{\tau\in T}\sum_{m\in M^{CORR}} C_p^{DTC}(p-P_{m\tau}^{BD})\gamma_{pm\tau} \tag{1e}$$

$$+ \sum_{p\in P}\sum_{\tau\in T}\sum_{m\in M^{CORR}}\sum_{v\in V} C_p^{DTC} \frac{t_{pmv\tau}^{LIN}}{24M_v^{CREW}} \tag{1f}$$

$$+ \sum_{\tau\in T}\sum_{m\in M^{CORR}} C_p^{DTC}\beta_{m\tau}(|P|-P_{m\tau}^{BD}) \tag{1g}$$

$$+ \sum_{n\in N}\sum_{p\in P_n}\sum_{v\in V} C_v^V u_{npv} T_v^T \tag{1h}$$

$$+ \sum_{m\in M}\sum_{\tau\in T} C_m^P \beta_{m\tau} \tag{1i}$$

$$z^{Emissions} = \sum_{n\in N}\sum_{p\in P_n}\sum_{v\in V} C_v^{GHG-TRANSIT} u_{npv} \tag{2a}$$

$$+ \sum_{p\in P}\sum_{v\in V}\sum_{m\in M}\sum_{\tau\in T} C_v^{GHG-IDLE} \frac{t_{pmv\tau}}{M_v^{CREW}} \tag{2b}$$

$$z^{Availability} = 1 - \frac{1}{|P||T|}\left(\sum_{m\in M^{CORR}}\sum_{\tau\in T}\beta_{m\tau}(|P|-P_{m\tau}^{BD})\right. \tag{3a}$$

$$+ \sum_{p\in P}\sum_{\tau\in T}\sum_{m\in M^{CORR}}(p-P_{m\tau}^{BD})\gamma_{pm\tau} \tag{3b}$$

$$+ \sum_{p\in P}\sum_{\tau\in T}\sum_{m\in M^{CORR}}\sum_{v\in V}\frac{t_{pmv\tau}^{LIN}}{24M_v^{CREW}} \tag{3c}$$

$$\left.+ \sum_{p\in P}\sum_{\tau\in T}\sum_{m\in M^{PREV}}\sum_{v\in V}\frac{t_{pmv\tau}}{24M_v^{CREW}}\right) \tag{3d}$$

6. Constraints

Vessel balance constraints

$$\sum_{l \in L} x_{nvl} + w_{a(n)v} - \sum_{n' \in A_n} x_{n'v\,a(n)} = w_{nv} \qquad \forall n \in N \backslash \{1\}, v \in V, n \le l \tag{4}$$

$$\sum_{l \in L} x_{nvl} = w_{nv} \qquad \forall n = 1, v \in V \tag{5}$$

$$\sum_{v \in V} G_v w_{nv} \le M^D \qquad \forall n \in N \tag{6}$$

$$u_{npv} \le w_{nv} \qquad \forall n \in N, p \in P_n, v \in V \tag{7}$$

Weather accessibility constraints

$$(M_v^K - U_{pv}) \sum_{m \in M} \sum_{\tau \in T} t_{pmv\tau} \ge 0 \qquad \forall p \in P, v \in V \tag{8}$$

Maintenance constraints

$$\sum_{m \in M} \sum_{\tau \in T} t_{pmv\tau} \le E_v M_v^{CREW} (T^{MAX} - T_v^T) u_{npv} \qquad \forall n \in N, p \in P_n, v \in V \tag{9}$$

$$\sum_{p \in P} \sum_{v \in V} t_{pmv\tau} \ge T_{m\tau}^M (1 - \beta_{m\tau}) \qquad \forall m \in M, \tau \in T \tag{10}$$

$$\sum_{p' \in \{(p+1),...,|P|\}} \sum_{v \in V} t_{p'mv\tau} \le T_{m\tau}^M (1 - \gamma_{pm\tau}) \qquad \forall p \in P, m \in M, \tau \in T \tag{11}$$

$$\sum_{p \in P} \gamma_{pm\tau} + \beta_{m\tau} = 1 \qquad \forall m \in M, \tau \in T \tag{12}$$

$$\sum_{v \in V} \left(\frac{t_{pmv\tau}}{M_v^{CREW}} \right) \le T^{MAX} \qquad \forall m \in M, \tau \in T, p \in P \tag{13}$$

$$(p - P_{m\tau}^{BD}) \sum_{v \in V} t_{pmv\tau} \ge 0 \qquad \forall p \in P, m \in M^{CORR}, \tau \in T \tag{14}$$

$$\sum_{v \in V} t_{pmv\tau} \ge \gamma_{pm\tau} \qquad \forall p \in P, m \in M, \tau \in T \tag{15}$$

$$\sum_{v \in V} \sum_{p' \in \{0,...,p\}} t_{p,m_2,v,\tau} \le (1 - \gamma_{p,m_1,\tau}) T_{m_2}^M \qquad \forall p \in P, \tau \in T \tag{16}$$

Big M constraints

$$t_{pmv\tau}^{LIN} \ge t_{pmv\tau} - M^{BIG}(1 - \gamma_{pm\tau}) \qquad \forall v \in V, p \in P, m \in M^{CORR}, \tau \in T \tag{17}$$

$$t_{pmv\tau}^{LIN} \le M^{BIG} \gamma_{pm\tau} \qquad \forall v \in V, p \in P, m \in M^{CORR}, \tau \in T \tag{18}$$

$$0 \le t_{pmv\tau}^{LIN} \le t_{pmv\tau} \qquad \forall v \in V, p \in P, m \in M^{CORR}, \tau \in T \tag{19}$$

Integrality constraints

$$t_{pmv\tau} \in \mathbb{R}_{\ge 0} \qquad \forall p \in P, v \in V, m \in M, \tau \in T \tag{20}$$

$$x_{nvl} \in \mathbb{Z}_{\ge 0} \qquad \forall n \in N, v \in V, l \in L \tag{21}$$

$$w_{nv} \in \mathbb{Z}_{\ge 0} \qquad \forall n \in N, v \in V \tag{22}$$

$$t_{pmv\tau}^{LIN} \in \mathbb{R}_{\ge 0} \qquad \forall p \in P, v \in V, m \in M, \tau \in T \tag{23}$$

$$u_{npv} \in \mathbb{Z}_{\ge 0} \qquad \forall n \in N, p \in P_n, v \in V \tag{24}$$

$$\gamma_{pm\tau} = \begin{cases} 1 \\ 0 \end{cases} \qquad \forall p \in P, m \in M, \tau \in T \tag{25}$$

$$\beta_{m\tau} = \begin{cases} 1 \\ 0 \end{cases} \qquad\qquad \forall m \in M, \tau \in T \qquad (26)$$

The first term of the cost objective function z^{Cost} in eq. (1a) are the charter costs for chartering a vessel of type v from month n until month l. The variable x_{nvl} is defined as the number of vessels of type v that are chartered from month n until month l. In the case that $x_{1,4,2} = 3$, this would indicate that 3 units of vessel type 4 should be chartered from month 1 to month 2, meaning that the vessel is chartered for 2 months in total. The parameter C_{nvl}^{TC} denotes the costs of chartering a vessel of type v from month n until month l. The set N is the set of all months. A set V is defined as the set that includes all vessel types. The set L is the set that indicates until which months vessels can be chartered.

The second term consists of the fixed costs of owning a vessel fleet. The variable w_{nv} denotes the number of vessels of type v in month n. The variable w_{nv} is different from x_{nvl} as the latter denotes the number of contracts and the length of the contracts that are required, while the former denotes the actual fleet size in a certain month as a result of the contract length x_{nvl}. The parameter C_{nv}^{F} denotes the fixed costs of owning a vessel of type v in month n.

The term in eq. (1c) are the costs due to conducting maintenance per manhour of work. The variable $t_{pmv\tau}$ is the variable that denotes the number of manhours a vessel of type v conducts on maintenance task m. The parameter C_{mv}^{M} are the costs of conducting maintenance on task m while using vessel v per manhour worked on a task.

The term in eq. (1d) is the downtime costs due to preventive maintenance. The parameter M_{v}^{CREW} represents the amount of crew that is onboard a vessel. The amount of days that the wind turbine is offline due to maintenance on the wind turbine is expressed as the number of manhours $t_{pmv\tau}$ divided by the amount of crew M_{v}^{CREW} and by 24 hours. The parameter C_{p}^{DTC} is a parameter that is equal to the number of costs lost for every 24 hour of wind turbine downtime on a given day p.

The downtime costs due to corrective maintenance can be found in eq. (1e), eq. (1f) and eq. (1g). The variable $\gamma_{pm\tau}$ is a binary variable that is equal to 1 if a maintenance operation m on wind turbine τ is completed on day p and is equal to 0 if this is not the case. The binary variable $\beta_{m\tau}$ is a binary variable that is equal to 1 if the maintenance task m on wind turbine τ is not completed by the end of the planning horizon and equal to 0 if it is completed somewhere in the planning horizon. The parameter $P_{m\tau}^{BD}$ denotes the day on which the breakdown happens. The parameter $|P|$ stands for the total amount of days in the planning horizon. In case a maintenance task is completed on the day p, eq. (1e) counts the number of days between the occurrence of the breakdown and the repair of the breakdown. This term is only added when the maintenance is completed on that specific day because only then it is multiplied with $\gamma_{pm\tau} = 1$. The number of days between the breakdown and the repair is then multiplied by the costs of downtime C_{p}^{DTC}. It could be that there is still time that is spent on a maintenance task on the day it is completed and still

causes the wind turbine to be broken down in the first part of the day. This is accounted for by eq. (1f), by summing up the number of hours that are being worked on a wind turbine on the day that it is completed. Note that $t_{pmv\tau}^{LIN}$ is a linearization of $t_{pmv\tau}\gamma_{pm\tau}$ using the big-M method, so only the amount of hours that are worked on the day on which the maintenance tasks are completed are nonzero. In the case that a maintenance task is not completed, there are still downtime costs. However, $\gamma_{pm\tau} = 0$ for all days and eq. (1e) will not capture these costs as $\gamma_{pm\tau}$ is never equal to 1. Therefore, the amount of downtime is formulated in eq. (1g) as a function of the variable $\beta_{m\tau}$ in case the maintenance task is not completed in the planning horizon.

The costs due to using a maintenance vehicle to travel to the wind farm and back and additional penalty costs if maintenance operations are not completed by the end of the month can be found in eq. (1h) and eq. (1i), respectively. The variable u_{npv} is defined as the number of vessels of type v that are used to travel to the wind farm and back in month n on the day p. The parameter C_{v}^{V} denotes the number of costs of using a maintenance vehicle at operating speeds per hour, while the parameter T_{v}^{T} denotes the amount of time it takes for a vessel of type v to travel to the wind farm and back.

The terms in eq. (3a), eq. (3b) and eq. (3c) represent the total downtime due to corrective maintenance. The second term in eq. (3d) is the loss of wind farm availability due to preventive maintenance operations. The first part in eq. (3a) is the total amount of availability, represented by 1. The availability function will be divided by the total number of turbines and the total number of days in the planning horizon, $|P|$ and $|T|$ respectively. This will return the wind farm availability over the entire planning horizon, rather than the availability of individual turbines.

Constraint eq. (4) relates the number of vessels of type v in month n that are available to use for maintenance activities, w_{nv}, to the sum of newly chartered vessels in month n until month l, $\sum_{l \in L} x_{nvl}$, plus the number of available vessels from last month, $w_{a(n)v}$, minus the number of vessels of which the contract ended in the previous month, $\sum_{n' \in A_n} x_{n'v\,a(n)}$. The set A_n is the set of all months that lie behind month n. E.g. the set $A_{n=3} = \{1, 2\}$ and the set $A_{n=5} = \{1, 2, 3, 4\}$. Additionally, $a(n)$ denotes the ancestor node before node n. E.g. if $n = 3$, then $a(3) = 2$ and if $n = 5$, then $a(5) = 4$. This constraint holds for all $n \in N$ with the exception of $n = 1$, because no ancestor nodes exist for the first month. Additionally, this constraint only holds such that $n \leq l$ because a vessel cannot be chartered until a month that lies in the past.

Constraint eq. (5) serves the same purpose as constraint eq. (5), but is specifically for the first month. It relates the number of vessels of type v in month n to the number of charter contracts that start in month $n = 1$ until month l.

In eq. (6), the term on the left-hand side of the equation represents the number of vessels of type v that are part of the fleet

in month n, multiplied by the size G_v of the vessel. The right-hand side of the equation is the maximum available space of the maintenance base M^D.

Constraint eq. (7) ensures that the number of vessels that are used for maintenance, u_{npv}, cannot exceed the number of vessels that are available in the fleet, w_{nv}.

Constraint eq. (8) makes sure that vessels cannot be used for maintenance if the weather conditions exceed the maximum conditions that the vessel can operate in. The parameter M_v^K is defined as the weather condition in which a vessel of type v can operate. The parameter U_{pv} denotes the weather condition in month n on day p. Some maintenance vehicles could have different limiting types of weather conditions, e.g. wave height for vessels and wind speed for helicopters. For that reason, U_{pv} could also be a different type of weather condition depending on the vessel type v. The constraint subtracts U_{pv} from M_v^K and is multiplied by the sum of manhours that a spends on a task on a given day. In the case that $M_v^K - U_{pv}$ is smaller than 0, the sum of manhours that a vessel spends working on a task has to be equal to zero in order to not violate the right-hand side condition. This can only occur if the weather value U_{pv} is higher than the maximum weather conditions that a vessel can operate in M_v^K. In the case that $M_v^K - U_{pv}$ is larger than 0, the sum of manhours that a maintenance vehicle works on, is not constrained by the weather.

Constraint eq. (9) ensures that if the total amount of manhours that is worked on a maintenance task m on vessel τ on day p in month n by vessel v, $t_{pmv\tau}$, is larger than 0, the right amount of vessels u_{npv} are used for the maintenance operation. Additionally, this constraint sets an upper limit to the amount of time that can be worked on a maintenance task by u_{npv} amount of vessels. This is defined as $T^{MAX} - T_v^T$, which is the maximum amount of operating time minus the time needed to travel to the wind farm and back. An efficiency factor E_v can be set to account for the loss of productivity of the crew, e.g. due to breaks.

Constraint eq. (10) makes sure that if not enough time is spent on a maintenance operation, the task will be assigned as uncompleted. The parameter T_m^M is the required amount of manhours needed to complete maintenance task m.

Constraint eq. (11) ensures that once a maintenance task is completed, no more hours are put into the maintenance operation on the following days after the completed maintenance task. Additionally, it limits the number of hours that are put in the task on the following days if the task is not completed to no more than the maximum amount of hours that are required for a maintenance task. In the case that $\gamma_{pm\tau} = 1$, the right-hand side of the equation becomes equal to 0. If the right-hand side of the equation is equal to zero, that means that the left-hand side of the equation has to be less or equal to zero. Since negative worked manhours $t_{pmv\tau}$ do not represent anything realistic, this means that the only feasible condition that satisfies this constraint is that the left-hand side sum is equal to 0 as well. Note that the sum of manhours that are being worked on is summed over $p' \in \{(p+1), ..., |P|\}$, which represents the set of remaining days after day p.

Constraint eq. (12) makes sure that a maintenance task is either completed on a particular day or that a maintenance task is not completed by the end of the month. This is ensured by summing up the variable which is defined to be equal to 1 if a maintenance task is completed on a particular day p, $\gamma_{pm\tau}$ and adding the binary variable $\beta_{m\tau}$ that is defined to be equal to 1 if the maintenance task is not completed by the end of the year. As all variables are binary variables, this constraint makes sure that only one of the variables on the left-hand side can be equal to 1. Therefore, the maintenance task can only be completed once or can remain uncompleted at the end of the planning horizon.

Constraint eq. (13) ensures that the maximum amount of hours that all vessels can work on a maintenance task on a given day does not exceed the maximum amount of hours that can be worked on a day. The reason for adding this constraint is to avoid situations where several maintenance vehicles can work on the maintenance task simultaneously and complete it faster, while this might be infeasible. In the constraint, this is expressed on the left-hand side by summing up the number of hours that each vessel of type v works on a task m from turbine τ on the day p in month m and dividing this value by the crew size M_v^{CREW}. On the right-hand side, there is the maximum amount of hours that can be worked on maintenance tasks each day.

Constraint eq. (14) makes sure that no hours can be worked on a corrective maintenance task if the breakdown of the turbine did not occur yet. This is expressed by subtracting the current day p by the parameter that represents the day that the breakdown occurs $P_{m\tau}^{BD}$ and multiplying this with the number of manhours that each vessel puts in this task. In the case that the current day is less or equal to the day that the breakdown occur, $p - P_{m\tau}^{BD} \leq 0$, that means that the sum of manhours that is worked on that task has to be equal to 0 in order to satisfy the right-hand side of the constraint. In other words, the maintenance tasks cannot be worked on. In the case that the current day is larger than the day that the breakdown occurs, the sum of manhours can take on any positive value or 0, thus the maintenance tasks can be worked on.

Constraint eq. (15) says that $\gamma_{pm\tau}$ can only be equal to 1 if at least one manhour has been worked on the task on that day and ensures that $\gamma_{pm\tau} = 1$ once a maintenance task is completed.

The constraint in eq. (16) ensures that a task m_2 cannot be started before a task m_1 is completed. The variable $\gamma_{p,m_1,\tau} = 1$ if the first maintenance task is completed. If this is the case, the right-hand side of this constraint becomes equal to 0. The remaining left-hand side of the constraint is the number of man-hours that are worked on the second maintenance task from day 0 until day p. The left-hand side and right-hand side together make sure that the number of man-hours that is worked on the second maintenance task m_2 is equal 0 up until m_1 is completed.

Constraint eq. (17), eq. (18), and eq. (19) are constraints that are used for the big-M method. They ensure that $t_{pmv\tau} = t_{pmv\tau}^{LIN}$ only if $\gamma_{pm\tau} = 1$. The variable $t_{pmv\tau}^{LIN}$ is used in the cost and availability objective functions in eq. (1f) and eq. (3c). Constraint eqs. (20) to (26) are integrality constraints.

B. Epsilon constraint method

Models with multiple objective functions are known as multi-objective optimization models. The methods for solving multi-objective models are classified into two types[22]. The first method is the scalarization method, which combines multiple objective functions into a single scalar fitness function and yields only one solution. The second method is the Pareto method, which treats the objective functions as independent vectors and yields one or more solutions. The Pareto method has one advantage over the scalarization method in that it shows an overview of the trade-offs between solutions, whereas the scalarization method does not show trade-offs between solutions.

The epsilon constraint method is a Pareto method that changes the model formulation by setting some of the objectives as constraints. The model is then solved several times, with the objective functions set as constraints being perturbed with each iteration. This method does not solve the optimization model directly but modifies the model formulation so that it can be used to find and estimate a set of non-dominated solutions on the Pareto front.

Let us define an arbitrary multi-objective optimization model in which the three objective functions $f_1(x_n)$, $f_2(x_n)$ and $f_3(x_n)$ should be minimized. The objective functions are subjected to equality constraints $h_i(x_n)$ and inequality constraints $g_j(x_n)$, such that:

$$\text{minimize}\{f_1(x_n), f_2(x_n), f_3(x_n)\} \tag{27}$$

$$h_i(x_n) = 0 \qquad\qquad \forall i \in I \tag{28}$$
$$g_j(x_n) \leq 0 \qquad\qquad \forall j \in J \tag{29}$$

This problem will now be reformulated by setting only one of the objective functions as an objective function, which will be $f_1(x_n)$ in the current example. The objective functions $f_2(x_n)$ and $f_3(x_n)$ are placed on the left-hand side of less-than-equal constraints. The right-hand side of these constraints will contain C_2 and C_3, which are parameters that will be perturbed, such that:

$$\text{minimize}\{f_1(x_n)\} \tag{30}$$

$$h_i(x_n) = 0 \qquad\qquad \forall i \in I \tag{31}$$
$$g_j(x_n) \leq 0 \qquad\qquad \forall j \in J \tag{32}$$
$$f_3(x_n) \leq C_3 \tag{33}$$
$$f_2(x_n) \leq C_2 \tag{34}$$

There are two important concepts to the epsilon constraint method. The first concept is that a MIP solver can be used to solve the model. By doing so, the solver will try to find the lowest possible value for $f_1(x_n)$ in the feasible space (assuming the model should be minimized). The second concept is that parts of the feasible space of the original optimization model can become infeasible once $f_3(x_n)$ and $f_2(x_n)$ are set as constraints. Solving the reformulated single-objective model

for different perturbations can be used to approximate solutions that lie on the Pareto front if the perturbations of C_3 and C_2 are chosen correctly.

The epsilon constraint method is visualized in fig. 5 and fig. 6. Setting objective functions as constraints can be represented by planes that cut off sections of the feasible region, as shown in fig. 5. The location of each of these planes is determined by the values for C_3 and C_2. Changing these values causes the red planes to move along their respective objective function axes.

Finding a good selection of values for C_3 and C_2 is one of the challenges of the epsilon constraint method. The constraint can cut off the entire feasible region if the values for C_3 and C_2 are set too low. If the values for C_3 and C_2 are set too high, the constraints may not effectively cut off the feasible space, resulting in an inaccurate estimate of the Pareto front shape. The method for defining a set of perturbations for C_3 and C_2 is to find upper and lower bounds for the perturbed values. A simple approach is to define the lower bound as the minimum value of the feasible space of the respective objective function, and the upper bound as the maximum value of the feasible space of the respective objective function. The first objective function to do this for could be either $f_3(x_n)$ or $f_2(x_n)$, but $f_3(x_n)$ has been selected for demonstration purposes. The lower bound is found by solving:

$$\text{minimize}\{f_3(x_n)\} \tag{35}$$

$$h_i(x_n) = 0 \qquad\qquad \forall i \in I \tag{36}$$
$$g_j(x_n) \leq 0 \qquad\qquad \forall j \in J \tag{37}$$

Similarly, the upper bound can be found by solving:

$$\text{maximize}\{f_3(x_n)\} \tag{38}$$

$$h_i(x_n) = 0 \qquad\qquad \forall i \in I \tag{39}$$
$$g_j(x_n) \leq 0 \qquad\qquad \forall j \in J \tag{40}$$

The lower and upper bound values for $f_3(x_n)$ will be referred to as $\min(f_3)$ and $\max(f_3)$, respectively. They are represented as the white planes in fig. 5 b). Now that a upper and lower bound for C_3 are found, perturbations of C_3 that lie between $\min(f_3)$ and $\max(f_3)$ can be made. For now it is assumed that the values of are C_3 are evenly spaced, such that:

$$C_3 = \min(f_3) + \mathscr{E}_n \qquad n \in \{0, 1, ..., N\} \tag{41}$$

and

$$\mathscr{E}_n = n/N(\max(f_3) - \min(f_3)) \qquad n \in \{0, 1, ..., N\} \tag{42}$$

So far, the upper and lower bounds for $f_3(x_n)$ are defined, but not for $f_2(x_n)$. Before the bounds on $f_2(x_n)$ are defined, one must realize that the lower and upper bounds of $f_2(x_n)$ of subsets of the feasible solution space are equal or less to that of the feasible solution space. This means that for certain subsets of the feasible region, i.e. when a portion of the feasible solution space is cut off by imposing a constraint of

$f_3(x_n)$, the upper and lower bounds of $f_2(x_n)$ in this subset may differ from the upper and lower bounds of $f_2(x_n)$ in the full feasible space. As a result, using the full feasible space upper and lower bounds for perturbations of C_2 can lead to models without a feasible solution.

To avoid C_2 values that cause the model to have no feasible solutions, the upper and lower bounds for $f_2(x_n)$ must be calculated for each perturbed C_3 value. For every perturbed C_3 value, two additional optimization models will be solved to find corresponding upper and lower bounds for $f_2(x_n)$ that belongs to the perturbed value of C_3. This will be achieved by adding the $f_3(x_n)$ constraint with the corresponding value for C_3 when finding the upper and lower bounds for $f_2(x_n)$. This can be observed in fig. 5 c), where the $f_3(x_n)$ constraint is visible (red plane) when calculating the upper and lower bounds for $f_2(x_n)$ that belong to this constraint (transparent planes).

Finding the upper and lower bounds of $f_2(x_n)$ for a given C_3 can be mathematically formulated as solving:

$$\text{minimize}\{f_2(x_n)\} \tag{43}$$
$$\text{maximize}\{f_2(x_n)\} \tag{44}$$

$$h_i(x_n) = 0 \qquad \forall i \in I \tag{45}$$
$$g_j(x_n) \leq 0 \qquad \forall j \in J \tag{46}$$
$$f_3(x_n) \leq \min(f_3) + \mathscr{E}_n \qquad n \in \{0, 1, ..., N\} \tag{47}$$

The upper and lower bounds of $f_2(x_n)$ are referred to as $\min(f_2)$ and $\max(f_2)$. The perturbed values of C_2 range over $\min(f_2)$ and $\max(f_2)$. If they are evenly spread, it can be defined as:

$$C_2 = \min(f_2) + \mathscr{E}_m \qquad m \in \{0, 1, ..., M\} \tag{48}$$

and

$$\mathscr{E}_m = m/M(\max(f_2) - \min(f_2)) \quad m \in \{0, 1, ..., M\} \tag{49}$$

Now that the values for C_2 and C_3 are defined, the optimization model in eq. (30) can be solved multiple times for each combination of C_2 and C_3 to find Pareto optimal points. The number of optimization models that are solved is dependent on the number of perturbations of C_2 and C_3 in between their respective upper and lower bounds. A higher amount of points results in a higher number of points on the Pareto front, but also requires more optimization models to be solved.

1. Improving the selection of C_2 and C_3

The values that were set for the bounds of C_2 and C_3 ensure that the constraints for the objective functions iterate over the fullll feasible region of the solution space. However, the disadvantage of this method is that some solutions may accumulate in the same location in the feasible space. The accumulated solutions require a model to be solved, but they do not provide a new Pareto optimal solution with unique corresponding objective values. To avoid wasting computational resources, each Pareto point should ideally have objective function values that differ from other solutions. Simultaneously, the range over which the Pareto points are calculated

should ideally still cover the entire Pareto front. This can be achieved by using the Nadir point to determine the maximum bound. The Nadir point is defined as the combination of the worst possible values for each objective in the set of all non-dominated Pareto optimal solutions. For models with more than two objective functions, the Nadir point can be found using the anchor points. For models with more than two objective functions, anchor points can no longer be used to find the exact Nadir point and can only be used as an estimate[23,24]. Algorithms have been developed to determine the exact Nadir point[25], but combining this with the epsilon constraint method can significantly complicate the algorithm[26]. The current study will not incorporate an exact method to find the Nadir point and instead use a similar approach to payoff tables made up of anchor points from Mavrotas and Florios[27]. This keeps the implementation of the epsilon constraint method relatively simple, but it can lead to underestimation of upper bounds.

The following changes are made to find the bounds for C_2 and C_3. First, the upper and lower bounds for C_3 are determined. The method for determining the lower bound remains the same, and it is determined by solving the model and minimizing $f_3(x_n)$ independently of the other objective functions. The problem that has to be solved is formulated as:

$$\text{minimize}\{f_3(x_n)\} \tag{50}$$

$$h_i(x_n) = 0 \qquad \forall i \in I \tag{51}$$
$$g_j(x_n) \leq 0 \qquad \forall j \in J \tag{52}$$

Finding the upper bound is now slightly different, as the model is solved twice now. The first time it is solved for $f_1(x_n)$, independently of the other objective functions, and the second time it is solved for $f_2(x_n)$, independently of the other objective functions. The highest value of f_3 from both solutions is then set as the upper bound for $f_3(x_n)$. This is formulated as solving the problems:

$$\text{minimize}\{f_1(x_n)\} \tag{53}$$
$$\text{minimize}\{f_2(x_n)\} \tag{54}$$

$$h_i(x_n) = 0 \qquad \forall i \in I \tag{55}$$
$$g_j(x_n) \leq 0 \qquad \forall j \in J \tag{56}$$

A similar process follows for the bounds of C_2. The upper and lower bounds for C_2 must be found for every perturbation of C_3. Finding the lower bound of C_2 is obtained by solving the model for $f_2(x_n)$.

$$\text{minimize}\{f_2(x_n)\} \tag{57}$$

$$h_i(x_n) = 0 \qquad \forall i \in I \tag{58}$$
$$g_j(x_n) \leq 0 \qquad \forall j \in J \tag{59}$$
$$f_3(x_n) \leq C_3 \tag{60}$$

Since an equality constraint for $f_3(x_n)$ is added to the model while finding the bounds for C_2, the value of $f_3(x_n)$ is fixed. To find the upper bound of C_2, only the minimum of $f_1(x_n)$ now has to be found and the value of f_3 that belongs to this solution is extracted.

$$\text{minimize}\{f_1(x_n)\} \tag{61}$$

$$h_i(x_n) = 0 \qquad \forall i \in I \tag{62}$$
$$g_j(x_n) \le 0 \qquad \forall j \in J \tag{63}$$
$$f_3(x_n) \le C_3 \tag{64}$$

The current method that is used to improve the selection of C_2 and C_3 is similar to the payoff table method as both approaches use anchor points to estimate the upper bounds. However, the current method calculates the bounds for C_2 for each perturbation of C_3. The advantage is that it ensures that the combinations of C_2 and C_3 are within the feasible space, thus not leading to infeasible models. The disadvantage of this is that it requires two additional problems to be solved to find the upper and lower bounds of C_2 for each perturbation of C_3. Although the epsilon constraint method in the current model is solved with an exact solving method by using MIP, this condition is not sufficient to guarantee that all solutions are non-dominated[28].

III.   RESULTS

A.   Case study definition

Two case studies are evaluated in the current research. Both case studies are based on the Princess Amalia Wind Farm, which is a wind farm that is currently operational. This wind farm is located offshore of IJmuiden in the Netherlands and was commissioned in 2008. It consists of 60 Vestas V80 wind turbines, each with a maximum rated power of 2 MW, for a total capacity of 120 MW. In both case studies, only one maintenance base is considered, which is assumed to be located in the port of IJmuiden. Case study 1 has a one-year time horizon, while Case Study 2 has a six-month time horizon. Each year consists of 12 months and each month in a year is assumed to consist of 30 days. Each year is assumed to have 12 months, with each month having 30 days.

Case study 1 has only a visual inspection of the wind turbine blades, which is modeled as a preventive maintenance task that must be performed on all wind turbines in the Princess Amalia wind farm. Case study 2 adds two more maintenance types on top of the visual inspection. The first is leading edge protection maintenance for some turbines, and the second is a critical failure corrective maintenance task. Critical failures are assumed to occur once a month at a single turbine in the wind farm. Maintenance engineers can work on a maintenance task for a maximum of 10 hours. The parameters used for maintenance tasks are listed in table II.

The choice can be made between three different maintenance vehicles for both case studies 1 and 2. The three op-

tions are CTVs with various hull designs: mono-hull, catamaran, and trimaran. The various designs of the vessel hulls give them unique characteristics, such as transit speed. In any given month, the maximum fleet size cannot exceed four vessels. It is assumed that each vessel can only transport one maintenance team of three technicians at a time. The vessel costs are assumed to be charter costs, fuel costs, and fixed costs related to upkeep costs. The significant wave height H_s is assumed to be a limiting factor for vessel access to the wind farm. Each vessel has a maximum wave height H_s that it can operate at. On any given day, the wave height H_s is determined using historical data. The parameters used for the vessels can be found in table V and table VI.

The vessels used for maintenance are assumed to be the only sources of direct emissions. These vessels consume fuel while in transit between the maintenance base and the wind farm. Additionally, vessels burn fuel using generators to power auxiliary systems on board the vessel while the crew is conducting maintenance tasks at the wind turbine. Because the fleet optimization model in the current study only models transit between the wind farm and the maintenance base, the emissions from transit between wind turbines are not included. Some of the parameters on the emissions can be found in table III and table IV.
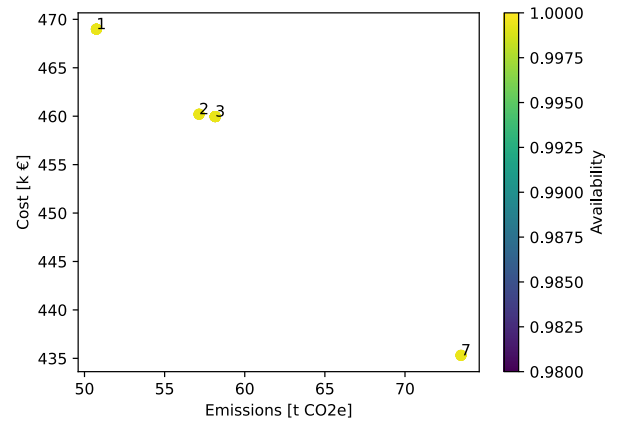
FIG. 1. Plot of the Pareto front of case study 1.

B.   Computational setup

The model perturbations are solved using an academic license of the commercial MIP solver Gurobi v.10.0.1. Python is used to model the epsilon constraint method, and Gurobi is used with a Python API. A computing cluster with two Intel Xeon Gold 6326 16 cores 32 threads CPUs running at 2.90GHz and 130762 MB of RAM is used.

Some termination criteria have been established in order to avoid lengthy solution times. The first termination criterion is when a solution with a MIP gap less than 2% is found. The second stopping criterion is after running the model for longer than 10800 seconds. The value of 10800 seconds was deter-

	Optimization model		UWiSE O&M Planner	
	Solution 1	Solution 7	Solution 1	Solution 7
Vessel type 0	-	1 [June, July]	-	1 [June, July]
Vessel type 1	1 [June, July]	-	1 [June, July]	-
Vessel type 2	-	-	-	-
Total costs	€469.0k	€435.3k	€476.7k	€408.3k
Time-based availability	99.93%	99.93%	99.76%	99.77%
GHG emissions	50.7 t CO2e	73.5t CO2e	-	-

TABLE I. Table with a summary of the small case study results from the optimization model and the UWiSE O&M Planner

	Maintenance type	Hours required [h]	Costs per task [€]
Task 1	Critical failure (Corrective)	6	500
Task 2	Visual inspection (Preventive)	6	250
Task 3	Coating reapplication (Preventive)	8	500

TABLE II. Table with maintenance task parameters.

	CO2PerLFuel $[kgCO2e/l]$	CH4PerLFuel $[kgCH4/l]$	N2OPerLFuel $[kgN2O/l]$
MFO	11.27	0.45E-3	0.09E-3

TABLE III. Table with the amount of CO2, CH4 and N2O emissions per fuel type.

CH4Factor $[kgCO2e/kgCH4]$	N2OFactor $[kgCO2e/kgN2O]$
25	298

TABLE IV. Table of the emission factors of CH4 and N2O.

	Type	Crew [teams]	Weather limits	Speed [m/s]	Docking space
CTV 1	Monohull	1	$H_s^{max} = 1.1[m]$	8	1 [Dock space]
CTV 2	Catamaran	1	$H_s^{max} = 1.35[m]$	14	1 [Dock space]
CTV 3	Trimaran	1	$H_s^{max} = 1.6[m]$	16	1 [Dock space]

TABLE V. Table with maintenance vehicle parameters.

		Fuel	Costs		
	Type	Consumption [l/h]	Charter [€/day]	Fuel [€/l]	Fixed [€/month]
CTV 1	MFO	180	3500	1.64	2000
CTV 2	MFO	130	4500	1.64	2000
CTV 3	MFO	150	5000	1.64	2000

TABLE VI. Table with maintenance vehicle parameters on fuel and costs.

	Fleet composition		
	Monohull	Catamaran	Trimaran
1	-	1 [Jun, Jul]	-
2	1 [Apr]	1 [Sep]	-
3	1 [Apr]	1 [Feb]	-
7	1 [Jun, Jul]	-	-

TABLE VII. Table with the objective function values and fleet compositions of a selection of solutions of case study 1.

mined by experimenting and determining which time limits would result in either good convergence of the MIP gap or a MIP gap less than 2%.

C. Case study results

The Pareto front of case study 1 is depicted in fig. 1 by plotting the solutions to the model perturbations. The x-axis of the plot represents the objective function for the GHG emissions, while the y-axis represents the objective function for the costs. The color of the plotted points represents the availability objective function. It can be seen that the Pareto front in fig. 1 shows four distinct solutions with unique objective function values. The first thing to notice is that the values for the time-based wind farm availability objective function are identical across all solutions. This is consistent with the observation that all maintenance tasks in case study 1 are preventive maintenance. Preventive maintenance is modeled so that wind turbines are only shut down when maintenance tasks are completed. Because each solution in the Pareto front plot must complete the same number of preventive maintenance

tasks and each task requires the same number of hours to be worked on, the solutions have the same time-based wind farm availability estimates. The fleet composition of each unique solution in the Pareto front in fig. 1 varies. The fleet compositions are shown in table VII. Solution number 1 charters a vessel of type 1 (catamaran) beginning in June and ending at the end of July. Solutions 2 and 3 have similar compositions, but the months in which the vessels are chartered differ. Solution 2 charters a vessel of type 0 in April and a vessel of type 1 in September, whereas solution 3 charters a vessel of type 0 in April and a vessel of type 1 in June. Finally, solution 7 charters a vessel of type 0 in June and July.

The Pareto front of case study 2 is plotted in fig. 2. Similarly to the Pareto front plots of case study 1, this was achieved by creating a scatter plot of the objective functions from the case study 2 solutions. There are two plots with the same

Objectives			Fleet composition		
f^{Cost}	$f^{Emissions}$	$f^{Availability}$	Mono-hull	Catamaran	Trimaran
1	732	67.2	0.981	-	1 [Jun]	1 [Apr]
39	731	97.3	0.990	1 [Mar, May, Jun]	1 [Apr]	-
42	756	73.5	0.991	1 [Apr]	1 [Feb, Jun]	-
45	741	88.9	0.991	1 [Apr, Jun]	1 [Feb]	-
48	879	66.9	0.995	-	1 [Feb, Mar]	1 [May, Jun]
52	796	83.5	0.994	1 [Jan, May, Jun]	1 [Mar]	-
55	778	97.3	0.994	1 [Jan, Mar, May, Jun]	-	-
58	986	70.0	0.998	-	-	1 [Jan, Feb, Mar, Apr, May, Jun]
63	960	79.0	0.998	1 [Mar, Apr, May, Jun]	-	1 [Jan, Feb]

TABLE VIII. Table with the objective function values and fleet compositions of a selection of solutions.
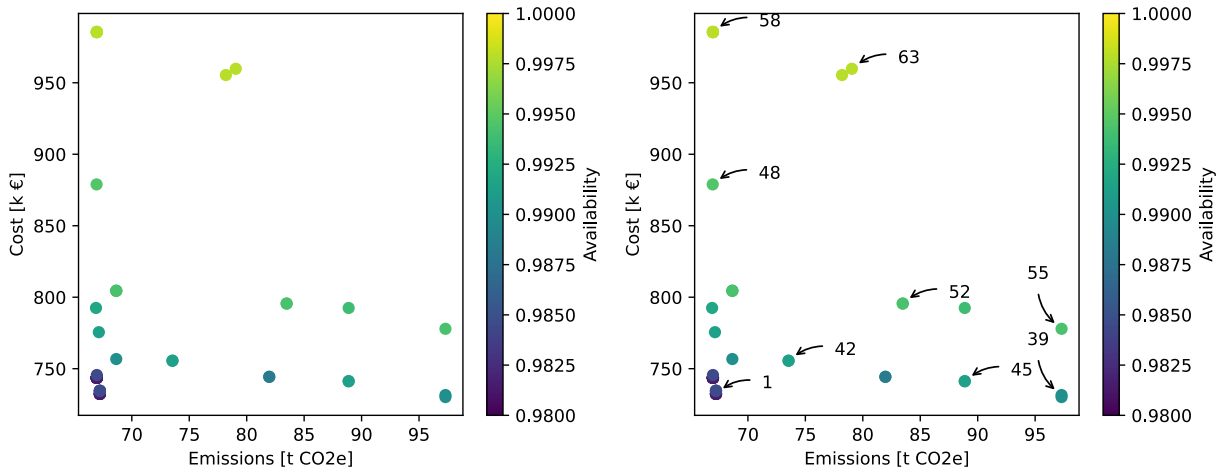
FIG. 2. Plot of the Pareto front of case study 2.

Pareto front in fig. 2. The left and right plots differ in that the right plot highlights some of the solutions by indicating the solution number with an arrow, whereas the left plot is left blank. The x-axis of both plots represents the GHG emission objective function and the y-axis represents the cost objective function. The color of the plotted points represents the availability objective function. When compared to the results of case study 1, it is evident that the amount of unique solutions is greater for case study 2. It can also be seen that the solutions now have distinct time-based wind farm availability objective function values, as the plotted points have different color shades. The fleet compositions that belong to the set of numbered solutions in fig. 2 can be found in **??**. The objective function values that belong to the numbered solutions can be found in table VIII. The results of the fleet compositions in table VIII show that not all solutions have at least one vessel available each month, despite the fact that critical failure corrective maintenance tasks occur once a month. Some solutions have the same vessel in their fleet every month (e.g., solution 58), whereas others have mixed fleet compositions across multiple months (e.g. solution 63). In any given month, none of the solutions have a fleet that consists of more than one vessel.

Convergence to optimality can be visualized by plotting the incumbent (best integer solution), best bound (lower bound to the model), and MIP gap over time. A plot like this can be found in fig. 3 for solution number 60. An arrow marks the points where the fleet composition variables w_{nv} are updated during the solving procedure. This plot shows that the solution has converged to a MIP gap less than the stopping criterion of 2% at just over 200 seconds. Another convergence plot can be found in fig. 4 for solution number 48, but this time without highlighting the points in time during the solving procedure where the fleet composition variables w_{nv} are updated. It is clear that the solution did not reach a MIP gap of less than 2% before the 10800 seconds stopping criteria was met. The difference between the incumbent and best bound ceased to improve after 2000 seconds. A similar phenomenon occurred with solution 24, where the MIP gap ceased to grow. All other solutions reached a MIP gap of less than 2% before the time limit of 10800 seconds was reached.
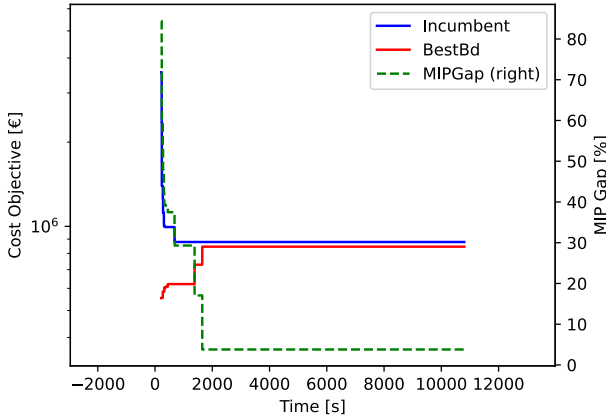
FIG. 3. Plot of the incumbent, the best bound and the MIP gap convergence over time for solution 60.
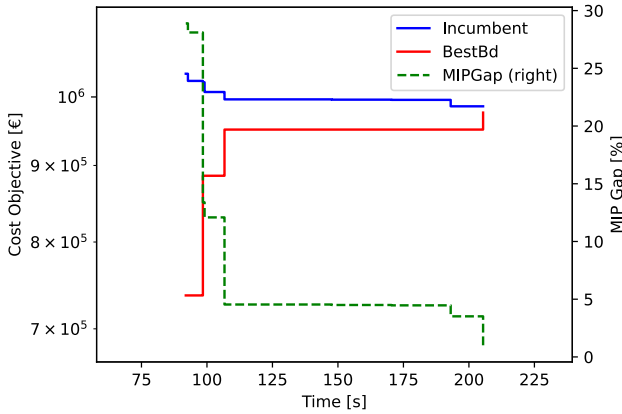
FIG. 4. Plot of the incumbent, the best bound and the MIP gap convergence over time for solution 48

IV. DISCUSSION

Case study 2 yielded a greater number of unique solutions than case study 1. Because the maintenance types in case study 1 were limited to preventive maintenance, all solutions resulted in the same amount of wind turbine downtime. As a result, all solutions had a constant wind farm availability function value. Case study 2 included corrective maintenance, which resulted in solutions with a wider range of wind farm availability values.

When the cost estimates for Case Study 1 were compared in table I, the fleet optimization model and the UWiSE O&M Planner showed good similarities in the cost estimation results. The UWiSE O&M Planner estimated a higher cost for one of the solutions, whereas the optimization model estimated a higher cost for another. This hints at inherent differences between the two models. It is possible that these differences become more pronounced in other case studies, and a

broader range of case studies should be evaluated to see under what conditions the differences become more pronounced.

Before the time limit was reached, most solutions for Case Study 2 and all solutions for Case Study 1 converged to a MIP gap of less than 2%. An interesting phenomenon was observed in two solutions of case study 2 that did not converge in time. The MIP gap appeared to stop improving at a certain point during the solving procedure, as shown in fig. 4. Stuck MIP bounds have been linked to weak MIP model formulation[29], but this does not explain why it occurred in such a small number of perturbed models. The cause of this phenomenon is unknown, and identifying it could improve the consistency of the results.

The effects of the simplifications of routing in the model became evident during the evaluation of the variables. On a single day, multiple preventive maintenance tasks were partially completed. As a result, the maintenance tasks were carried out in parallel rather than serially. This would be inefficient planning because the vessels would spend a significant amount of time in transit between turbines. The model is unable to quantify transit time between wind turbines, resulting in an underestimation of associated fuel consumption and time loss.

The current study has successfully integrated GHG emissions as an objective function in an offshore wind fleet optimization model. The use of multi-stage stochastic fleet optimization models, as found in many other fleet optimization studies, is a reasonable modeling choice given the inherent uncertainty in offshore wind O&M. However, these multi-stage optimization models can be computationally expensive. This study solves a multi-objective model using the epsilon constraint method in conjunction with MIP, which gives insights into the trade-offs between solutions. This comes with a high computational cost, as multiple perturbations of the model have to be solved.

Since the model does not include uncertainty, it is recommended to take a conservative approach when selecting parameters and setting up the fleet optimization model. For instance, it is suggested to check if the historical weather data includes unusually good weather in a month where rough weather conditions are expected. At last, it is recommended to limit the vessel types to those that move to the wind farm and back to shore once a day, such as CTVs. Although the model is not necessarily limited to specific vessel types, it is expected that the fleet optimization model does not accurately model other vessel types such as SOVs, as they can stay offshore for multiple days.

V. CONCLUSION

This research includes the development of the first offshore wind O&M fleet optimization model with GHG emissions as an objective function based on the model of Stålhane et al.[16] and Bolstad et al.[17]. The optimization model that is proposed in this study is formulated as a deterministic MIP model that includes the costs, GHG emissions, and time-based wind farm availability as objective functions. The model supports fleet

decisions on the amount of, charter length, and type of vessels. The cost objective function consists of vessel utilization costs, vessel charter costs, fuel costs, downtime costs, and maintenance costs. The GHG emissions include direct emissions of vessels in transit and idling/loitering. The wind farm availability is based on the amount of downtime of the wind turbines.

Future research should evaluate the possibilities of including stochastics in the model. This could help with incorporating uncertainty into the fleet composition decision-making. Another suggestion for future research is to include the quantification of transit between turbines in the model. This should increase the fidelity of the cost and the GHG emission quantification as a result of transit.

[1] L. Moosmann, A. Siemons, F. Fallasch, L. Schneider, C. Urrutia, N. Wissner, R. Mendelevitch, H. Hermann, and S. Healy, "The cop27 climate change conference, status of climate negotiations and issues at stake," Study for the committee on the Environment, Public Health and Food Safety, Policy Department for Economic, Scientific and Quality of Life Policies, European Parliament (2022), european Parliament, Luxembourg.

[2] Paris Agreement, "United Nations. United Nations Treaty Collection, Chapter XXVII 7. d," (2015).

[3] IRENA, "Future of wind: Deployment, investment, technology, grid integration and socio-economic aspects (a global energy transformation paper)," International Renewable Energy Agency, Abu Dhabi (2019).

[4] I. Komusanac, G. Brindley, D. Fraile, and L. Ramirez, "Wind energy in europe," (2020).

[5] Wind & water works, "Dutch offshore wind guide," (2022).

[6] WindEurope, "Windeurope position on non-price criteria in auctions," (2022).

[7] I. B. Sperstad, M. Stålhane, I. Dinwoodie, O.-E. V. Endrerud, R. Martin, and E. Warner, "Testing the robustness of optimal access vessel fleet selection for operation and maintenance of offshore wind farms," Ocean Engineering 145, 334–343 (2017).

[8] R. Martin, I. Lazakis, S. Barbouchi, and L. Johanning, "Sensitivity analysis of offshore wind farm operation and maintenance cost and availability," Renewable Energy 85, 1226–1236 (2016).

[9] A. Garcia-Teruel, G. Rinaldi, P. R. Thies, L. Johanning, and H. Jeffrey, "Life cycle assessment of floating offshore wind farms: An evaluation of operation and maintenance," Applied Energy 307, 118067 (2022).

[10] E. E. Halvorsen-Weare, C. Gundegjerde, I. B. Halvorsen, L. M. Hvattum, and L. M. Nonås, "Vessel fleet analysis for maintenance operations at offshore wind farms," Energy Procedia 35, 167–176 (2013), deepWind'2013 – Selected papers from 10th Deep Sea Offshore Wind R&D Conference, Trondheim, Norway, 24 – 25 January 2013.

[11] D. D. Diran, "Marine fleet optimization for offshore substation maintenance: An application for the german and dutch offshore transmission grid," TU Delft (2018), master thesis.

[12] C. Gundegjerde, I. B. Halvorsen, E. E. Halvorsen-Weare, L. M. Hvattum, and L. M. Nonås, "A stochastic fleet size and mix model for maintenance operations at offshore wind farms," Transportation Research Part C: Emerging Technologies 52, 74–92 (2015).

[13] M. Stålhane, H. Vefsnmo, E. E. Halvorsen-Weare, L. M. Hvattum, and L. M. Nonås, "Vessel fleet optimization for maintenance operations at offshore wind farms under uncertainty," Energy Procedia 94, 357–366 (2016), 13th Deep Sea Offshore Wind R&D Conference, EERA DeepWind'2016.

[14] A. Gutierrez-Alcoba, E. Hendrix, G. Ortega, E. Halvorsen-Weare, and D. Haugland, "On offshore wind farm maintenance scheduling for decision support on vessel fleet composition," European Journal of Operational Research 279, 124–131 (2019).

[15] M. Stålhane, E. E. Halvorsen-Weare, L. M. Nonås, and G. Pantuso, "Optimizing vessel fleet size and mix to support maintenance operations at offshore wind farms," European Journal of Operational Research 276, 495–509 (2019).

[16] M. Stålhane, K. H. Bolstad, M. Joshi, and L. M. Hvattum, "A dual-level stochastic fleet size and mix problem for offshore wind farm maintenance operations," INFOR: Information Systems and Operational Research 59, 257–289 (2020), https://doi.org/10.1080/03155986.2020.1857629.

[17] K. H. Bolstad, M. Joshi, L. M. Hvattum, and M. Stålhane, "Composing vessel fleets for maintenance at offshore wind farms by solving a dual-level stochastic programming problem using grasp," Logistics 6 (2022), 10.3390/logistics6010006.

[18] Y. Dalgic, I. Dinwoodie, I. Lazakis, D. Mcmillan, and M. Revie, "Optimum ctv fleet selection for offshore wind farm o&m activities," European Safety and Reliability Conference ESREL 2014 (2014), 10.1201/b17399-164.

[19] Y. Dalgic, I. Lazakis, I. Dinwoodie, D. Mcmillan, M. Revie, and J. Majumder, "Cost benefit analysis of mothership concept and investigation of optimum chartering strategy for offshore wind farms," Energy Procedia 80, 63–71 (2015).

[20] G. Rinaldi, P. Thies, and L. Johanning, "A coupled monte carlo-evolutionary algorithm approach to optimise offshore renewables o&m," 12th European wave and tidal energy conference (2017).

[21] G. Rinaldi, A. C. Pillai, P. R. Thies, and L. Johanning, "Multi-objective optimization of the operation and maintenance assets of an offshore wind farm using genetic algorithms," Wind Engineering 44, 390 – 409 (2019).

[22] N. Gunantara, "A review of multi-objective optimization: Methods and its applications," Cogent Engineering 5 (2018), 10.1080/23311916.2018.1502242, https://doi.org/10.1080/23311916.2018.1502242.

[23] H. Isermann and R. E. Steuer, "Computational experience concerning payoff tables and minimum criterion values over the efficient set," European Journal of Operational Research 33, 91–97 (1988).

[24] K. Deb and K. Miettinen, "A review of nadir point estimation procedures using evolutionary approaches: A tale of dimensionality reduction," (2009).

[25] J. M. Jorge, "An algorithm for optimizing a linear function over an integer efficient set," European Journal of Operational Research 195, 98–103 (2009).

[26] A. Nikas, A. Fountoulakis, A. Forouli, and H. Doukas, "A robust augmented ε-constraint method (augmecon-r) for finding exact solutions of multi-objective linear programming problems," Operational Research 22 (2022), 10.1007/s12351-020-00574-6.

[27] G. Mavrotas and K. Florios, "An improved version of the augmented ε-constraint method (augmecon2) for finding the exact pareto set in multi-objective integer programming problems," Applied Mathematics and Computation 219, 9652–9669 (2013).

[28] G. Mavrotas, "Effective implementation of the ε-constraint method in multi-objective mathematical programming problems," Applied Mathematics and Computation 213, 455–465 (2009).

[29] E. Klotz and A. M. Newman, "Practical guidelines for solving difficult mixed integer linear programs," Surveys in Operations Research and Management Science 18, 18–32 (2013).

[30] J. Kaldellis and D. Apostolou, "Life cycle energy and carbon footprint of offshore wind energy. comparison with onshore counterpart," Renewable Energy 108, 72–84 (2017).

[31] IEA, "Average co2 intensity of power generation from coal power plants, 2000-2020," IEA, Paris (2020).

[32] L. Moosmann, A. Siemons, F. Fallasch, L. Schneider, C. Urrutia, N. Wissner, and D. Oppelt, "The cop26 climate change conference, status of climate negotiations and issues at stake," Study for the committee on the Environment, Public Health and Food Safety, Policy Department for Economic, Scientific and Quality of Life Policies, European Parliament (2021), european Parliament, Luxembourg.

[33] R. Mckenna, P. Leye, and W. Fichtner, "Key challenges and prospects for large wind turbines," Renewable and Sustainable Energy Reviews 53, 1212–1221 (2016).

[34] G. Shafiullah, A. M.T. Oo, A. Shawkat Ali, and P. Wolfs, "Potential challenges of integrating large-scale wind energy into the power grid–a review," Renewable and Sustainable Energy Reviews 20, 306–321 (2013).

[35] J. Szpytko and Y. Salgado, "Integrated maintenance decision making platform for offshore wind farm with optimal vessel fleet size support system," TransNav, the International Journal on Marine Navigation and Safety of Sea Transportation 13, 823–830 (2019).

[36] D. Liapodimitris, "Vessel fleet optimisation for offshore wind power maintenance," Uppsala University (2017).

[37] E. E. Halvorsen-Weare, I. Norstad, M. Stålhane, and L. M. Nonås, "A metaheuristic solution method for optimizing vessel fleet size and mix for maintenance operations at offshore wind farms under uncertainty," Energy

Procedia **137**, 531–538 (2017), 14th Deep Sea Offshore Wind R&D Conference, EERA DeepWind'2017.

[38] Y. Dalgic, I. Lazakis, and O. Turan, "Vessel charter rate estimation for offshore wind o&m activity," (2013).

[39] E. Gonzalez, E. M. Nanos, H. Seyr, L. Valldecabres, N. Y. Yürüşen, U. Smolka, M. Muskulus, and J. J. Melero, "Key performance indicators for wind farm operation and maintenance," Energy Procedia **137**, 559–570 (2017), 14th Deep Sea Offshore Wind R&D Conference, EERA Deep-Wind'2017.

[40] A. Gray, "Setting a benchmark for decarbonising o&m vessels of offshore wind farms," ORE Catapult (2021).

Appendix A: Appendixes
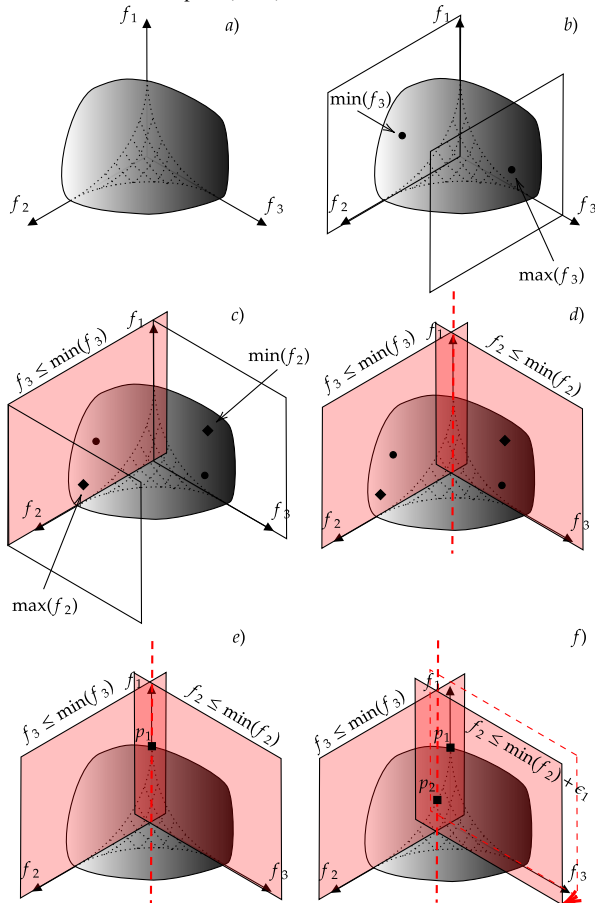
FIG. 5. Visual representation of the development of a three dimensional Pareto front using the epsilon constraint method with three objectives
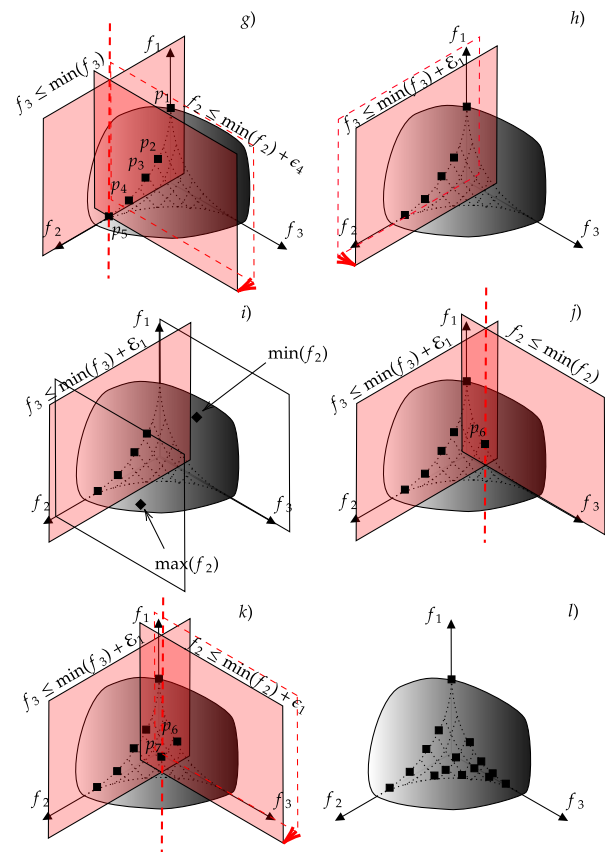
FIG. 6. Visual representation of the development of a three dimensional Pareto front using the epsilon constraint method with three objectives

B. Appendix

B.1. Optimization methodologies

Some types of problems that are encountered in engineering, finance, logistics and many other disciplines, require a best selection out of a group of options. These problems are known as optimization problems. Optimization is interested in finding optimal values to a problem, like minimizing the amount of costs or maximizing profits. Minimization of costs is a common objective to minimize in optimization problems, but numerous different objectives in optimization can be used in disciplines such as engineering, where optimization problems can be used to find optimal designs and shapes.

The amount of different variants and sub-variants of optimization problems and solution methodologies is large. Some frameworks have been presented in literature, but the taxonomy of optimization is not commonly agreed upon. There are approaches for the taxonomy of optimization, as optimization problems typically consist of two major parts. The first one is by categorizing the different types of optimization problems. The second one is by categorizing the different types of optimization methods. Some optimization methods might perform better for some types of problems, while others might not work at all for a given problem. For this reason, it is important that the type of problem is identified and evaluated beforehand, so a fitting method can be selected to solve the optimization model.

For the taxonomy on optimization methodologies, the following literature includes different frameworks and approaches. The work of Affenzeller et al. (2008) includes a taxonomy on different types of optimization techniques, such as calculus, random and enumerative based optimization techniques. The work of Janga Reddy and Kumar (2020) includes a state-of-the-art review on a variety of heuristic methods with applications on water resource engineering and also provides a taxonomy on optimization methods.

To authors best knowledge, the taxonomy on different optimization problems is covered to a lesser extend compared to optimization methodologies. A dichotomy on some of the more general characteristics of optimization problems has been addressed in the work of Nocedal and Wright (2006). A more detailed taxonomy on different types of optimization problems has been shared in the work of NEOS Guide (n.d.).

The following sections will address some optimization problems and some optimization methodologies. Since the optimization problem in the fleet optimization problem in the current report is solved using the Gurobi commercial software, a selection of optimization problems and optimization methodologies is made that are deemed relevant as background information to Gurobi. Some additional topics that are related to the work in the current report are also introduced. The full list of relevant optimization problems and methodologies is presented below and will be addressed in more detail in the sections that follow:

- *Mathematical optimization*: The first section will be on mathematical optimization problems, which introduces a way of formulating optimization models that is used in many different optimization problem sub-variants. The formulation will also be used for the

formulation of the fleet optimization problem that is solved using Gurobi in the current report.

- *Convex optimization*: Convex optimization problems are a subset of mathematical optimization problems, which come with numerous characteristics that are convenient for solving optimization problems. One of these is that convex optimization problems guarantee that a local optimal value is a global optimal value. Linear optimization problems are a subset of convex optimization problems. Being able to guarantee global optimal results is a commonly sought after trait in optimization, thus making convex optimization problems an important subcategory of optimization problems.

- *Multi-objective optimization*: Some problems have multiple objectives, which can sometimes be conflicting. Changing one variable can increase one objective function, while it decreases another objective function. Pareto dominated results play a important role into finding optimal (sets of) solutions for multi-objective optimization problems. The problem that is defined in the current report is a multi-objective optimization problem.

- *Stochastic optimization*: Many optimization models are deterministic by nature, meaning that they do uncertainty is not incorporated in the model. However, there are methods to account for uncertainty by defining the deterministic equivalent of a stochastic problem. For some optimization problems, it might be an unrealistic assumption that the model is deterministic if some parts of the model are prone to uncertainty. Many fleet optimization models from existing literature use stochastic models and thus an introduction to modelling uncertainty in optimization problems will be given.

- *Mixed integer programming*: For some optimization problems, the variables cannot be represented by a continuous variable. This is a common restriction when variables represent products or items. If variables in an optimization problem have both continuous variables and variables that are limited to integer values only, it is known as a mixed integer programming problem. Unfortunately, mixed integer problems cannot be solved identically to its continuous variant. Gurobi is a commercial program that is used to solve mixed integer programming problems in the current report and the fleet optimization problem that is proposed in the current report is a mixed integer problem.

- *Duality*: The principle of duality is a key principle in many theories and algorithms regarding optimization. The idea behind duality is that a optimization problem which requires an objective function to be minimized (primal problem), can be reformulated as another problem that requires to be maximized (dual problem). A solution to the primal problem is an upper bound to the solution of the dual problem and a solution to the dual problem is a lower bound to the primal problem. If a problem has strong duality, the optimal solution of the dual problem is equal to the optimal solution of the primal problem. Convex optimization problems have strong duality and this is exploited for many types of algorithms.

- *Karush-Kuhn-Tucker conditions*: Under certain conditions, the Karush-Kuhn-Tucker conditions proof that a solution of an optimization problem is optimal. Among these conditions falls convexity, although with some additional conditions for the constraints. A category of optimization methods known as interior point methods, are used to solve the Karush-Kuhn-Tucket conditions. An interior point based algorithm can also be used by Gurobi to solve optimization problems.

- *Optimization algorithms*: Different kinds of optimization algorithms can be used as a method to solve optimization problems. Some algorithms include the simplex algorithm and interior point methods, which are both incorporated by Gurobi. Another

branch of algorithms includes genetic algorithms, which are used to verify and validate a Pareto front method method that is introduced in the current report.

B.1.1. Mathematical optimization

Mathematical optimization is a broad category of optimization problems of which its purpose is to find the optimal values for a given function, which is typically referred to as the objective function. These optimal values lie on a minimum or a maximum of the objective function, depending on whether or not the problem is a minimization or a maximization problem. Typically, minimization is used as standard notation so the objective function $f(x)$ which should be minimized minimized can be generically defined as:

$$\text{minimize} \qquad f(x_1, x_2, ..., x_n) \qquad \forall n \in N \tag{B.1}$$

The variables that define the objective function are all x_n for some number of variables N. Optimization problems can also have constraints that they are subjected to. Constraints describe relationships between variables which it must satisfy. The constraints can either be an inequality constraints $g_i(x)$, or an equality constraint $h_j(x)$, such that:

$$h_i(x_1, x_2, ..., x_n) = 0 \qquad \forall n \in N, i \in I \tag{B.2}$$

$$g_j(x_1, x_2, ..., x_n) \leq 0 \qquad \forall n \in N, j \in J \tag{B.3}$$

Optimization problems do not necessarily have to be subjected to constraints, although many practical optimization problems have at least some sort of constraints.

B.1.2. Convex optimization

Convex optimization is a field of optimization problems that studies optimization problems of convex functions and convex sets. Convex optimization problems have characteristics that make the problem solving more convenient than generic mathematical optimization problems. One of these characteristics is that convex optimization problems are guaranteed to be strong-dual problems as well. This means that both the primal and the dual problem and the Karush-Kuhn-Tucker can be used to solve the problem, which will be elaborated on in appendix B.1.7.

A function is considered a convex function if the line that is spanned between any two arbitrary picked points above the function, lies above the function. In other words, any line between two arbitrary picked points above the function do not cross the graph of the function. This is visualized in fig. B.1. Convex sets follow a similar definition, where any line between two arbitrary picked points in this set does not fall outside of the set in Euclidean space. This is visualized in fig. B.2. Optimization problems are convex optimization problems if the following conditions hold true:

- Objective function $f(x)$ is a convex function

- Equality constraints $h(x) = 0$ are linear functions

- Inequality constraints $g(x) \leq$ are convex functions

Figure B.1.: Convex function (left) and a non-convex function (right).

Figure B.2.: Convex set (left) and a non-convex set (right).

Note that the condition for optimization problems to qualify as convex optimization problems requires the equality constraints to be linear functions, rather than convex functions. The reason for this is that the equality constraint $h(x) = 0$ can be rewritten into two inequality constraints $h(x) \leq 0$ and $-h(x) \leq 0$. The only conditions that makes sure that the function $h(x)$ is convex and that both $h(x) \leq 0$ and $-h(x) \leq 0$, are linear functions.

B.1.3. Multi-objective optimization

Multi-objective optimization is a class of optimization problems in which multiple objective functions are optimized simultaneously. The objective functions can be defined as follows:

$$\text{minimize} \quad \{f_1(x_1, x_2, ...x_n), f_2(x_1, x_2, ...x_n), ..., f_m(x_1, x_2, ...x_n)\} \quad \forall n \in N, m \in M \quad \text{(B.4)}$$

where f_m are the objective functions of the problem and M represents the total number of objective functions. The objective functions can be subjected to a set of constraints:

$$h_i(x_1, x_2, ..., x_n) = 0 \qquad \forall n \in N, i \in I \tag{B.5}$$
$$g_j(x_1, x_2, ..., x_n) \leq 0 \qquad \forall n \in N, j \in J \tag{B.6}$$

where $h_i(x_n)$ are the equality constraints and $g_j(x_n)$ are the inequality constraints of optimization problem.

Gunantara (2018) defines two methods on how multi-objective optimization problems can be solved. The first method is based on scalarization of the objective function. The other method is the Pareto method, in which the objective functions are treated as independent vectors.

Scalarization approach

The scalarization method adds all objective functions into one objective function and adding weights to them:

$$f_{scalar}(x_1, x_2, ..., x_n) = \sum_{m=1}^{M} w_m f_m(x_1, x_2, ..., x_n) \tag{B.7}$$

The weights of the scalars can be determined individually if some objectives should be prioritized over others. Alternatively, if equal weights are desired, the individual weights can be found by:

$$w_m = \frac{1}{M} \tag{B.8}$$

Other weight methods exist to make the prioritization of objectives easier and more systematic. This can be done by assigning ranks to objectives. The most important objective is given the lowest index number and the least important objective is given the highest index number. All the other objectives are given an index number in between, based on their priority. The rank order centroid method (Roszkowska, 2013) can then be used to define weights based on the given rank of the objective functions and is defined as:

$$w_m = \frac{1}{M} \sum_{k=m}^{M} \frac{1}{k} \tag{B.9}$$

Another method that assigns higher weights or lower weights w_m based on their rank is the rank-sum method (Roszkowska, 2013), which is defines as:

$$w_m = \frac{2(M + 1 - m)}{M(M + 1)} \tag{B.10}$$

One of the issues with the scalarization method is that the objectives can have different dimensions, e.g. costs is expressed in currency units, while the emisions could be expressed in kilograms of CO2. Adding them up as scalar values would not be meaningful due to their differnet dimensions. Normalization of the objective functions can help overcome this issue. This is done by calculating each individual objective function $f_m(x_1, x_2, ..., x_n)$ first. Then, each individual objective and its respective weight from eq. (B.7) can be divided by this optimal value for the individual solution:

$$f_{scalar}(x_1, x_2, ..., x_n) = \sum_{m=1}^{M} w_m \frac{f_m(x_1, x_2, ..., x_n)}{f_m^{Optimal}(x_1, x_2, ..., x_n)} \tag{B.11}$$

One of the advantages of using the scalarization method is that it can be solved using traditional single-objective optimization algorithms, as all objectives have been reformulated as a single objective. One of the downsides is that it does not give much information on sensitivities of the compromises once weights are slightly shifted. In other words, it could be that a slight sacrifice for objective function $f_1(x_1, x_2, ..., x_n)$ drastically increases objective function $f_2(x_1, x_2, ..., x_n)$, but this is hidden due to the attributed weights.

Pareto approach

One of the mentioned downsides of the scalarization method was that choices based on the relative sensitivity between the objective functions could not be made. An alternative

approach to avoid this issue is to treat each objective function as a set of independent vectors. All objective function vectors $\vec{f}_m(x_1, x_2, ..., x_n)$ now form a solution space of rank M together since the objectives are treated as independent vectors. If all decision variables x_n are also treated as independent vectors, they form the decision space of rank N together. They relate to one another in the sense that every single feasible point in the decision space will map to a point in the solution space, as is depicted in fig. B.3.
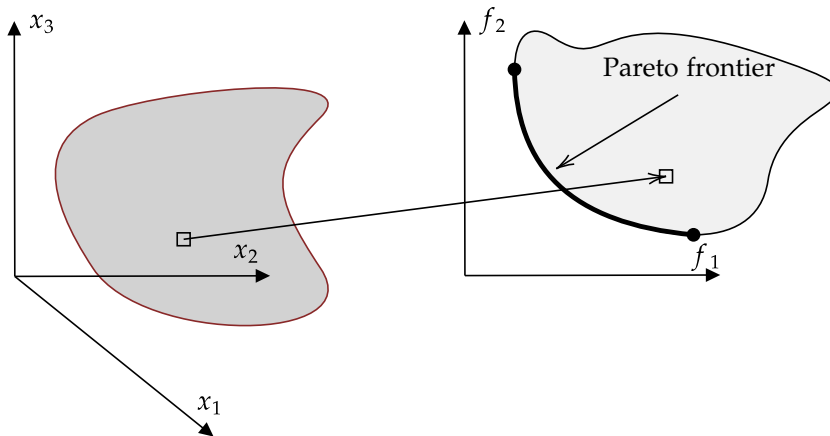
Figure B.3.: Feasible variable space (left) mapped to feasible objective space (right).

Pareto optimal solutions are defined as solutions that cannot increase one objective without reducing another objective. The set of all Pareto optimal solutions is the Pareto front, as can be seen in fig. B.3. The Pareto front in this figure can be represented by a line segment. Solutions that do not lie on the Pareto front are not considered optimal solutions. This is because for any solution that does not lie on the Pareto front, there is a solution that lies on the Pareto front that can increase both objective functions. In other words, a better solution can be found without any sacrifices.

The Pareto front can be evaluated manually for low dimension problems in order to find an optimal solution. Any solution can be considered optimal on the Pareto front, depending on how much one objective function is preferred over the other. Although the decision to go with a single Pareto optimal solution over the other solutions is not inherently done by calculating the Pareto front, it can still be useful to help with this decision making since it shows the sensitivity between choices.

However, Pareto fronts become less intuitive for larger amount of objective functions, as plotting them will require more than two dimensions. Alternative decision making methods exist to pick optimal solutions. This discipline is known as multi-criteria decision making and many approaches exist in order to pick one solution. One of these approaches is by finding the Utopia point and then selecting the Pareto optimal solution with the smallest Euclidean distance to the Utopia point (Gunantara, 2018). The Utopia point is a point with the values of the objective functions $\vec{f}_m(x_1, x_2, ..., x_n)$ if they were to be solved independently as single objective functions. Another method is by the weighed sum method, which is analogous to the scalarization approach and scores all objectives by summing them up and giving them a corresponding weight.

One of the advantages of using the Pareto method for multi-objective optimization problems is that the Pareto front provides more information than the scalarization approach. One of the disadvantages is that not all algorithms are suited to independently optimize multiple

objective functions simultaneously and its typically more computational expensive than the scalarized approach.

B.1.4. Stochastic optimization

The basic form of an mathematical optimization problem, as introduced in appendix B.1.1, uses a deterministic formulation of the objective function and the constraints. In practical problems, some parameters cannot be treated with certainty. Some examples are the fluctuation of prices in the future or uncertainty of the weather forecast.

A selection of stochastic optimization problems will be introduced in this report, based on the work of C. Li and Grossmann (2021). However, this small selection only scratches the surface of the stochastic optimization topology as introduced by Powell (2019). The inclusion of all approaches is beyond the scope of this research, thus only stochastic programming, chance-constrained programming and robust optimization are addressed.

Stochastic programming (multi-stage programming)

Stochastic programming is a sub-community of stochastic optimization methodologies according to a categorization of stochastic optimization by Powell (2019). Two-stage and multi-stage programming belong to the stochastic programming sub-community. Multi-stage programming is a generalized version of two-stage programming, but it has greater complexity over the two-stage variant (Powell, 2019). The two-stage variant will be addressed in this report and its mathematical formulation will be follow from the work of Powell (2019).

The key principle of two-stage models is splitting up a problem into two separate problems. During the first problem, a set of decisions x_0 have to be made. After that, some uncertainty is revealed and another set of decisions have to be made in the second problem. This revealed uncertainty is discretized into a number of possible realizations ω (also known as scenarios), where $\omega \in \Omega$ and each of these scenarios has a chance $p(\omega)$ of occurring. The minimization of the objective function can then be defined as:

$$\min_{x_0}(c_0 x_0 + \sum_{\omega \in \Omega} p(\omega) \min_{x_1(\omega) \in X_1(\omega)} c_1(\omega) x_1(\omega)) \tag{B.12}$$

where the first part is the first stage variables x_0 multiplied with the coefficients c_0 of the first stage problem. The second part sums all second stage variables x_1 multiplied with the coefficients c_1 from the second stage scenarios, multiplied with their respective chance of occurring. The first problem will have a set of constraints in the form:

$$A_0 x_0 \leq b_0 \tag{B.13}$$

where A_0 and b_0 are coefficients and parameters, respectively. The second problem has a set of constraints in the form:

$$A_1 x_1 \leq b_1 \tag{B.14}$$

Typically, problems in the first stage denote something like a type of inventory decision such that x_0 represents the amount of inventory. In the second stage, the inventory can then be distributed. In this form, additional constraints for the second stage could look something like:

$$B_1 x_1 \leq x_0 \tag{B.15}$$

such that the amount of distributed inventory x_1 cannot exceed the value of the initial inventory x_0. Two-stage models are matured in the field of mathematics (Powell, 2019), which therefore grants access to a wide range of existing literature such as papers and books. This makes them one of the more well known stochastic modelling methodologies. However, the computational complexity of the problem scales with the amount of scenarios Ω, thus making problems with large sets of scenarios computationally heavy.

Robust optimization

Robust optimization is a stochastic optimization sub-community that optimizes the problem for the worst case scenario (Powell, 2019). Let there be an objective function $f(x, w)$ where x is a decision variable such that $x \in X$ and w is a uncertain parameter that can take on any value from a set such that $w \in W$. A robust optimization problem can then be formulated as:

$$\min_{x \in X} \max_{w \in W} f(x, w) \tag{B.16}$$

such that a value is chosen for $w \in W$ which is the worst case for the objective function. Analogous to an objective function, a constraint with uncertain coefficients $a \in A$ on the left hand side and uncertain parameters $b \in B$ at the right hand side can be defined as:

$$\min_{a \in A} ax \leq \max_{b \in B} b \tag{B.17}$$

where the values for a and b are now chosen such that the constraints tighten the feasible space the most. Robust optimization can be a good method if the probability that this can occur is not a contributor to the decision making. After all, it makes ensures that feasibility holds due to its conservative characteristic. However, robust optimization might be too restrictive if the worst case scenario has a low probability of occurring and if some amount of risk is tolerable.

Chance-constrained programming

Chance constrained programming is another stochastic optimization approach. It includes constraints that ensure feasibility holds under a certain probability (Küçükyavuz & Jiang, 2021). The definition of a generic chance constrained programming problem will be based on the definition given by P. Li et al. (2008). A objective function $f(x, w)$ is defined with variable x and uncertainty variable w. An output variable $y(w)$ and a probability α are defined. A constraint that limits the range of the output variable y can be defined as:

$$y^{min} \leq y(w) \leq y^{max} \tag{B.18}$$

The probability that the constraint is violated can than be defined as $\Pr\left(y^{min} \leq y(w) \leq y^{max}\right)$. If the probability of the constraint violation should be restricted, this can then be defined as:

$$\Pr\left(y^{min} \leq y(w) \leq y^{max}\right) \geq \alpha \tag{B.19}$$

Other variants of chance constraint notation are provided by (Küçükyavuz & Jiang, 2021). One of the advantages of using chance constraints programming over robust optimization is that chance constraints can tolerate constraint violations of values that are very unlikely to occur.

B.1.5. Mixed integer programming

Mixed integer programming (MIP) is a category of optimization problems that includes a combination of continuous with integer and/or binary variables. Many practical optimization problems require integer or binary decision variables in order to be realistic, e.g. if a decision variable determines the amount of vehicles in a routing problem, then it would be physically infeasible to have an answer that is a fraction. Similarly, if a decision variable determines whether a vehicle is used by assigning the value 1 to it, or if it is not used by assigning the value 0 to it, this variable should only give answers within the feasible binary decision space.

We can mathematically define continuous variable x such that $x \in \mathbb{R}$, where $\mathbb{R}$ is the set of all real values. Similarly, we can define integer variable z such that $z \in \mathbb{Z}$, where $\mathbb{Z}$ is the set of all integer values and define binary variable b such that $b \in \{0, 1\}$.

B.1.6. Duality

Some of the methodologies that are used to find optimal values for optimization problems, rely on the principle of duality. The idea behind duality is that a problem can be divided into a primal problem and a dual problem. Given that the problem has strong duality, the optimal solution to the dual problem is equal to the optimal solution of the primal problem. In some cases, solving the dual problem is easier than solving the primal problem and therefore is a convenient way to solve problems. The derivations for duality below are based on the the work of Freund (2014), Luptácik (2010) and Boyd and Vandenberghe (2009).

First, we assume we have an objective function

$$f(x) \tag{B.20}$$

where and a set of inequality constraints

$$g_i(x) \leq 0 \qquad \forall i \in m \tag{B.21}$$

Every "$\geq$" constraint can be rewritten as a "$\leq$" constraint by multiplying both sides of the constraint with -1. Each "$=$" constraint can be redefined as a combination of a "$\leq$" and a "$\geq$" by setting the upper and lower bound of these constraints such that they will be a equality constraint.

To construct the dual of the problem, the Lagrangian $L(x, u)$ has to be defined:

$$L(x, u) = f(x) + \sum_{i=1}^{m} u_i g_i(x) \tag{B.22}$$

One way to interpret the Lagrangian of the optimization problem, is that it takes the original objective function $f(x)$ and adds the constraint violations $g_i(x)$ to the objective function as a penalty with a weight u_i. Now the dual function $L^*(u)$ can be defined as follows:

$$\min_x f(x) + \sum_{i=1}^{m} u_i g_i(x) \tag{B.23}$$

The dual problem can now be defined as the maximum of the dual function $L^*(u)$ when $u \geq 0$. Since all u_i can be interpreted as coefficients that determine the slope of $g_i(x)$, u_i

should be chosen such that it penalizes the penalty function (i.e. the constraint violation) the most.

$$\max_{u} \min_{x} f(x) + \sum_{i=1}^{m} u_i g_i(x) \tag{B.24}$$

In any case, a problem has at least weak duality characteristics which means that the solution to the dual problem is always equal or greater than the solution to the primal problem. This means that the dual problem bounds the problem at the very least. Strong duality on the other hand guarantees that the optimal solution to the dual problem is also the optimal solution to the primal problem. Convex optimization problems have strong duality. Linear optimization is also part of convex optimization and convex optimization can be seen as a more generalized category of strong duality optimization problems.

B.1.7. Karush-Kuhn-Tucker conditions

In this section, the Karush-Kuhn-Tucker (KKT) conditions will be introduced. If the KKT conditions are satisfied, this will guarantee that a solution x is optimal. The proof of the Karush-Kuhn-Tucker will not be included in this section and more emphasis will be given on a intuitive interpretation of these conditions. The derivations can be found in the work of Luptácik (2010) and Boyd and Vandenberghe (2009).

First, lets reintroduce the Lagrangian form of the optimization problem.

$$L(x,u) = f(x) + \sum_{i=1}^{m} u_i g_i(x) \tag{B.25}$$

For x to be a optimal value for the optimization problem, we have the following condition that should hold true.

$$\nabla f(x) + u \nabla g(x) = 0 \tag{B.26}$$
$$g(x) \leq 0 \tag{B.27}$$
$$u \geq 0 \tag{B.28}$$
$$u g(x) = 0 \tag{B.29}$$

Where ∇ is the gradient operator. To understand eq. (B.26) should hold, it must be understood that following the gradient of a function will increase the values of the function and following the opposite direction of the gradient of a function will decrease the values of the function. Recall that we are interested in finding the minimum of the optimization problem, so it is desirable to move in the negative direction of the gradient of the objective function $f(x)$ and in the negative direction of the gradient of the constraints $g(x)$ to improve the solution. In fact, they can actually both be improved if at a given solution x, it is possible to move to another solution of which its direction is at least partially in the direction where $-\nabla f(x)$ and $-\nabla g(x)$ overlap. If a value for x is found that does not cause $\nabla f(x)$ and $\nabla g(x)$ to overlap anymore, there can be no more further improvements to the solution and x is optimal. The condition to prevent overlap is eq. (B.26), as $\nabla f(x)$ and $\nabla g(x)$ are now inversely proportional to each other. Additionally, eq. (B.27) makes sure that x is a feasible solution. Then, eq. (B.28) limits u to positive values only. At last, eq. (B.29) is necessary to make sure that the optimal value of the objective function is not altered by nonzero values of $ug(x)$.

These four conditions are the KKT conditions and can prove that a given value for x is optimal. The usefulness of the KKT conditions lies in the fact that they allow the optimization problem to be solved as a set of equality and non-equality equations, rather than by solving it as a optimization problem.

B.1.8. Optimization algorithms

Optimization algorithms are algorithms that can be used to solve optimization problems. The algorithms that can be used depend on the type of optimization problem. For instance, there are numerous algorithms that can be used for convex optimization problems, but they are not guaranteed to work for non-convex optimization problems as well. Additionally, combinations of algorithms are sometimes used to increase performance or to work around some of the shortcomings. The many types and sub-variants of algorithms therefore make a full taxonomy on all algorithms difficult. Among the many traits that algorithms can have, some of the common ones are listed below:

- *Global/local minimum*: Some algorithms are designed such that they try to find global solutions, while others can get stuck in a local optimum.

- *Single objective or multi-objective*: Not all algorithms are suitable for multi-objective optimization problems without modifications, e.g. for the Pareto approach with multi-objective optimization problems.

- *Finitely terminating/iterative/heuristic algorithms*: Some optimization problems are guaranteed to find the optimal solution in a finite amount of time. Other optimization problems iteratively converge towards this solution but are not guaranteed to find the exact optimum. Heuristics are a good approach to get solutions that lie close enough to the optimal value for some application and typically require less computational power, but not all are guaranteed to come close the the actual optimal solution.

Simplex method

The simplex method is an algorithm that can solve linear optimization problems. A brief introduction on the simplex method will be given in this section. The explanation that follows in this section is based on the book of Nocedal and Wright (2006), which could be consulted for a more detailed description. One of the recognizable characteristics of the simplex method is that the algorithm follows the vertices of the feasible space of the optimization problem. The feasible space is a space of possible solutions that is bounded by the constraints and that does not violate these constraints.

A simplified visual representation of the simplex method can be found in fig. B.4. The axis are variables x_1 and x_2 and the objective function is dependent on x_1 and x_2. The feasible space is shown as the grey surface and the outlines of the feasible space are formed by its surrounding constraints.

The concept of the simplex algorithm is to first find a feasible solution to begin with in the feasible space. After this feasible solution has been found, the algorithm moves to a neighbour vertex. In the case that there are multiple vertices to choose from, the vertex that improves the objective function the most will be chosen. The process of moving to the next vertex will continue until no more improvements can be made, which is when optimality has been reached.

The conceptual explanation that was given in combination with fig. B.4 makes the method look simple. However, the traveling over the vertices of the feasible space is a bit more complex under the hood. It is out of scope of the current report to provide a full description of the algorithm, as this is already covered in great detail in the work of Nocedal and Wright (2006) and other literature. Manual calculation of these points is usually done using a so

called "simplex tableau". However, like many types of algorithms, this is tedious work and is better suited to solve using computers.

To this day, the simplex method is still actively used as a linear optimization method. It is intuitively easy to understand due to the sensible visual feedback after each iteration. The simplex method scales exponentially with the problem size, but win practice the simplex method performs very well and only very specific problems perform poorly (Nocedal & Wright, 2006). An alternative to the simplex method that has variants that scale in polynomial time is the interior point method, which will be discussed in the next section
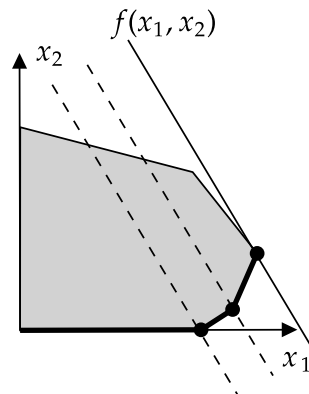
Figure B.4.: Simplex algorithm.

Interior point method

Interior point methods are a category of optimization methods that can be used to solve convex optimization problems. The explanation in this section on the interior point method will only scratch the surface behind the theory. The explanation is based on the book of Boyd and Vandenberghe (2009) and this book should be consulted for a more in depth explanation.

Unlike the simplex method, the interior point methods moves inside of the feasible space. This is visually simplified in fig. B.5.

Although the visual representation of the interior point method looks rather simple, its relationship to the steps in the algorithm are a lot less intuitive than with the simplex method. The interior point method solves a modified version of the KKT conditions. Recall in appendix B.1.7 where the KKT conditions were briefly introduced, that if a solution satisfies the KKT conditions, the solution is optimal. The modified version that is solved using the interior point method is easier to solve, as introducing a perturbation t to eq. (B.28) will simplify the KKT conditions to a unconstrained optimization problem. Unconstrained optimization problems can be solved using techniques like Newthon's method to get to a solution. If the perturbation t is selected very small, it will be very close to the actual solution because it approaches the initial condition without a perturbation in eq. (B.28). However, selecting t too close to zero in the beginning usually results in Newtons method to converge very slowly.

To overcome the slow converging issue, several iterations of Newthon's method are then conducted that slowly converge towards $t = 0$. First, the solution is solved for a given t, which results in a solution x that is not yet optimal. Then a new problem will be solved with $t' = 0.9t$ and the initial position will be the x from the previous step. Note that the

multiplication with 0.9 is arbitrary here and different values could provide better or worse results and finding good values is one of the challenges of the interior point method. The process will continue with $t'' = 0.9t'$ and so on until a perturbation value is found that is close enough to zero. This process of iteratively making t smaller lets the problem converge a lot faster than selecting a too small perturbation t at the beginning.

Variations and different approaches exist for the interior point method and the book of Nocedal and Wright (2006) provides a brief overview on the history of the interior point methods and some of their variants. It is also stated in this book that although some interior point methods scale polynomial with the problem size, that this did not necessarily made them faster in practice for quite some problems compared to the simplex method that scales exponentially with the problem size.
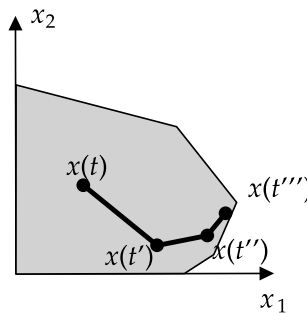
Figure B.5.: Interior point method.

Genetic algorithms

Genetic algorithms are a category of heuristic methods that can be used to solve a wide range of optimization problems. As their name already suggests, some aspects are analogous to evolutionary processes in nature.

A genetic algorithm has a cost function that it will evaluate. This cost function can be expressed as the objective functions if they are used to solve optimization problems. Genetic algorithms also have a population and each individual in the population includes a solution to the problem. The individuals can be considered as a fit solution if the objective function is relatively good compared to the rest of the population. The population will iterate through generations and some of the population of the previous generation will survive, while another part of the previous generation its population will die off. The part of the population which will survive are a selection of the fittest individuals. Some of the fittest individuals will then mate and produce new solutions to replace the individuals that died. Parts of the individuals that mate will be combined to produce a new solution. This process continues until a termination criterion is met. Besides mating, some individuals might also be subjected to random mutations.

Genetic algorithms are not inherently designed to deal with constraints, unlike the simplex algorithm and interior point methods. One method that allows genetic algorithms to deal with constraints is to let individuals die off if they violate constraints. However, if the feasible region of the optimization problem is heavily constrained, then it could be that the population has difficulty to move through the feasible space or to find initial feasible solutions that are spread out. Another method is to include the constraint violation as part of the objective function. This makes all solutions feasible, but infeasible solutions get a penalty.

The magnitude of the penalty is important to select, as setting the penalty too low could benefit solutions that violate the constraints if the penalty is lower than the improvement of the cost function by violating the constraints.

Genetic algorithms are well suited for solving multi-objective optimization problems. The reason for this is that plotting individuals will estimate the Pareto front, once the solution is sufficiently converged. Other methods like the Simplex algorithm and interior point methods only produce a single solution.

The parameters of a genetic algorithm make a large impact on its performance. A large population could provide a more spread out initial population, but can require more computational power to compute new generations. The optimal values for the parameters of a genetic algorithm are often problem dependent.

One of the downsides of genetic algorithms over the simplex and interior point methods is that it is not guaranteed to converge or find an optimal value. In practice, it can often be a good approximation and for some problems be a lot more computational efficient.

Methods for mixed integer programming

In the previous sections, we have given a brief introduction to the simplex method, the interior point method and genetic algorithms. Both the simplex method and the interior point method can deal with continuous variables effectively. However, some problems have variables that are limited to integer values only. One example of this is the optimal number of maintenance vessels, which can only be an integer value. After all, 1.3 vessels would not make sense from a physical perspective. One simple approach to deal with this would be to round the solution, but unfortunately, it has been shown that rounding the value does not guarantee that the rounded value is optimal. That means that rounding 1.3 vessels to 1 vessel does not make 1 vessel the optimal solution and other approaches should be used.

There are dedicated (commercial) programs and applications, which are specialized in solving mixed integer programming problems. Although most of these programs and applications operate somewhat in a similar fashion compared to one another, there is a large amount of different techniques and operations that can be used to find the MIP equivalent of the problem. Not all techniques will be handled in this section, but some of the fundamental concepts of mixed integer programming will be addressed. The explanations and methods that are discussed in this section will be based on the commercial MIP software Gurobi (Gurobi Optimization LLC, 2022).

Branching First, we consider a linear MIP. This MIP will first be solved without its integrality constraints, meaning that the solution will be solved as if the integer variables are continuous variables. Because the problem is now solved using continuous variables instead of integer variables, the problem is a convex optimization problem and can be solved using the simplex method and/or interior point method that were introduced in earlier sections. Solving the problem without the integrality constraints is also called a relaxation of the problem. Lets assume that the relaxation solution of the MIP is found and returns a variable $x = 8.4$, which should be an integer variable in the MIP. The problem will now be split up in two separate problems; one problem with a constraint such that $x \leq 8$ and one problem with a constraint $x \geq 9$. For the sake of clarity, we can call the first problem that was solved and resulted in $x = 8.4$ problem P_0, while the sub problems with the constraints are labeled as P_1 and P_2. The same process of solving the relaxed problem can be repeated for P_1 and P_2. This process is called branching. The problem P_0 is also commonly known as the root node of the

problem and the problems P_1 and P_2 are also called nodes of the search tree. Nodes that are not yet branched are called leaf nodes. Generally, a problem is solved once there are no more leaf nodes on the search tree.

Incumbents and best bounds   There are a couple of things that can occur when branching leave nodes. First of all, a solution can be returned that does not violate any of the integrality constraints, i.e. it is a feasible solution to the MIP. This means that no matter what, the optimal solution to the MIP can not be higher than the optimal solution of the feasible MIP solution (assuming it is a minimization problem, it is an upper bound). If a lower feasible solution is found during the branching of the search tree, this will be the new upper bound. This upper bound is also known as an incumbent node. It should be noted that there is also a lower bound the the MIP, which is the minimal value of all leaf nodes. We know this is a lower bound because leaf nodes include a relaxed solution to the optimization problem and an integer solution can at best be equal to the relaxed solution. So no matter what, the MIP solution of a leaf node can never be better than the relaxed solution to the problem and therefore the lowest value of all leaf nodes is an lower bound to the MIP. This lower bound to the MIP is also known as the best bound. Iterating through the search tree will eventually lead to improvements of the incumbent and improvements of the best bound. The difference between the incumbent and the best bound is also known as the gap. As the gap becomes smaller by improving the incumbent and best bound, it will become smaller. Once the gap is equal to 0, optimality has been proven.

Fathoming nodes   If solving a leaf node leads to a solution that does not violate any of the integrality constraints, the node is considered fathomed. This means that there are no more better solutions that can be found by branching the leaf node. Another thing that can lead to a node being fathomed is when a leaf node returns an infeasible solution. Since the leaf node solves a relaxation of the optimization problem, there can be no feasible integer solution if there is also no feasible continuous solution, thus the node can be considered fathomed. The last condition that can lead to a leaf node being fathomed is when a feasible solution is found to the relaxed problem, but it has a worse objective value than the incumbent. This means that the lowest possible integer solution that could come out of this node would be no better than the best integer solution and it can therefore be fathomed.

Solve time enhancing techniques   Some MIP solvers can be significantly faster compared to others for the same problem, even though they share the same basic principles on how they operate. The reason for this difference in performance is due to som underlying techniques are used to find the optimal solution faster. Although there are many different types of techniques being used, the most common ones are:

- *Presolve*: The purpose of presolving the optimization problem is to make the problem size smaller and to tighten the formulation of the MIP. An example of presolving is when a set of constraint can tighten the feasible space of variables such that a variable is only viable for one single value. Instead of obtaining this through branching, this value can already be assigned to the variable before the branch and bound procedure.

- *Cutting planes*: Cutting planes is a set of different techniques that can improve the performance of the MIP solver. The principle of cutting planes is removing undesired fractional solutions, as these do not satisfy the integer variable integrality constraints. While presolving techniques have similar goals, one key difference between presolve and cutting planes is that presolve tries to simply the problem before the branch and

bound procedure starts, while cutting plane techniques are done during the branch and bound procedure. The reason for doing the cutting plane techniques during the branch and bound technique is that there are a lot of opportunities to apply a cutting plane technique and doing this for every opportunity will make the problem size enormous. The advantage of doing cutting plane techniques during the branch and bound procedure, is that cutting planes will only be applied in scenarios where it is known it will actually help the problem.

- *Heuristics*: The principle of heuristics is to find good incumbent solutions. In the case that MIP's are too difficult to proof optimality within a reasonable time, the next best thing to have is usually a good feasible solution. Another reason for wanting to find good incumbents is that it helps to make the search tree smaller, as incumbents can fathom some parts of the search tree. It can sometimes be helpful to put more effort into some nodes of the search tree to see if a good feasible solution can be extracted. One method of doing so is by rounding some of the integer variables that do not have an integer value in the relaxation of the problem, but are very close to an integer value, hoping to find a good feasible solution without having to conduct multiple branch and bound steps to acquire the same solution.

- *Parallelism*: There is a trend where increasingly more cores are available in computing chips. However, not all computational problems can take advantage of that. For mixed integer programming, there are numerous techniques that are used to take advantage of multiple cores. Finding root nodes is hard to do in parallel in general, but searching through the search tree can be done more efficiently in parallel. Additional methods that are used by Gurobi to take advantage of multiple cores, is by solving the problem using different algorithms or settings simultaneously and stopping once one of them finds a solution.

B.2. Big-M method

B.2.1. Proof and limitations of the linearization

To see how these constraints collectively make the problem linear, the value $\gamma_{pm\tau} = 1$ will be once again substituted in all the new defined constraints. Substituting this value in eq. (3.20), eq. (3.21) and eq. (3.22) will respectively change the constraints into:

$$t^{LIN}_{pmv\tau} \geq t_{pmv\tau} \qquad \forall v \in V, p \in P, m \in M^{CORR}, \tau \in T \qquad (B.30)$$

$$t^{LIN}_{pmv\tau} \leq M^{BIG} \qquad \forall v \in V, p \in P, m \in M^{CORR}, \tau \in T \qquad (B.31)$$

$$0 \leq t^{LIN}_{pmv\tau} \leq t_{pmv\tau} \qquad \forall v \in V, p \in P, m \in M^{CORR}, \tau \in T \qquad (B.32)$$

It can be observed that eq. (B.30) and eq. (B.32) are causing $t_{pmv\tau} = t^{LIN}_{pmv\tau}$ and thus $t^{LIN}_{pmv\tau}$ will take on the same value as $t_{pmv\tau}$.

If $\gamma_{pm\tau} = 0$ is substituted in the constraints then eq. (3.20), eq. (3.21) and eq. (3.22) will respectively change the constraints into:

$$t^{LIN}_{pmv\tau} \geq t_{pmv\tau} - M^{BIG} \qquad\qquad \forall v \in V, p \in P, m \in M^{CORR}, \tau \in T \qquad (B.33)$$

$$t^{LIN}_{pmv\tau} \leq 0 \qquad\qquad \forall v \in V, p \in P, m \in M^{CORR}, \tau \in T \qquad (B.34)$$

$$0 \leq t^{LIN}_{pmv\tau} \leq t_{pmv\tau} \qquad\qquad \forall v \in V, p \in P, m \in M^{CORR}, \tau \in T \qquad (B.35)$$

Now it can also be observed that eq. (B.34) and eq. (B.35) cause $t^{LIN}_{pmv\tau} = 0$, which is also the desired outcome in the nonlinear formulation. This will not make $t^{LIN}_{pmv\tau} = t_{pmv\tau}$ so they have different values. This is also intended, as only the nonlinear part should have $t_{pmv\tau}$ substituted with $t^{LIN}_{pmv\tau}$.

Adding these constraints to the original problem, substituting $t_{pmv\tau}$ with $t^{LIN}_{pmv\tau}$ in the nonlinear formulation of the objective function and removing $\gamma_{pm\tau}$ in the nonlinear formulation of the objective function will make the problem linear. The catch of using this method is that additional constraints and additional variables are required, thus making the problem larger than the original nonlinear problem. On top of this, the value of M^{BIG} should be selected such that $M^{BIG} >> t_{pmv\tau}$, otherwise the constraints do not work as intended. Simultaneously, selecting extreme large values of M could result in numerical issues if the problem is solved using computational methods.

B.3. Verification of the epsilon constraint method

Although the epsilon constraint method is a well known method in multi-objective optimization literature, the author of the current report is unaware of an identical methodology that is used to determine the bounds of both $f_2(x_n)$ and $f_3(x_n)$ in current literature. Additionally, the implementation of this methodology can be prone to errors. For these reasons, a verification of both the methodology and the implementation will be conducted to check and evaluate its performance.

The verification will be done by defining a test problem first. The Pareto front of this test problem will be approximated using the three dimensional epsilon constraint method and it will also be approximated using a genetic algorithm. The results of both Pareto fronts will then be plotted against each other to see if they form the same Pareto front. The reason why a test problem is used to verify the results of the epsilon constraint method, rather than the developed problem offshore wind fleet optimization problem, is that the author of the current paper has attempted to implement the fleet optimization in a genetic algorithm before. Preliminary testing with the fleet optimization problem using genetic algorithms indicated that the unmodified genetic algorithms were not successful at finding solutions to the optimization problem, which was likely due to the fact that the fleet optimization problem is highly constrained. The results for the fleet optimization problem of the genetic algorithm are therefore expected to be poor in comparison to simpler and less constrained problems. A less constrained test case will make the genetic algorithm more likely to converge, thus making it better to verify with.

The verification methodology will go as follows:

1. The test problem will be implemented using a genetic algorithm

2. The test problem will be implemented using a MIP solver and the proposed three dimensional epsilon constraint method

Genetic algorithm settings and parameters	
Genetic algorithm	NSGA 3 (Blank & Deb, 2020)
Population size	300
Offspring number	150
Reference directions	Das-Dennis method (Das & Dennis, 1998)
Number of reference direction partitions	30
Stopping criteria	3 minute run time

Table B.1.: Table with genetic algorithm parameters used in the verification.

3. The Pareto points of both solutions will be plotted in the solution space and compared against each other.

4. A matching Pareto front indicates that the three dimensional epsilon constraint method works as intended.

Verification test problem

$$I = \{0, 1, 2, 3\}$$
$$J = \{0, 1, 2\}$$

$$\text{minimize}\{f_1(z_{i,j}), f_2(z_{i,j}), f_3(z_{i,j})\}$$

$$f_1 = 3z_{0,0} - 5z_{1,0} + z_{2,0} + 2z_{3,0} - 0.5z_{0,1} + z_{1,1} + 5z_{2,1} - 8z_{3,1} + z_{0,2} + z_{1,2} - z_{2,2} - z_{3,2}$$
$$f_2 = 4z_{1,0} + 0.1z_{2,0} + 5z_{3,0} - 3z_{1,1} - z_{2,1} - z_{3,1} + z_{0,2} - z_{3,2}$$
$$f_3 = -z_{0,0} - 2z_{1,0} - z_{2,0} - 4z_{3,0} + 0.5z_{0,1} - 3z_{1,1} - 5z_{2,1} + 8z_{3,1} - z_{0,2} - 8z_{1,2} + z_{2,2} + z_{3,2}$$

$$\sum_{i \in I} \sum_{j \in J} z_{i,j} \leq 5$$

Genetic algorithm

Genetic algorithms inherently have the trait that they approach the Pareto front for many problems. This is because each generation that is calculated using the genetic algorithm contains many solutions. Given that these solutions have converged towards Pareto optimal solutions sufficiently, they will approximate the Pareto front. The genetic algorithm type and parameter settings for this test case can be found in table B.1.

Epsilon constraint method

The epsilon constraint method for three objectives requires some parameters to be set. As was discussed section 4.2, selecting the step size between each ϵ and the range over which the epsilons are iterated are some of the changeable parameters. The epsilon constraint method that is used in the current report, iterates between the minimum and maximum values of

Three objective epsilon constraint	
Number of f_3 constraint shifts	15
Number of f_2 constraint shifts	15
$(\mathcal{E}_{n+1} - \mathcal{E}_n)$ step size in f_3	Constant, 1/15
$(\epsilon_{m+1} - \epsilon_m)$ step size in f_2	Constant, 1/15
Number of Pareto points calculated p_i	(15+1)(15+1)=256
Stopping criteria	MIP GAP = 0%

Table B.2.: Table with three objective epsilon constraint method parameters used in the verification.

f_3 and f_2. The settings of the three objective epsilon constraint method can be found in table B.2.

Results

The results of the Pareto front that is found by the genetic algorithm and the Pareto front that is found by the epsilon constraint method are shown in fig. B.6 and fig. B.7. Both plots are the same results, but the plots have a different angle and orientation such that the depth of the Pareto front can be better visualized.

As can be observed, the front of both the genetic algorithm and the Pareto front match and form the same plane. It is assumed that the test problem is sufficient simple enough that the genetic algorithm converges towards the actual Pareto front. Since both the methods match, this result helps to verify the proposed epsilon constraint method.
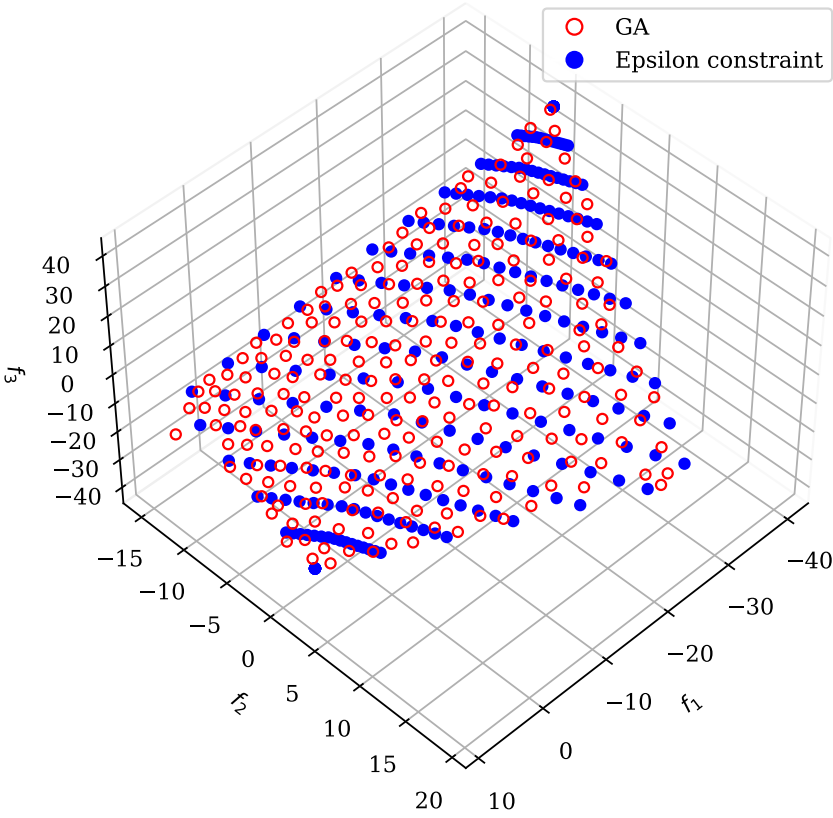
Figure B.6.: Pareto front genetic algorithm and epsilon constraint method.
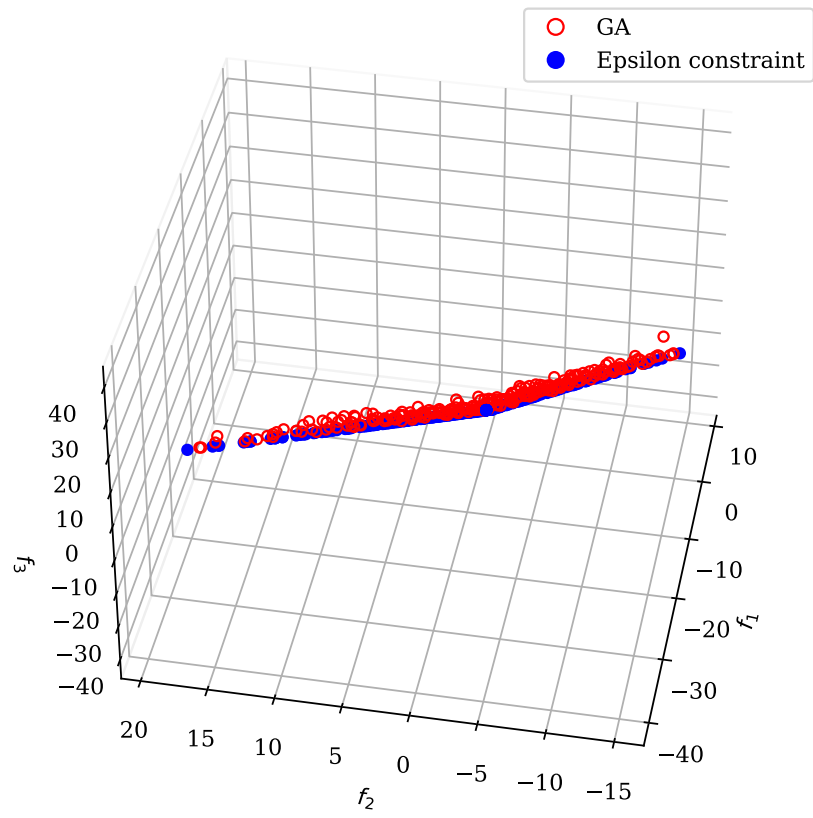
Figure B.7.: Pareto front genetic algorithm and epsilon constraint method (rotated).

C. Appendix

C.1.
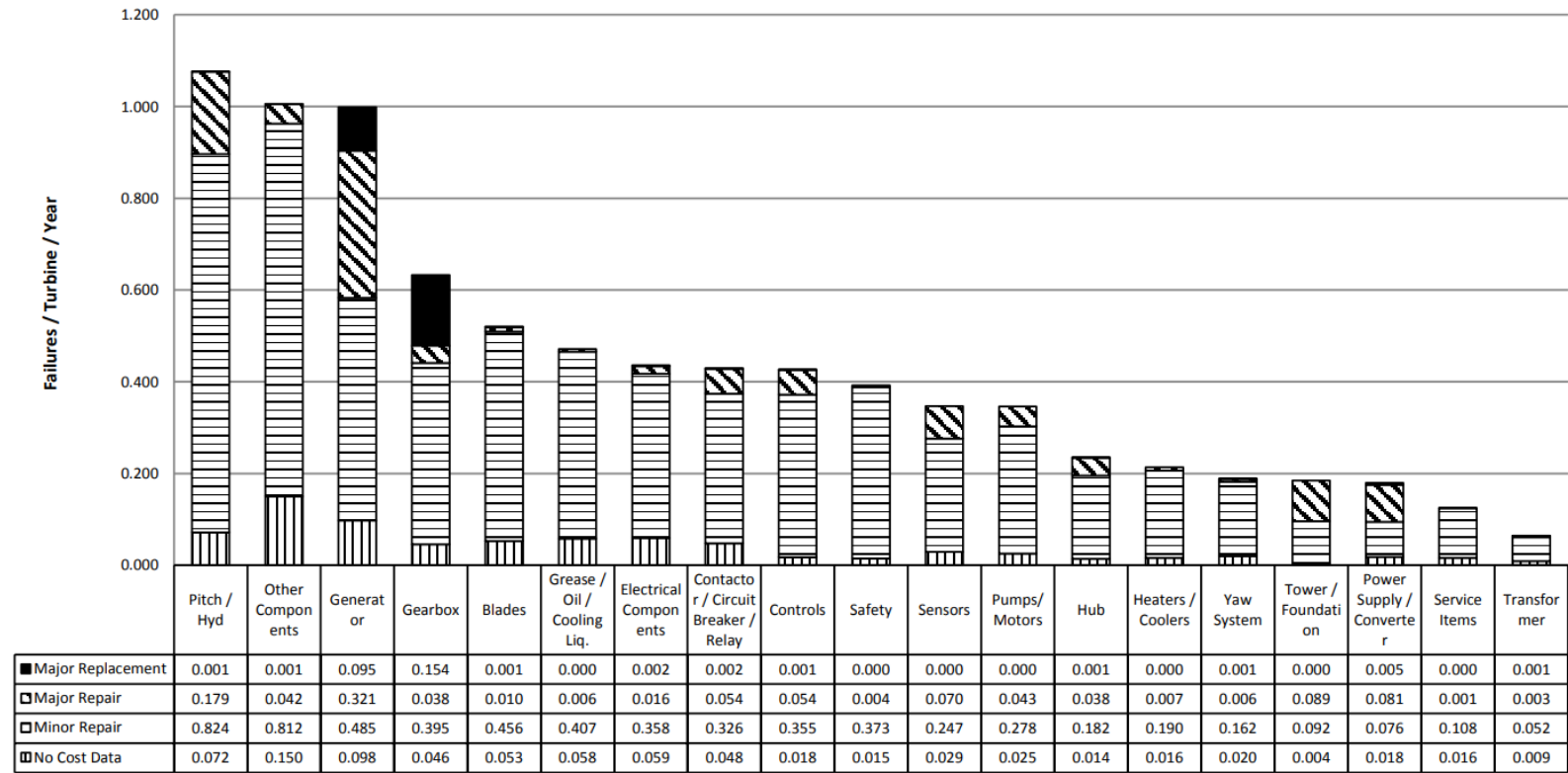
Figure C.1.: Failure rate Pareto chart for subassembly and cost category.
Reprinted from "Failure rate, repair time and unscheduled O&M cost analysis of offshore wind turbines", by Carroll et al. (2015), *Wind Energy*, *19*(6), 1107-1119

C.2.
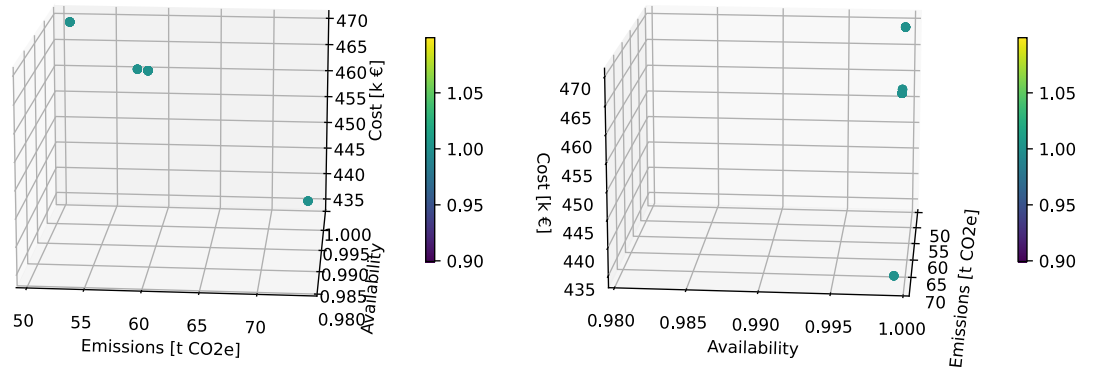
Figure C.2.: Pareto front of case study 1 (3D).
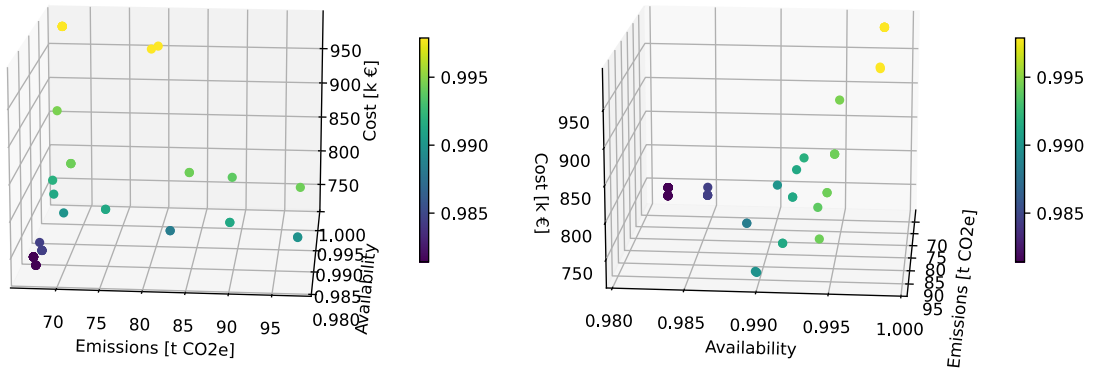
Figure C.3.: Pareto front of case study 2 (3D).
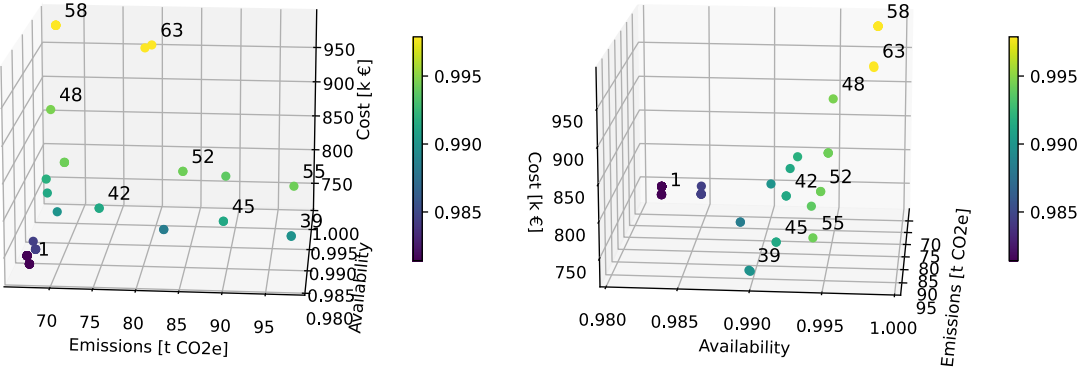
Figure C.4.: Pareto front of case study 2 (3D, numbered).

Bibliography

Affenzeller, M., Winkler, S., & Wagner, S. (2008). Evolutionary system identification: New algorithmic concepts and applications. In W. Kosinkski (Ed.), *Advances in evolutionary algorithms* (pp. 29–48). I-Tech Education; Publishing. https://doi.org/10.5772/6138

Blank, J., & Deb, K. (2020). Pymoo: Multi-objective optimization in python. *IEEE Access*, *8*, 89497–89509. https://doi.org/10.1109/ACCESS.2020.2990567

Bolstad, K. H., Joshi, M., Hvattum, L. M., & Stålhane, M. (2022). Composing vessel fleets for maintenance at offshore wind farms by solving a dual-level stochastic programming problem using GRASP. *Logistics*, *6*(1). https://doi.org/10.3390/logistics6010006

Boyd, S., & Vandenberghe, L. (2009). *Convex optimization* (7e). Cambridge University Press. https://doi.org/10.1017/CBO9780511804441

Carroll, J., McDonald, A., & Mcmillan, D. (2015). Failure rate, repair time and unscheduled O&M cost analysis of offshore wind turbines. *Wind Energy*, *19*(6), 1107–1119. https://doi.org/10.1002/we.1887

Colin Cooke. (2016). *Aberdeen, Sikorsky S-92A Babcock offshore helicopter* [photograph] [*Aberdeen, Sikorsky S-92A Babcock offshore helicopter* [Photograph]. Flickr. https://flic.kr/p/MruAD3]. https://flic.kr/p/MruAD3

Dalgic, Y., Dinwoodie, I., Lazakis, I., Mcmillan, D., & Revie, M. (2014). Optimum CTV fleet selection for offshore wind farm O&M activities. *Proceedings for the European Safety and Reliability Conference ESREL 2014*. https://doi.org/10.1201/b17399-164

Dalgic, Y., Lazakis, I., Dinwoodie, I., Mcmillan, D., Revie, M., & Majumder, J. (2015). Cost benefit analysis of mothership concept and investigation of optimum chartering strategy for offshore wind farms. *Energy Procedia*, *80*, 63–71. https://doi.org/10.1016/j.egypro.2015.11.407

Dalgic, Y., Lazakis, I., & Turan, O. (2013). Vessel charter rate estimation for offshore wind O&M activity. In C. G. Soares & F. L. Peña (Eds.), *Proceedings for the 15th international congress of the international maritime association of the mediterranean IMAM 2013*. https://doi.org/10.1201/b15813-113

Das, I., & Dennis, J. E. (1998). Normal-boundary intersection: A new method for generating the pareto surface in nonlinear multicriteria optimization problems. *SIAM Journal on Optimization*, *8*(3), 631–657. https://doi.org/10.1137/S1052623496307510

Deb, K., & Miettinen, K. (2009). A review of nadir point estimation procedures using evolutionary approaches: A tale of dimensionality reduction. https://www.diva-portal.org/smash/record.jsf?pid=diva2%5C%3A498801&dswid=-9088

Dewan, A., & Asgarpour, M. (2016). *Reference O&M concepts for near and far offshore wind farms* (Report No. ECN-E—16-055). ECN. ECN Petten. https://projecten.topsectorenergie.nl/storage/app/uploads/public/5d3/ff0/cc1/5d3ff0cc19673456604507.pdf

Dighe, V. V., Pergod, L., & Yung, C. (2022). *Offshore wind access report 2022* (Report No. TNO 2022 R12419). TNO. http://resolver.tudelft.nl/uuid:d6cefbf6-2916-42fc-bb3d-b2d713938e09

Diran, D. D. (2018). *Marine fleet optimization for offshore substation maintenance: An application for the german and dutch offshore transmission grid* [Master's thesis, TU Delft]. TU Delft Repository. https://repository.tudelft.nl/islandora/object/uuid%5C%3Aa364a0e7-f8ca-463b-9204-31bc3a761580

Freund, R. M. (2014). *Duality theory of constrained optimization*. Massachusetts Institute of Technology. https://ocw.mit.edu/courses/15-084j-nonlinear-programming-spring-2004/ac15ee761a195e0fa56df107942f6373_lec18_duality_thy.pdf

Garcia-Teruel, A., Rinaldi, G., Thies, P. R., Johanning, L., & Jeffrey, H. (2022). Life cycle assessment of floating offshore wind farms: An evaluation of operation and maintenance. *Applied Energy*, 307, 118067. https://doi.org/https://doi.org/10.1016/j.apenergy.2021.118067

Gray, A. (2021). *Setting a benchmark for decarbonising O&M vessels of offshore wind farms*. ORE Catapult. https://ore.catapult.org.uk/analysisinsight/setting-benchmark-decarbonising-om-vessels-offshore-wind-farms/

Gunantara, N. (2018). A review of multi-objective optimization: Methods and its applications (Q. Ai, Ed.). *Cogent Engineering*, 5(1). https://doi.org/10.1080/23311916.2018.1502242

Gundegjerde, C., Halvorsen, I. B., Halvorsen-Weare, E. E., Hvattum, L. M., & Nonås, L. M. (2015). A stochastic fleet size and mix model for maintenance operations at offshore wind farms. *Transportation Research Part C: Emerging Technologies*, 52, 74–92. https://doi.org/10.1016/j.trc.2015.01.005

Gurobi Optimization LLC. (2022). Gurobi Optimizer Reference Manual. https://www.gurobi.com

Gutierrez-Alcoba, A., Hendrix, E., Ortega, G., Halvorsen-Weare, E., & Haugland, D. (2019). On offshore wind farm maintenance scheduling for decision support on vessel fleet composition. *European Journal of Operational Research*, 279(1), 124–131. https://doi.org/10.1016/j.ejor.2019.04.020

Halvorsen-Weare, E. E., Gundegjerde, C., Halvorsen, I. B., Hvattum, L. M., & Nonås, L. M. (2013). Vessel fleet analysis for maintenance operations at offshore wind farms. *Energy Procedia*, 35, 167–176. https://doi.org/10.1016/j.egypro.2013.07.170

Halvorsen-Weare, E. E., Norstad, I., Stålhane, M., & Nonås, L. M. (2017). A metaheuristic solution method for optimizing vessel fleet size and mix for maintenance operations at offshore wind farms under uncertainty. *Energy Procedia*, 137, 531–538. https://doi.org/10.1016/j.egypro.2017.10.382

Hu, B., & Yung, C. (2020). *Offshore wind access report 2020* (Report No. TNO 2020 R11992). TNO. TNO. https://publications.tno.nl/publication/34637592/uSPDJu/TNO-2020-R11992.pdf

IRENA. (2019). *Future of wind: Deployment, investment, technology, grid integration and socio-economic aspects (a global energy transformation paper)*. International Renewable Energy Agency. https://www.irena.org/publications/2019/Oct/Future-of-wind

Isermann, H., & Steuer, R. E. (1988). Computational experience concerning payoff tables and minimum criterion values over the efficient set. *European Journal of Operational Research*, 33(1), 91–97. https://doi.org/https://doi.org/10.1016/0377-2217(88)90257-3

Janga Reddy, M., & Kumar, D. N. (2020). Evolutionary algorithms, swarm intelligence methods, and their applications in water resources engineering: A state-of-the-art review. *H2Open*, 3(1), 135–188. https://doi.org/10.2166/h2oj.2020.128

Jorge, J. M. (2009). An algorithm for optimizing a linear function over an integer efficient set. *European Journal of Operational Research*, 195(1), 98–103. https://doi.org/https://doi.org/10.1016/j.ejor.2008.02.005

Kang, J., Sobral, J., & Soares, C. G. (2019). Review of condition-based maintenance strategies for offshore wind energy. *Journal of Marine Science and Application*, 18, 1–16. https://doi.org/10.1007/s11804-019-00080-y

Klotz, E., & Newman, A. M. (2013). Practical guidelines for solving difficult mixed integer linear programs. *Surveys in Operations Research and Management Science*, 18(1), 18–32. https://doi.org/10.1016/j.sorms.2012.12.001

Kolios, A., & Brennan, F. (2018). *Review of existing cost and o&m models, and development of a high fidelity cost/revenue model for impact assessment* (Report No. Ares(2018)6044833). ROMEO Project. https://romeoproject.eu/wp-content/uploads/2018/12/D8.1_RO MEO_Report-reviewing-exsiting-cost-and-OM-support-models.pdf

Komusanac, I., Brindley, G., Fraile, D., & Ramirez, L. (2020). *Wind energy in europe* (R. O'Sullivan, Ed.). WindEurope. https://windeurope.org/intelligence-platform/product/wind-e nergy-in-europe-2020-statistics-and-the-outlook-for-2021-2025/

Küçükyavuz, S., & Jiang, R. (2021). *Chance-constrained optimization: A review of mixed-integer conic formulations and applications*. https://doi.org/10.48550/arXiv.2101.08746

Kyoto Protocol. (1997). United Nations. United Nations Treaty Collection, Chapter XXVII 7. a. https://treaties.un.org/doc/Treaties/1998/09/19980921%5C%2004-41%20PM/C h_XXVII_07_ap.pdf

Li, C., & Grossmann, I. E. (2021). A review of stochastic programming methods for optimization of process systems under uncertainty. *Frontiers in Chemical Engineering*, 2. https://doi.org/10.3389/fceng.2020.622241

Li, P., Arellano-Garcia, H., & Wozny, G. (2008). Chance constrained programming approach to process optimization under uncertainty. *Computers & Chemical Engineering*, 32(1-2), 25–45. https://doi.org/10.1016/j.compchemeng.2007.05.009

Liapodimitris, D. (2017). *Vessel fleet optimisation for offshore wind power maintenance* [Master's thesis, Uppsala University]. DiVA. https://www.diva-portal.org/smash/get/diva2: 1151086/FULLTEXT01.pdf

Luptácik, M. (2010). *Mathematical optimization and economic analysis* (Vol. 36). Springer. https://doi.org/10.1007/978-0-387-89552-9

Mark Kilner. (2018). *North Foreland, Vattenfall Tempest* [photograph]. https://flic.kr/p/Q7xL5 P

Martin, R., Lazakis, I., Barbouchi, S., & Johanning, L. (2016). Sensitivity analysis of offshore wind farm operation and maintenance cost and availability. *Renewable Energy*, 85, 1226–1236. https://doi.org/https://doi.org/10.1016/j.renene.2015.07.078

Mavrotas, G. (2009). Effective implementation of the ϵ-constraint method in multi-objective mathematical programming problems. *Applied Mathematics and Computation*, 213(2), 455–465. https://doi.org/https://doi.org/10.1016/j.amc.2009.03.037

Mavrotas, G., & Florios, K. (2013). An improved version of the augmented ϵ-constraint method (augmecon2) for finding the exact pareto set in multi-objective integer programming problems. *Applied Mathematics and Computation*, 219(18), 9652–9669. https://doi.org /https://doi.org/10.1016/j.amc.2013.03.002

Merizalde, Y., Hernández-Callejo, L., Duque, O., & Alonso Gómez, V. (2019). Maintenance models applied to wind turbines. a comprehensive overview. *Energies*, 12, 225. https: //doi.org/10.3390/en12020225

Mesquita-Cunha, M., Figueira, J. R., & Barbosa-Póvoa, A. P. (2022). New ϵ-constraint methods for multi-objective integer linear programming: A pareto front representation approach. *European Journal of Operational Research*, 306(1), 286–307. https://doi.org/1 0.1016/j.ejor.2022.07.044

Moosmann, L., Siemons, A., Fallasch, F., Schneider, L., Urrutia, C., Wissner, N., Mendelevitch, R., Hermann, H., & Healy, S. (2022). *The COP27 Climate Change Conference: Status of climate negotiations and issues at stake*. European Parliament. https://www.europarl.e uropa.eu/RegData/etudes/STUD/2022/733989/IPOL_STU(2022)733989_EN.pdf

Naji Tahan, B. D. (2005). Chapter 14 - offshore installation. In S. K. CHAKRABARTI (Ed.), *Handbook of offshore engineering* (pp. 1055–1126). Elsevier. https://doi.org/10.1016/B 978-0-08-044381-2.50021-7

NEOS Guide. (n.d.). *Optimization problem types*. https://neos-guide.org/guide/types/

Nikas, A., Fountoulakis, A., Forouli, A., & Doukas, H. (2022). A robust augmented ϵ-constraint method (augmecon-r) for finding exact solutions of multi-objective linear programming problems. *Operational Research*, *22*. https://doi.org/10.1007/s12351-020-00574-6

Nocedal, J., & Wright, S. J. (2006). *Numerical optimization* (2e). Springer. https://doi.org/10.1007/978-0-387-40065-5

Norbert Möller. (2018). *Cuxhaven, Innovation Jack-Up Vessel* [photograph] [*Cuxhaven, Innovation Jack-Up Vessel* [Photograph]. Flickr. https://flic.kr/p/LuTjH7]. https://flic.kr/p/LuTjH7

Paris Agreement. (2015). United Nations. United Nations Treaty Collection, Chapter XXVII 7. d. https://treaties.un.org/pages/ViewDetails.aspx?src=TREATY&mtdsg_no=XXVII-7-d&chapter=27&clang=_en

Powell, W. B. (2019). A unified framework for stochastic optimization. *European Journal of Operational Research*, *275*(3), 795–821. https://doi.org/10.1016/j.ejor.2018.07.014

Ramachandran, R., Desmond, C., Judge, F., Serraris, J.-J., & Murphy, J. (2021). *Floating offshore wind turbines: Installation, operation, maintenance and decommissioning challenges and opportunities*. European Academy of Wind Energy. https://doi.org/10.5194/wes-2021-120

Ranganathan, J., Corbier, L., Bhatia, P., Schmitz, S., Gage, P., Oren, K., Dawson, B., Spannagle, M., McMahon, M., Boileau, P., Frederick, R., Vanderborght, B., Thomson, F., Koichi, K., Woo, C., Pankhida, N., Miner, R., Segalen, L., Koch, J., . . . Cook, E. (2004). *Greenhouse gas protocol: A corporate accounting and reporting standard*. World Business Council for Sustainable Development. https://doi.org/10.13140/RG.2.2.34895.33443

Ren, Z., Verma, A. S., Li, Y., Teuwen, J. J., & Jiang, Z. (2021). Offshore wind turbine operations and maintenance: A state-of-the-art review. *Renewable and Sustainable Energy Reviews*, *144*. https://doi.org/10.1016/j.rser.2021.110886

Rinaldi, G., Pillai, A. C., Thies, P. R., & Johanning, L. (2019). Multi-objective optimization of the operation and maintenance assets of an offshore wind farm using genetic algorithms. *Wind Engineering*, *44*, 390–409. https://doi.org/10.1177/0309524X19849826

Rinaldi, G., Thies, P., & Johanning, L. (2017). A coupled monte carlo-evolutionary algorithm approach to optimise offshore renewables O&M. *Proceedings of the 12th European Wave and Tidal Energy Conference*. https://www.researchgate.net/publication/319955237_A_coupled_Monte_Carlo-Evolutionary_Algorithm_approach_to_optimise_offshore_renewables_OM

Rinaldi, G., Thies, P., & Johanning, L. (2021). Current status and future trends in the operation and maintenance of offshore wind turbines: A review. *Energies*, *14*, 2484. https://doi.org/10.3390/en14092484

Roszkowska, E. (2013). Rank ordering criteria weighting methods – a comparative overview. *Optimum. Economic Studies*, *5*(65), 14–33. https://doi.org/10.15290/ose.2013.05.65.02

Shafiee, M. (2015). Maintenance logistics organization for offshore wind energy: Current progress and future perspectives. *Renewable Energy*, *77*, 182–193. https://doi.org/10.1016/j.renene.2014.11.045

Shenton, S., Mallett, C., & Frampton, M. (2014). *Jack-up vessel optimisation*. The Crown Estate. https://www.thecrownestate.co.uk/media/1780/ei-km-in-om-construction-072014-jack-up-vessel-optimisation.pdf

Sperstad, I. B., Stålhane, M., Dinwoodie, I., Endrerud, O.-E. V., Martin, R., & Warner, E. (2017). Testing the robustness of optimal access vessel fleet selection for operation and maintenance of offshore wind farms. *Ocean Engineering*, *145*, 334–343. https://doi.org/10.1016/j.oceaneng.2017.09.009

Stålhane, M., Bolstad, K. H., Joshi, M., & Hvattum, L. M. (2020). A dual-level stochastic fleet size and mix problem for offshore wind farm maintenance operations. *INFOR: Information Systems and Operational Research*, *59*(2), 257–289. https://doi.org/10.1080/031 55986.2020.1857629

Stålhane, M., Halvorsen-Weare, E. E., Nonås, L. M., & Pantuso, G. (2019). Optimizing vessel fleet size and mix to support maintenance operations at offshore wind farms. *European Journal of Operational Research*, *276*(2), 495–509. https://doi.org/10.1016/j.ejor.20 19.01.023

Stålhane, M., Vefsnmo, H., Halvorsen-Weare, E. E., Hvattum, L. M., & Nonås, L. M. (2016). Vessel fleet optimization for maintenance operations at offshore wind farms under uncertainty. *Energy Procedia*, *94*, 357–366. https://doi.org/10.1016/j.egypro.2016.09.1 95

Szpytko, J., & Salgado, Y. (2019). Integrated maintenance decision making platform for offshore wind farm with optimal vessel fleet size support system. *TransNav, the International Journal on Marine Navigation and Safety of Sea Transportation*, *13*(4), 823–830. https://doi.org/10.12716/1001.13.04.15

Thomsen, K. E. (2014). *Offshore wind: A comprehensive guide to successful offshore wind farm installation* (Second). Elsevier. https://doi.org/10.1016/C2012-0-07272-9

Wind Denmark. (2008a). *Burbo Bank, offshore wind turbine* [photograph]. https://flic.kr/p/7v rQu3

Wind Denmark. (2008b). *Horns Rev I, Turbine* [photograph]. https://flic.kr/p/7jKLcL

Wind & water works. (2022). *Dutch offshore wind guide*. Netherlands Enterprise Agency. https ://www.rvo.nl/sites/default/files/2021/10/Dutch%5C%20Offshore%5C%20Wind %5C%20Guide%5C%202022.pdf

WindEurope. (2022). *Windeurope position on non-price criteria in auctions*. https://windeurope.o rg/policy/position-papers/windeurope-position-on-non-price-criteria-in-auctions/

Wright, S., & Falbe-Hansen, L. (2017). *Definitions of availability terms for the wind industry* (Document No. EAA-WP-15). DNV-GL. https://www.ourenergypolicy.org/wp-content /uploads/2017/08/Definitions-of-availability-terms-for-the-wind-industry-white-p aper-09-08-2017.pdf

Colophon

This document was typeset using LaTeX, using the KOMA-Script class `scrbook`. The main font is Palatino. The figures and diagrams were mostly drawn using Mathcha, Ti*kz* and Microsoft PowerPoint.